UNIVERSITÀ DEGLI STUDI DI MILANO

Scuola di Dottorato in
Scienze molecolari e biotecnologie agrarie, alimentari ed ambientali
Molecular Sciences and Plant, Food and Environmental Biotechnology

Dottorato di Ricerca in
Chimica, Biochimica ed Ecologia degli Antiparassitari (XXVII ciclo)
Chemistry, Biochemistry and Ecology of Pesticides

New strategies based on natural compounds for controlling biofilm formation

CRISTINA CATTO'
No. Matr. R09731

Supervisor: Dr. Fabio Forlani
Co-supervisor: Dr. Francesca Cappitelli
Coordinator: Prof. Daniele Daffonchio

Academic year 2013/2014

Contents

Abstract

Direct observations of a wide variety of natural habitats have established that 99 % of microorganisms grow in form of biofilms, complex structured communities of microorganisms associated with surfaces and embedded in a self-produced extracellular polymeric substances. Biofilms are able to colonize every surface that offers minimal conditions for the life included all human artefact surfaces. Consequently, industrial installations, work benches, water distribution systems and also medical devices can be covered by biofilm with devastating consequences in terms of social and economic impact. The most detrimental property of biofilms is that conventional biocidal practices often prove inadequate. Indeed, adopting the sessile mode of life, microorganisms improve their resistance to antimicrobial agents up to several orders of magnitude. In addition, increasingly restrictive regulations limiting the use of substances hazardous to human health and the environment, have resulted in several biocides being banned. In this contest the development of new improved effective solutions able to replace the presently dominating drug/device products is becoming imperative.

An innovative approach could be the use of biocide-free anti-biofilm compounds with novel targets, unique modes of action and properties that are different from those of the currently used antimicrobials. Recently, the use of sub-lethal doses of bio-inspired molecules able to interfere with specific key steps that are needed to establish biofilms have been proposed as an alternative strategy to prevent biofilm formation. Since this approach deprives microorganisms of their virulence properties without affecting their existence, the selection pressure for antibiotics and biocides resistance mutations decreases. In this contest, nature represents an immense source of new bioactive substances with unrivalled structural diversity and complexity. Recently, the natural compounds zosteric acid (ZA) and salicylic acid (SA) have been proposed as alternative biocide-free agents able to significantly reduce, at sub-lethal concentrations, both bacterial and fungal adhesion and to play a role in shaping biofilm architecture, in reducing biofilm biomass and thickness and in extending the antimicrobial agents performance.

In this project, ZA and SA were selected as suitable anti-biofilm compounds to provide new effective preventive or integrative solutions against bacterial and fungal biofilm formation available for a wide range of applications. Specifically, the aim of the project was to develop new anti-biofilm materials by covalently anchoring ZA and SA to commercial available polymeric materials, allowing the anti-biofilm compounds to preserve the biological function upon the conjugation process and over a working timescale.

The conjugation reaction was performed in such a way to orient the molecules with their active scaffold externally exposed on the surface so that to ease the interaction with the target microorganism. In this study, a detailed chemical and functional information necessary to ZA and SA to exert their anti-biofilm activity was obtained without affecting the active structure of the investigated molecules.

In Chapter 3 a 43-member library of small molecules based on ZA scaffold diversity was designed and screened against *Escherichia coli* to identify important structural chemical determinants for ZA anti-biofilm activity in order to select potential functional groups that could be exploited for the covalent linkage to an abiotic surface. The compounds were characterized by: i) the introduction of substituents at different positions on phenyl ring; ii) the removal of the insaturation; iii) the substitution of the carboxylic acid with an alcohol, an aldehyde and ester functionalities. Both E/Z isomers were also prepared in order to explore the role of the double bond. All the molecules were submitted to biological assays in order to evaluate their ability to be a carbon and energy source and to affect both planktonic growth and microbial adhesion at several concentrations. Structure/anti-biofilm activity relationship considerations revealed that the carboxylic acid moiety conjugated to the double bond in

trans configuration was an essential requirement in ZA chemical structure to guarantee a good anti-biofilm performance. In contrast, the deletion of the sulphate ester group seemed not to compromise the ZA anti-biofilm activity. Moreover, the biological results revealed that the *para* position on the phenyl ring could be considered a good point for the coupling to a polymer. Indeed, *p*-aminocinnamic (*p*-ACA) acid bearing the same ZA active scaffold and an amino group in the *para* position of the phenyl ring was selected as suitable compound to form a covalent linkage with appropriate functional groups of the polymeric material.
Besides cinnamic acid analogs, another class of derivatives related to the scaffold of salicylic acid has been investigated. Also in this case, the addition of an amino group in the *para* position of the phenyl ring of SA structure did not affect the molecule anti-biofilm performance. Indeed, *p*-aminosalicylic acid (p-ASA) bearing the chemical structure of salicylic acid and an amino group in the *para* position of the phenyl ring was selected to be covalently coupled to a polymeric materials.
In Chapter 4 the molecular mechanisms and pathways by which ZA and SA affect the biofilm formation in *E. coli* were investigated. In this study, a pull-down system combined with a mass spectrometry-based approach was successfully employed to screen the whole *E. coli* proteome in order to identify the molecular targets implicated in ZA and SA anti-biofilm responses. By successfully exploiting the information obtained from the previous work, *p*-ACA and *p*-ASA were chosen as suitable molecules to successfully immobilize ZA and SA active scaffold on a chromatography solid phase support via an amide bond. Mass spectrometry analysis of SDS-PAGE-resolved pull-down proteins revealed that both ZA and SA in *E. coli* directly interact with the same protein WrbA. On the basis of previous studies reported in the literature, we supposed a mechanism by which ZA and SA interact with WrbA negatively modulating its activity and leading to an enhanced production of both the cell signal indole and reactive oxygen species that cooperate in a complex network of events leading to the inhibition of biofilm formation. The blast search inside Bacteria and Fungi databases revealed that WrbA sequences exist in a diversity of microorganisms with a high percentage of identity, suggesting a possible important role of this protein in the microbial life, probably associated to the response against environmental stresses. Because of the presence inside other microorganisms of a protein with a similar sequence and activity, it can be supposed that ZA and SA interact with these proteins with a potential anti-biofilm effect also in these microorganisms. Only related to SA, FkpA and Tdh were also identified as possible molecular targets, suggesting the presence of a complex and overlapping regulatory network controlling quorum sensing, motility and biofilm formation.
Based on the information provided by experiment reported in the previous chapters, in Chapter 5, ZA and SA were successfully covalently immobilized on low density polyethylene surface, providing new no-leaching bio-hybrid materials available for a wide range of applications. A specific protocol to expose ZA and SA active scaffold on the external surface of a polymeric material via an amide bond was set up, allowing the anti-biofilm compound active moieties to directly interact with bacterial cells and successfully exerting their function even immobilized. Firstly, oxygen plasma treatment was employed to activate the low density polyethylene surface. Subsequently, the graft-polymerization with 2-hydroxyethyl methacrylate and the immobilization of the selected bioactive molecules on the polymeric surface successfully provided the new materials. Attenuated total reflectance Fourier transform infrared spectroscopy and confocal laser scanner microscope (CSLM) analyses proved that the polyethylene surface was successfully functionalized with ZA and SA molecules. The anti-biofilm performance of the innovative materials was investigated against *E. coli* biofilm using the CDC reactor able to simulate flow conditions normally encountered in vivo. The number of adhered cells on both traditional and functionalized polyethylene surface was established by plate count assays. Biofilm grown on both treated and control material was also submitted to live/dead staining procedure and analyzed by epifluorescence microscope. Both plate count assays and microscope observations showed a 60 % percentage reduction of biofilm growth on both ZA and SA functionalized materials, with a mechanism that did not affect bacterial viability. CLSM analysis also revealed a dramatic impact of immobilized zosteric acid and salicylic acid on biofilm morphology, showing a biofilm with a

significantly reduced thickness and polysaccharide matrix amount. Moreover, biofilm grown on functionalized surfaces showed enhanced susceptibility to ampicillin and ethanol, that further reduced biofilm biomass up to 95 %.
In conclusion, in this study a polyethylene surface was successfully functionalized with the antibiotic-free natural compounds ZA and SA, providing new, improved solutions able to reduce the incidence of biofilm formation. In this approach, no molecules are leached from the surface, sidestepping the problem of the compound kinetic release, providing long term protection against bacterial colonization, and reducing the risk of developing resistant microbial strains, as the concentration of the anti-biofilm agent is constantly below the lethal level. In addition, the knowledge of ZA and SA structure/anti-biofilm activity relationship and molecular targets involved in their anti-biofilm activity open the way to new additional studies to generate more potent derivatives based on the same target and activity structure.

Introduction

The nature of biofilms

Direct observations of a wide variety of natural habitats have established that 99 % of microorganisms grow in form of biofilms, complex structured communities of microorganisms associated with surfaces and embedded in a self-produced extracellular polymeric substances (EPS). Biofilms are able to colonize every surface that offers minimal condition for the life, both abiotic and biotic, including extreme environments such as the walls of pores in glaciers, hot vents or the bottom of the ocean (Costerton et al., 1987). Biofilm formation also appears early in the fossil record and is common throughout a diverse range of organisms in both the Archaea and Bacteria domains (Hall-Stoodley et al., 2004).

The ability to form biofilms is an ancient and integral characteristic of prokaryotes and probably biofilms are the first form of life recorded on earth, dating back 3.5 billion years, and the most successful one. In the context of evolution and adaptation it is likely that biofilms provided homeostasis in the face of the fluctuating and harsh conditions of the primitive earth. However, the protective conditions offered by life on surfaces and the necessity to colonize new environments might have led to the concurrent development of both sessile and planktonic forms (Hall-Stoodley et al., 2004). It is believed that planktonic cells are important for rapid proliferation and spread into new territories, whereas sessile populations are focused on perseverance thanks to their ability to survive in hostile environments (Pace et al., 2006). Anyway the inclination for bacteria to become surface bound is so ubiquitous in diverse ecosystems that it suggests a strong survival and/or selective advantage for surface dwellers over their free-floating counterparts (Dunne, 2002). When residing within a biofilm, microorganisms experience a certain degree of shelter and homeostasis that helps them to persist in the environment. One of the key component of this microniche is the surrounding EPS, a mixture of components such as polysaccharides, proteins, nucleic acids and lipids that form the scaffold for the three-dimensional architecture of the biofilm. EPS immobilize biofilm cells and keep them in close proximity, thus allowing for intense interactions, including cell–cell communication, and the formation of synergistic microconsortia, often leading to a strict mutual metabolic dependence of microorganisms within the biofilm (Davey et al., 2000). In particular, cell to cell communication system, known as quorum sensing, allows bacterial cells to communicate resulting in a cohesiveness of function that benefits an entire population and allows the community to operate as a living system (Smith et al., 2010). Moreover, since cells are maintained in close proximity to each other, horizontal gene transfer is facilitated promoting the genetic information exchange and maintaining a large and well-accessible gene pool. Significantly higher rates of conjugation in bacterial biofilms compared to planktonic populations have been reported (Flemming, 2008). In addition, owing to the retention of extracellular enzymes, EPS generate a versatile external digestive system, sequestering dissolved and particulate nutrients from the environment and allowing them to be utilized as nutrient and energy sources. It is also reported that matrix increases levels of protection against environmental stresses, such as depleted nutrient, moisture and oxygen levels, inhospitable surrounding pH and salinity, excessive shear forces and UV exposure, and even metal toxicity. Additionally, life in a biofilm protects against attacks by a host immune system's protective proteins and signaling molecules, phagocytes, antibiotics and disinfectants (Flemming et al., 2010).

Biofilm formation is a complex dynamic process by which cells undergo a range of phenotypic switches over time. During some stages of biofilm development, as much as 50 % of the proteome can be differentially produced compared with the same cells growing in planktonic culture (Southey-Pillig et

al., 2005). Earlier studies in environmental and industrial microbiology have examined biofilm formation in various ecosystems, and concluded that bacteria form biofilms in essentially the same manner regardless which environment they inhabit (Costerton, 1997). In the first step of biofilm formation, planktonic microorganisms move into close proximity with the surface, which may have several physico-chemical characteristics that are important to determine the rate and the extent of the attachment process. The process of microbial adherence to surfaces is also largely dictated by a number of variables such as the species of bacteria, cell surface composition, nutrient availability, hydrodynamics, and global regulatory networks (Dunne, 2002). Some studies also suggest that motility is very important for planktonic cells initial contacts with a surface since flagella-mediated motility can bring the cell within close proximity of the surface to overcome repulsive forces between bacterium and the surface (Pratt et al., 1998). This initial attachment is reversible and is generally mediated by non-specific interactions such as electrostatic, hydrophobic, or van der Waals forces. When the loosely bound microorganisms consolidate the adhesion process by producing exopolymers and adhesins that complex with surface materials, adhesion to the surface becomes irreversible and microorganisms can not dislodged by gentle rinsing (Dunne, 2002). Once bacteria have irreversibly attached to a surface, bacterial cells undergo phenotypic changes, and the process of biofilm maturation begins. Microorganisms grow and multiply, start to form microcolonies, produce extracellular polymers and communicate via quorum sensing signals. The results is an intricate structure composed by discrete matrix-enclosed communities of microbial cells that may include one or of many species (Davey et al., 2000). Depending on the species involved, the biofilm may be composed of 10-25 % cells and 75-90 % matrix, and the matrix material often appears to be most dense in the area closest to the core of the biofilm (Costerton, 1999; Flemming et al., 2010). Mature biofilms display discrete temporal and spatial structure because of differences in local conditions such as nutrient availability, pH, oxidizing potential, and so on. For example, cells near the surface of the biofilm are exposed to higher concentrations of oxygen, while near the center oxygen is rapidly depleted to near anaerobic levels. The steep oxygen gradients are paralleled by gradients for either nutrients or metabolites from the biofilm, which creates a heterogenic environment. In adapting to these local environmental conditions microorganisms within a biofilm display many genotypes and phenotypes with broad metabolic and replicative heterogeneity, providing the community as a whole with enormous capability to resist stresses (Steward, 2008). Finally, individual microcolonies from the mature biofilm may detach from the surface, reenter the planktonic state, translocate to a new location and may reattach to new areas, initiating a new cycle of biofilm formation. Therefore, biofilm formation may be cyclical in nature. Nutrient starvation, overexpression of alginate lyase, loss of EPS, and quorum sensing may be involved in the control of biofilm detachment. Mechanisms of biofilm dispersal can be dictated by survival for escaping unfavorable habitats aiding in the development of new niches or may be initiated by the bacteria themselves without any obvious perturbation (Stoodley et al., 2002; Pace et al., 2006).

The deleterious impact of biofilms on human world

The study of biofilms has skyrocketed in the past 20 years due to increased awareness of their pervasive effect on human life with devastating social and economic implication. On a global scale, biofilm-related costs incur billions of dollars to the agricultural, engineering, and medical sectors of the economy (Plyuta et al., 2013).

Especially in the clinical sector, biofilms create relevant problems. The correlation between biofilms and infectious disease is a connection that is becoming well documented in the medical community, and the National Institutes of Health in the USA estimates that 80 % of all bacterial infections occurring in the human body are biofilm related. An estimated 17 million new biofilm infections arise each year in the USA, which result in up to 550,000 fatalities annually (Davies, 2003). Biofilm infections are rarely

resolved by the host's immune system. Biofilm bacteria release antigens and stimulate the production of antibodies, yet bacteria residing in biofilms are resistant to these defence mechanisms (Davey et al., 2000). The role of biofilms in the contamination of medical implants has also been well established in the clinical area. Every day implantable medical devices such as prosthetic heart valves, cardiac pacemakers, total joint replacements, renal dialysis, ventricular shunts and various types of catheters are applied in almost all fields of medicine for managing critically ill patients (von Eiff et al., 2005; Hall-Stoodley et al., 2004). Unluckily, these implants become potential surface for biofilm formation causing devastating medical complications such as life-threatening systemic infections and malfunctions that in most of cases may require device removal (von Eiff et al., 2005). These drastic interventions bear obvious implications in term of patient morbidity, mortality, prolonged hospitalization and increased healthcare costs (Darouiche, 2007). It has been estimated that catheter-associated urinary tract infections are the most common source of hospital-acquired infections accounting for approximately 40 % of all nosocomial infections worldwide, with approximately 900,000 cases in the United States alone annually and cost that ranges from 296 million to 2.3 billion dollars each year (Jhonson et al., 2006; Lo et al., 2014).

The detrimental effects of biofilm, can be also felt across numerous industries causing a particular costly problem in nearly every industrial water-based process, including water treatment and distribution, food processing, utilities and marine-based industries. The result is the loss of billions of dollars each year related to the decrease in industrial productivity as well as to the industrial system physical deterioration such as pipe plugging and corrosion (Stowe et al., 2011). In particular, biofilms formed in food-processing environments are of special importance as they have the potential to act as a persistent source of microbial contamination that may lead to threaten the microbiological quality and safety of food products resulting in food-borne disease (Cappitelli et al., 2014). It has been estimated that in the USA, foodborne illness causes 9000 human deaths and affects 6-80 million people every year (Rayner et al., 2004). In addition, the presence of detrimental bacteria on food processing surfaces shortens the time between cleaning, reduces heat transfer efficacy or even equipment obstruction, produces metal corrosion in pipelines and tanks resulting at least in metal loss and food contamination with consequently economic losses (Van Houdt et al., 2010; Cappitelli et al., 2014). Biofilms are the predominant mode of microbial growth in drinking water networks and high purity water production and distribution systems (Farkas et al., 2013). Flemming and colleagues (2002) estimated that approximately 95 % of bacterial cells are attached to pipe walls as biofilm communities while less than 5 % are found in the water phase. Detrimental effects may occur, including microbially induced corrosion, disinfectant depletion, aesthetic problems i.e. colour, odour and taste degradation and microbiological deterioration of drinking water (Farkas et al., 2013; Polo et al., 2014). Biofilms are also ubiquitous in the marine world. The surfaces of ship hulls or underwater pipelines are rapidly conquered by biofilms of bacteria and fungi which mediate subsequent attachment and growth of mussels, polychaete worms, or barnacles. These biofilms contribute to early corrosion and higher fuel consumption during displacement due to increased hydrodynamic drag (Garcia-Fernandez et al., 2009).

Biofilm are found on almost every household surfaces, including toilets, sinks, countertops, and cutting boards in the kitchen and bath as well as air-conditioning and heating system surfaces. Also high-surface areas and repeated exposure to moisture and nutrients make kitchen surfaces ideal habitats for the concentration, growth and potential spread of bacterial biofilm. Raloff (1996) reported that the majority of 75 dishrags and 325 sponges harbored *Escherichia coli*, *Salmonella spp.*, *Pseudomonas spp.* and *Staphylococcus spp.* In another study involving 213 houses, 47.4 % tested positive for *Listeria monocytogenes*, with dishcloths and various other utensils and structural surfaces being the most highly contaminated items (Beumer et al., 1996). Poor disinfection practices and ineffective cleaning products may increase the incidence of illnesses associated with pathogenic organisms in the household environment as well as the deterioration of air quality (Rayner et al., 2004).

Unexpectedly biofilm also affect stone surface of stone buildings and monuments, both historic and modern (Crispim et al., 2003). As a consequence of complex interactions within microbial community and its substrate biodeterioration processes occur. Microrganisms may act by extracting nutrients from the substrate, by active penetration below the surface or by production of acid metabolites, siderophores, chelating materials and osmolytes that degrade minerals. The consequences are aesthetic and structural damages of stone and the decay of the buildings and monument in the long term period (Young et al., 2008).
It is estimated that more than 10,000 species of bacteria and fungi develop complex biofilm on plant surfaces causing diseases that damage plants and plants products. The kind and amount of losses caused by plant disease vary with plant or plant product, pathogen, locality, environmental, etc. and may range from slight to 100 % loss. The financial losses and social consequences are inevitable especially for countries who depend on their own plant produce for their existence (Agrios, 2012). For example *Xanthomonas oryzae* pv *oryzae* causes one of the most important disease of rice in many parts of the worlds and is very destructive in Japan, India and other parts of Asia. As more than 50 % of world population relies on rice for basic nutrition, it is clear that damage of rice production poses significant economic and social risk (Khoshkdaman et al., 2012).
However, it is very important to point out that biofilms are an integral part of the natural environment and can also serve very beneficial purposes, such as in the treatment of drinking water, wastewater and detoxification of hazardous waste (Ashraf et al., 2001; Farkas et al., 2013).

Anti-biofilm traditional strategies: biocides and antibiotics

For decades, abatement of biofilm growth has commonly been achieved by applying biocides and antibiotics to surfaces or by incorporating them into synthetic polymer-based products. In particular, the coating of device surfaces with one or two antimicrobial substances or the entrapping of these agents within the device material are the approaches most often used to obtain devices with different antimicrobial spectra and duration. Materials containing antibiotics and disinfectants are in part commercially available and already used in clinical applications (Francolini et al., 2010).
However, despite considerable efforts, the past 30 years have yielded little benefit from this practice or available products and reviews are not unanimous about their benefit (Jhonson et al., 2006; Nowatzky et al., 2012). In the recent years, the inherent resistance and/or tolerance of sessile microorganisms to antimicrobial has been found to be a general phenomenon. Sessile bacteria can be up to 1,000-fold more resistant to antibiotics and biocides treatment in comparison to planktonic bacteria of the same strain, depending on the species-drug combination. For example, a β-lactamase-negative strain of *Klebsiella pneumoniae* had a minimum inhibitory concentration of 2 μg/mL ampicillin in aqueous suspension. The same strain, when grown as a biofilm, was scarcely affected (66 % survival) by 4 h treatment with 5000 μg/mL ampicillin, a dose that eradicated free-floating bacteria (Anderl et al., 2000). Paradoxically, once dispersed from the biofilm, those bacterial cells typically revert to an antibiotic susceptible form which suggests that resistance of bacteria in biofilms is not acquired via mutations or mobile genetic elements (Davey et al., 2000; Pace et al., 2006). On the contrary the restricted susceptibility of biofilms to antimicrobials depends on the characteristics of the biofilm organisms as well as the antimicrobial agent and the environment (Harrison et al., 2007).
The presence of a diffusion barrier provided by the EPS has a potential to reduce the penetration of antibiotics or biocides either by physically slowing their diffusion or chemically reacting with them. Local accumulation of metabolic products may also lead to condition which can directly antagonise the action of an antimicrobial agent. For example EPS acts as an ion exchanger, and sequesters hydrophilic and positively charged molecules as in the case of the antibiotic category of aminoglycosides (Pace et al., 2006). In *Pseudomonas aeruginosa* biofilms, both tobramycin and gentamicin (aminoglycosides)

penetrate more slowly due to interaction with extracellular polymers such as alginate (Nichols et al., 1988). β-lactamase is believed to accumulate in the biofilm matrix as a result of secretion or cell lysis, deactivating β-lactam antibiotics in the surface layers more rapidly than they diffuse into the biofilm (Anderl et al., 2003). Similarly secreted catalase protects aggregated bacteria by preventing full penetration of hydrogen peroxide into the biofilm (Stewart et al., 2000). In addition tolerance could be related to restricted penetration into individual bacteria. A recent study identified a mutant of *P. aeruginosa* that expressed classical biofilm architecture, but remained fully susceptible to the three antibiotic classes tested. Because the mutant lacked periplasmic glucans, which were shown to bind tobramycin, tolerance in wild-type biofilms was attributed to the sequestration of antimicrobial agents in the periplasm (Mah et al., 2003; Van Bambeke et al., 2003).

The slow growth rates of biofilm communities have also been posited as a factor in increased biofilm resistance to eradication (Pace et al., 2006). Within a biofilm, there exists a heterogeneous population of cells which differ in growth rates dependent upon the area in which are located. Bacterial cells embedded deep within the biofilm matrix grow more slowly due to lack of nutrients and oxygen. Cells with reduced metabolic activity are also inherently more recalcitrant to antimicrobial therapies as almost all antibiotics target biosynthetic processes occurring in actively growing bacteria such as the biosynthesis of proteins, RNA, DNA, peptidoglycan and folic acid. Therefore most antibiotics that are capable of killing growing and dividing bacterial cells tend to be very inefficient at killing non-multiplying bacteria (Hurdle et al., 2011). This, coupled with the differential penetration distances into a biofilm that antimicrobials display, explains how some drugs fail to completely eradicate biofilm bacteria (Worthington et al., 2012). In particular a top-to-bottom gradient of decreasing antibiotic susceptibility is reported. This gradient originates in the surface layers of biofilms where there is almost complete consumption of oxygen and glucose, leading to anaerobic nutrition-depleted niches with restricted metabolic activity in their depths (Fux et al., 2005). Transmission electron microscopy revealed that sessile bacteria were affected by ampicillin near the periphery of the biofilm but were not affected in the interior, where bacterial cells probably grew slowly or entered in a stationary-phase state due to the limitation for nutrients and oxygen (Pace et al., 2006).

Genetic studies also indicated that sessile cells are more tolerant to antimicrobial agents since express certain resistance genes that protect biofilms from the killing effect of the antimicrobial agent. Bacteria may acquire antibiotic/biocide resistance through either horizontal gene transfer (such as genes encoded on plasmid, transposon, or integron) or through mutation in different chromosomal loci. Hausner and collaborators (1999) demonstrated that conjugation processes in biofilms were 1,000-fold higher than those determined by conventional plating techniques, indicating that gene transfer occurs far more frequently in biofilms than planktonic cell. In addition it is reported that microorganisms in a biofilm state mutate at higher rates to evolve resistance and alleviate the particular stress on the community (Blazquez, 2003). Approximately 20 % of *Psuedomonas* isolates from the lungs of cystic fibrosis patients display this phenomenon, making the task of treatment even more challenging (Oliver et al., 2000). Antibiotic resistance is becoming one of the most pressing clinical problems in modern medicine. The intensive use of antibiotics has dramatically increased the frequency of resistance among human pathogens reducing the possibility of treating infections effectively and increases the risk of complications and of a fatal outcome. New antibiotics and new therapeutic strategies are requested by healthcare sector to address this challenge. However, one of the major problems facing the antibiotic-drug discovery sector is the difficulty in identifying new drug-like compounds with suitable antibacterial activity (Wright et al., 2007; Cegelski et al., 2008).

Biofilms may also escape the effects of antibiotics without undergoing genetic mutation for the presence of a persistence subpopulation of microorganisms in highly protected phenotypic state similar to spore called persisters (Stewart et al., 2001). These persister cells arise due to a state of dormancy in which cells are metabolically inactive. As a consequence, persisters are less sensitive to antibiotics because the cells are not undergoing cellular activities that antibiotics can corrupt, which results in tolerance (i.e., no growth and slow death). Persister cells in biofilms appear to be responsible

for the recalcitrance of chronic infections since they are responsible for biofilm regrowth when the level of treatment drops (Wood et al., 2013).
Another problem concerning the use of antimicrobial agents is that the majority of them do not appear to have been tested against biofilm organisms, largely due to inherent technical difficulties and the lack of a suitable consensus method. Although one standardized biofilm method has been accepted by the American Society for Testing and Materials (ASTM E2196-12), there are no such methods that have been approved or endorsed by the regulatory agencies (EMPA technology report, 2013).
Considerations regarding the use of biocides should also take into account that chemical treatments to prevent biological damage often involve considerable amounts of potentially dangerous substances. Sooner or later biocides and antibiotics are released into the environment and, as they are not generally specifically targeted against deteriorating microorganisms, they are potentially dangerous for human health and the environment (Young et al., 2008; Shultz et al., 2011). Especially many of them are persistent in the environment since they do not break down into safer constituent parts but rather remain intact over prolonged periods of time (Sousa et al., 2014). For example, tetracycline antibiotics are one of the primarily antibiotics groups used for veterinary purposes, for human therapy and for agricultural purposes. Due to their extensive usage, most of the actual evidence suggests that they are omnipresent compounds found in different ecological compartments. In particular, their highly hydrophilic character and low volatility have resulted in significant persistence in the aquatic environment exhibiting serious environmental problems including ecological risks and human health damages. Antibiotics residues promote the development of antibiotic resistant microorganisms, which can induce adverse effect to human health by increasing the risk of certain infections. In addition, the occurrence of tetracycline antibiotics in the environment inhibits the growth of some terrestrial and aquatic species (Daghrir et al., 2013). Similarly over the past 40 years the biocidal organotin compounds tributyltin (TBT) have been intensively used for the protection of ship hulls and for this reason have been largely released into waters. This led to deleterious effects onto non-target aquatic organisms, such as abnormal growth, reproductive failure, sterility and premature death of various marine species at concentrations even below 1 ng/L (Xu et al., 2005a). Moreover, each year a large proportion of crop is lost due to plant pathogens and in order to maintain the productivity, more and more chemicals are being added in the natural environment (Oerke, 2006). These chemical pesticides enter the food chain resulting in serious harmful effects on human health. According to a survey made by the World Health Organization more than 50,000 people in developing countries are annually poisoned and 5000 die as result of the effect of toxic agents used in agriculture (Patel et al., 2013).
Recently the risk to human and animal health and their environmental impact have increasingly discouraged biocide use. This is readily seen in the number of recent policies, directives, technical reports, strategies, recommendations and regulatory decisions designed to reduce antimicrobial agents consumption, ensuring the prudent use of these fragile strategies, and protect specific agents that are critically important for human and animal health and wellbeing (Directive 98/8/EC; Recommendation 2002/77/EC; SCENIHR report 2009; EFSA Summary Report 2012). In particular the European Community Directive 98/8/EC of the European Parliament concerns the authorization for the marketing of biocidal products within the member states and, at the European Community level, establishes a list of approved active substances that may be used in biocidal formulations and banned such compounds that posed severe environmental and human risks, i.e. TBT-based compounds are completely banned. Approximately 18 compounds are currently used as antifouling booster biocides worldwide as alternatives to metal-based and TBT compounds. However, even the approved biocides, such as chlorothalonil, Irgarol 1051, and Sea-nine 211, pose the danger of causing a nonselective toxicity. For instance, the mode of action of Irgarol 1051 is based on the inhibition of photosynthetic electron transport in chloroplasts that can occur at concentrations < 1 mg/L, many times more the lowest EC50 values reported for algae and crustaceans (Xu et al., 2005b).

Innovative eco-friendly strategies for controlling biofilm formation

The numerous problems coming from the use of conventional approaches have directed the scientific community to develop alternative more effective strategies that are perceived as safe by the public and pose negligible risk to human health and the environment. An innovative approach could be the use of biocide-free anti-biofilm compounds with novel targets, unique modes of action and properties that are different from those of the currently used antimicrobials. Recently the use of sub-lethal dose of bio-inspired molecules able to interfere with specific key steps that are needed to establish biofilms has been proposed as alternative strategy to control biofilm formation (Villa *et al*., 2009; Villa *et al*., 2010; Villa *et al.*, 2012; Villa *et al.*, 2013). Since this approach deprives microorganisms of their virulence properties without affecting their existence, the selection pressure for antibiotics and biocides resistant mutations decrease, posing promising perspective to restore the efficacy of traditional antimicrobial agents (Rasko *et al.*, 2010). According to the biofilm formation process, different key steps are considered promising targets for developing innovative anti-biofilm products. The interaction with the surface sensing process keeps pioneering cells in a planktonic form limiting the adhesion of microorganisms to the surfaces. Cell-to-cell communication has also emerged a good point of attack since it is responsible of important mechanisms for controlling the development of highly structured and cooperative biofilm consortia. Such communication among Gram-negative bacteria involves N-acyl homoserine lactones, small secreted molecules that can be self-recognized in dose-dependent manner, and a complex set of transcription factors of quorum sensing-controlled genes (Karatan et al., 2009). The interference with these cell-to-cell communication processes inevitably results in biofilm matrix damages with destabilization of the biofilm physical integrity. Finally, detachment promotion of established biofilm have been presented as a further suitable mechanism to control biofilm formation (Cappitelli et al., 2011; Villa et al., 2013).

In this context nature represents an immense source of new potential bioactive substances with unrivalled structural diversity and complexity (Wong et al., 2008). Plants and animals have adaptively developed fascinating and sophisticated strategies over millions of years to prevent harmful bacterial colonization on their living tissues in response to an ever-present pathogen pressure. In particular both aquatic and terrestrial plants offer very interesting classes of biologically active, low-molecular-mass (<5 kDa) compounds, like alkaloids, terpenoids, flavonoids and coumarins, peptides, glycosides, nucleosides and polyphenols (Villa et al., 2013). Several studies on marine plants suggested that in most of the cases these compounds manipulate the expression of specific phenotypes that represent different stages of biofilm process rather than killing microorganism (Harder, 2008). The mime of these natural strategies is a promising starting point for novel improved effective anti-biofilm solution able to replace the presently dominating drug products (García-Fernández et al., 2013).

Several studies were carried out to explore the anti-biofilm performance of a multitude of compounds coming from nature. For example the extract from the root of *Rubus ulmifolius* was proved to inhibit *Staphilococcus aureus* biofilm formation interfering with cells surface adhesion without limiting bacterial growth (Quave et al., 2012). Differently furanones produced by the marine macroalga *Delisea pulchra* were demonstrated to perturb biofilm processes interfering with bacterial cell-to-cell communication without affecting the growth rate (Wu et al., 2004). Similarly a number of flavonoids found in citrus species were proved to be antagonists of N-acyl homoserine lactones and autoinducer-2-mediated cell–cell signaling affecting biofilm formation by *Vibrio harveyi* and *E. coli* (Vikram et al., 2010). The methanolic extract obtained from *Cuminum cyminum* was also shown to act as quorum-sensing inhibitor, interfering with the N-acyl homoserine lactone activity and inhibiting the swimming and swarming motility, the production of the extracellular polymeric substances and the biofilm formation in several bacterial pathogens (Issac Abraham et al., 2012). Finally the efficacy of sub-lethal concentrations of *Muscari comosum* bulb extract in modulating the extracellular signal responsible for biofilm dispersion was reported (Villa et al., 2012). Villa and collaborators (2013) highlighted that in most of the cases the response depicted by the surface in the presence of these natural compounds is

not dose molecule dependent but explain a non-linear pattern with a parabola-like shape profile. This profile resembles a hormetic property, an adaptive situation in which the response to an environmental stressor varies with the level of exposure (Calabrese et al., 2002).

New experimental approaches to identify promising natural anti-biofilm molecules

Recently, the scarcity of information about the molecular scaffolds that inhibit/disperse bacterial biofilms, has addressed the scientific community toward new experimental approaches consisting in high throughput screenings in which a thousand of molecules can be rapidly analyzed and identified as active compounds (Whortington et al., 2012; Khan et al., 2014). One of the first reports detailing the screening of a large library of compounds with the objective of identifying novel small molecules that possessed anti-biofilm activity was written by Schachter and co-authors (2003) who developed a high-throughput strategy for extracting, purifying and characterizing a library of more than 150,000 natural compounds coming from plants. In 2005, Ren and collaborators (2005) screened 13,000 compounds from 176 plant families and identified ursolic acid (3β-hydroxy-urs-12-en-28-oic acid) from the tree *Diospyros dendo* as a new biofilm inhibitor. Ursolic acid was demonstrated to be completely non-toxic towards *E. coli*, *P. aeruginosa*, *V. harveyi*, and successfully inhibited the formation of these bacterial biofilms. Transcriptome analyses on *E. coli* treated with ursolic acid suggested that this plant-derived compound may function as a signal that induces cells to remain too motile hindering cell adhesion or destabilizing already formed biofilm (Ren et al., 2005). Junker and co-author (2007) reported a high throughput screening to identify novel small molecules able to inhibit and disperse *P. aeruginosa* biofilm developing a new luminescence-based assay. A total of 66,095 molecules derived from libraries containing known bioactive compounds, natural products, and commercially available entities were screened for their anti-biofilm performance at concentration not affecting bacterial growth. Of the compounds analyzed, 61 (0.09 %) were shown to possess notable activities in bacterial anti-attachment assays. This screening led to the discovery of a novel benzimidazole able to inhibit biofilm formation by the pathogenic bacteria *P. aeruginosa*, *K. pneumoniae*, *Erwinia amylovora*, and *Shigella*, methicillin-resistant *S. aureus* and *S. aureus* Newman without affecting bacterial growth (Sambanthamoorthy et al., 2011). Panmanee and colleagues (2013) proposed a high-throughput screening of 42,865 compounds to identify compounds that inhibit formation of *Staphylococcus epidermidis* biofilms and found 16 able to act as anti-biofilm compounds at sub-lethal dose. Examples of other libraries also included the screening of 80 known eukaryotic protein kinase inhibitors with ATP-like scaffolds against *E. coli* biofilm formation by Wenderska and co-authors (2011), the analysis of 8000 for their ability to inhibit motility in *Vibrio cholera* by Rasmussen and colleagues (2011), the test of 312 marine-derived extracts for both biofilm inhibition and dispersal by Navarro and co-workers (2014).

All these studies allowed to isolate several natural or analogues of natural anti-biofilm compounds with a diverse array of chemical structures and biological activities. A number of natural products that possess the ability to inhibit or disperse bacterial biofilms have been used as the starting points for medicinal chemistry programs in which synthetic manipulation of the natural product scaffold has allowed for the design of more efficacious compounds (Worthington et al., 2012). A structure-based virtual screen for the identification of putative quorum-sensing inhibitors was carried out using a focused database comprising compounds that process structural similarities to known quorum-sensing inhibitors furanone 30, patulin, the *P. aeruginosa* LasR natural ligand and known a quorum sensing receptor. This screening led to the discovery of three compounds, which were all recognized drugs, namely salicilyc acid, nifuroxazide and chlorzoxazone, which were subsequently prove to inhibit quorum-sensing regulated gene expression at sub-lethal concentration (Yang et al., 2009).

Computer-aided drug design techniques have also been employed in the search for new biofilm modulators. One such study involved the investigation of 51 active compounds derived from traditional Chinese medicines which antibacterial properties had been previously documented. By virtually determining if any of the target compounds exhibited similar docking characteristics in a 3-D environment to a known inhibitor of the *Agrobacterium tumefaciens* quorum sensing transcriptional regulator protein TraR, the authors hypothesized that hits in the virtual screening would translate into compounds that would also display anti-biofilm activity against *P. aeruginosa*. Five compounds that performed well in the virtual screens were effectively able to inhibit biofilm development and completely disperse *P. aeruginosa* biofilms with no noticeable effect on bacterial growth (Zeng et al., 2008).

Zosteric acid a new promising anti-biofilm compound coming from seagrass

Zosteric acid or *p*-(sulphooxy)cinnamic acid, a secondary metabolite from the seagrass *Zostera marina*, was proved to be a powerful anti-biofilm compound against both bacteria and fungi with a species-specific activity. Xu and collaborators (2005a) observed a significant reduction (92.5 %) in marine bacterial biofilm coverage with 500 mg/L of zosteric acid while Stanley and colleagues (2002) reported that with 1000 mg/L of zosteric acid the fungal adhesion of *Colletotricum lindemuthianum* and *Magnaporthe grisea* on both abiotic and plant leaves surfaces was reduced by 40 %. Similarly Villa and coauthors (2010) demonstrated that 500 mg/L of zosteric acid decreased *E. coli* and *Bacillus cereus* cells adhesion more than 90 % whereas they reported that the zosteric acid effective concentration for *Aspergillus niger* and *Penicillium citrinum* was 1000 mg/L with a biofilm maximum reduction of 57%. Villa and collaborators (2011) also showed that 10 mg/L zosteric acid reduced *Candida albicans* adhesion by at least 70 % leading cells to the inability of forming filamentous structures. More recently Polo and colleagues (2014) proved that 200 mg/L of zosteric acid caused a reduction of 80 % *P. aeruginosa* biofilm coverage. Cryosectioning of different biofilms combined with microscopy observations also revealed a significant impact of zosteric acid on thickness and morphology of both bacterial and fungal biofilm (Villa et al., 2010; Villa et al., 2011, Polo et al., 2014). In addition, zosteric acid was reported to enhance the sensitivity to different antimicrobial agents such as chlorhexidine, chlorine, hydrogen peroxide, and cis-2-decenoic acid (Villa et al., 2011).
In order to study the zosteric acid mechanism of action whole cell proteome of *E. coli* without and with sublethal concentrations of zosteric acid has been studied. Proteomic analysis revealed that proteins with altered expression level in response to the anti-biofilm compound were involved in stress, motility, quorum-sensing and metabolism/biosynthesis mechanisms. Zosteric acid was also proved to increase the autoinducer-2 concentration, the reactive oxygen species, the tryptophanase and the indole synthesis. In addition, Villa and coauthors (2010) reported that zosteric acid is not a chemorepellent but it stimulates individual *E. coli* cell movement by increasing flagellin production, causing the bacteria to wander across the surface instead of adhering firmly and developing biofilm. Indeed it was supposed that zosteric acid acts as an environmental cue leading to global stress on bacterial cells, which favors the expression of various proteins necessary to escape from adverse conditions (Villa et al., 2012). Zosteric acid chemical structure is characterized by a sulfate ester group at one end and a conjugate carboxylic group on the other side. Stanley and colleagues (2002) hypothesized that the basis of the anti-biofilm effect lies in the high affinity for water shown by its sulfate group that increase the hydrophilicity of cell surface. However, a recent study demonstrated that the antifouling agent did not affect cell surface wettability and highlighted the role of the carboxylic group as the active moiety of the molecule since the methyl ester derivate of zosteric acid showed no anti-biofilm activity (Villa et al., 2011).

The potentiality of this molecule as a suitable anti-biofilm compound to replace the biocide-based anti-biofilm traditional strategies also resides in its very low toxicity towards the organisms and the environment. Xu and coauthors (2005b) evaluated a low toxicity of zosteric acid to *P. putida* and aquatic bacteria using the Microtox assay and static toxicity assessment. Moreover zosteric acid showed no measurable LD50 for larval fish with an acute toxicity profile similar to table sugar and had a half-life of a few days in seawater (Flemming, 2005). Using in vitro experiments with suitable primary cell based models, Villa and collaborators (2011) demonstrated that 10 mg/L of zosteric acid did not compromise the cellular activity, adhesion, proliferation or morphology of either the murine fibroblast line L929 or the human osteosarcoma line MG-63. Ecotoxicological tests also did not highlight direct toxicity effects toward the crustacean *Daphnia magna* (Polo et al., 2014). With the goal of determining the general features of its behavior in the environment, Polo and coauthors (2014) also obtained different chemical and physical properties of zosteric acid suggesting a low bioaccumulation potential and the water compartment as its main environmental recipient.
In the past, zosteric acid was isolated from *Zostera marina* through extraction with methanol (Zimmerman 1995, US Patent 5384176). However, more recently Villa and coauthors (2010) proposed a new non-patented process, providing the required amount for a scale-up application and avoiding the costly and time consuming extraction from a natural source.

Salicylic acid a suitable compound for new anti-biofilm strategies

Salicylic acid (salicylate) is a plant-produced phenolic phytohormone, isolated from a wide range of plants and fruits and known to play an important role in several plant physiological processes, such as the induction of plant defense responses against pathogen attack (Hara et al., 2012). For over 4000 years it has been used for the treatment of diseases becoming the most widely used drug in the world with a long list of medical purposes included both systemic and topical uses (Damman, 2013).
Recently, salicylic acid has been observed to be another promising compound suitable for alternative and innovative anti-biofilm strategies to replace the traditional less-effective biocides. Several studies demonstrated that salicylic acid at a concentration that does not affect microbial viability is able to counteract biofilm formation against a wide range of bacteria and fungi. Faber and colleagues (1993) reported that salicylic acid inhibited *P. aeruginosa*, *Enterobacter aerogenes*, *K. pneumoniae*, *E. faecalis*, and *C. albicans* cells adhesion on catheter surfaces with a reduction of biofilm formation over 90 % in the case of *Enterobacter* and *Pseudomonas*. In addition, Faber and co-workers (1995) demonstrated a satisfactory dose-related inhibition of *S. epidermidis* and *P. aeruginosa* biofilm formation on plastic contact lens, lens cases and commonly used medical polymers such as polyethylene and polystyrene surfaces treated with sodium salicylate. Muller and collaborators (1998) reported that *S. epidermidis* biofilm decreased up to 55 % in the presence of 5 mM (691 mg/mL) salicylic acid while Teichberg and collaborators (1993) using electron microscopy analysis demonstrated a dramatic impact of salicylic acid on *S. epidermidis* biofilm. Prithiviraj and co-workers (2005) also showed that when salicylic acid was added into the culture medium at physiologically relevant concentrations (0.1 to 1 mM) the ability of *P. aeruginosa* to form biofilm was diminished in a concentration-dependent manner. More recently, Abd El Aziz and co-workers (2012) found that salicylic acid inhibited *P. aeruginosa* biofilm production up to 68 % at the range of concentration 10-100 µg/mL and eradicated a pre-formed biofilm up to 64% in concentrations below 100 µg/mL acting in a dose dependent manner and with no or little effect on the bacterial viability. In addition these researchers reported that salicylate salt increase the therapeutic efficacy of traditional antibiotic against cells adhesion and subsequent biofilm formation. When salicylate was added to the antibiotic ciprofloxacin/*N*-acetylcysteine combination, the biofilm was reduced up to 99 %. Similarly, El-Banna and colleagues (2012) reported that salicylate at both concentration 10 µg/mL and 100 µg/mL inhibited biofilm production on catheter segments of *E. coli*,

K. pneumonia, *Proteus mirabilis* and *P. aeruginosa* up to 68 %, and disrupted pre-formed biofilms by up to 62 % depending on microorganism and salicylate concentration. In addition salicylate (100 µg/mL) in combination with gentamicin and amikacin showed a better dose-dependent inhibitory effect on biofilm production (up to 79 %) and an improved disruptive effect on the pre-formed biofilms (up to 78 %). The effect of salicylate combination with antimicrobials was also reported by Polonio and co-workers (2001). These researchers proved that the combination of salicylate (5 mM) with vancomycin 1 µg /mL inhibited biofilm formation of *S. epidermidis* by ≥99.9 % and when biofilm-coated polystyrene beads were exposed to 5 mM sodium salicylate and 4 µg/mL vancomycin there was a >99.9 % reduction in viable count. Sub-inhibitory concentrations of salicylic acid were also demonstrated to successfully attenuate biofilm formation by different plant pathogens such as *P. syringae pv syringae*, *Pectobacterium carotovorum* and *A. tumefaciens* (Logonenko et al., 2013; Plyuta et al., 2013). The performance of salicylic acid on a multi-species biofilm was also evaluated. Dowd and co-authors (2009) set up an vitro multi-species chronic wound biofilm model using *P. aeruginosa*, *E. faecalis* and *S. aureus* as model microorganisms and they found that salicylic acid at 10 mM and 20 mM differently targeted the three microorganisms with a major impact on *S. aureus* strain.

Beside these promising studies, the mechanism by which salicylic acid performs its anti-biofilm activity remains to be elucidated. It was hypothesized that salicylic acid interferes with bacterial quorum sensing signals involved in biofilm formation. Yang and colleagues (2009) experimentally showed the ability of salicylic acid to suppress the expression of genes associated with the las/rhl quorum sensing N-acyl homoserine lactone-based signaling system in *P. aeruginosa*. Similarly, Bandara and co-authors (2006) reported that salicylic acid reduced the production of N-acyl homoserine lactone signals and the expression of some virulence factors. Langonenko and co-authors (2013) also showed that salicylic acid affect *P. aeruginosa* biofilm production inhibiting the activity of LuxR-like regulator involved in cells-to-cells communication system and decreasing swimming motility. On the contrary Da and colleagues (2010) asserted that the quorum-sensing disruption is not the predominant mechanism of action since they proved that *P. aeruginosa* mutant lacking for the lasR gene, involved in the quorum-sensing system and an hypothetical salicylic acid target, exhibited an unexpected decreasing biofilm formation profile similar to the wild type strain after salicylic acid treatment, suggesting that the inhibitory effect of salicylic acid depends on more than just quorum-sensing disruption, which appears to play only a relatively small role in the cellular response. In addition, under the hypothesis that quorum-sensing disruption is the predominant mode of action and on the basis that some gene products of the quorum-sensing regulons are necessary for swarming motility, a salicylic acid dependent reduction in the swarming motility of *P. aeruginosa* would expected, with complete abolishment of swarming in the quorum-sensing mutant. However both the wild type and the quorum-sensing mutant were showed capable of swarming under the given experimental conditions, providing additional evidence that quorum-sensing interference is not the predominant mechanism of salicylic acid, as previously thought. To elucidate the salicylic acid mechanism of action, Chow and colleagues (2011) compared the ability of *P. aeruginosa fliC* mutants (flagellum knockout) and *pilB* mutants (type IV pilus knockout) strains to their respective wild-type for their swarming, swimming, and twitching ability under the presence of salicylic acid. Motility assays showed that sub-inhibitory concentrations of 25 and 50 mM salicylic acid significantly decreased bacterial swarming motility in a mutant strain while twitching and swimming motility showed less inhibitory results, supporting the idea that the motility structures are the targets of salicylic acid. However, since biofilm-forming capacity was still observed in both the motility mutants, the authors concluded that probably salicylic acid not preferentially targets on mechanisms or motility systems and hypothesized a possible salicylic acid pleiotropic effect on other factors implicated in biofilm formation. A potential explanation for the inhibitory effect on motility and biofilm formation is that salicylic acid may downregulate the expression of flagella genes by affecting their transcriptional activity which results in the reduction of flagellin protein forming the filament on the single polar flagellum of the bacterium (Dongo et al., 2012).

The various and sometimes contradictory effect of salicylic acid on these processes lets suggest the presence of complex and overlapping regulatory networks controlling QS, motility and biofilm formation which have still to be clarified (Lagonenko et al., 2013).

Functionalization of polymeric material with anti-biofilm natural compounds

The main bottleneck to spread and use the new powerful and eco-friendly anti-biofilm compounds is their incorporation into a system able to resist over a working time scale. In the recent years different passive and active anti-biofilm coating strategies have been investigated with the idea to create novel eco-friendly coating surfaces by the use of less toxic natural product instead of the traditional antimicrobial agents (Coenye *et al.*, 2011). In the passive coating approaches the surface is spread with one or more molecules able to reduce bacterial adhesion by altering the properties of the substrate so that conditioning films do not form and/or bacteria-substrate interactions are not favorable (Garcia-Fernandez et al., 2009). In an early research, glass slides coated with zosteric acid were proved to reduce the attachment of *Acinetobacter sp*. on the slide compared to the control surface (Todd *et al.*, 1993). In other field study, ceramic tiles were coated with crude zosteric acid and then placed into a marine environment; treated slides were proved to accumulate significantly fewer bacteria than controls for 48 h (Zimmerman *et al.*, 1995). Unfortunately, the effectiveness of passive coatings for reducing bacterial adhesion is limited in the time and varies greatly depending on bacterial species. Moreover the anti-biofilm properties of the coating surface can be masked by an adsorbed conditioning film, thereby diminishing the effectiveness (Hetrick *et al.*, 2006). In the active approaches the anti-biofilm molecule is superficially bound to the surface of a polymeric material or incorporated into the interior of the polymer the polymeric material, directly or by means of a carrier, and actively eluted from the surface by the contact with an aqueous environment (Garcia-Fernandez et al., 2009). The anti-biofilm activity is the result of the free-floating molecules that interact with bacteria in the surface surrounding area (Barrios *et al.*, 2005; Hetrick *et al.*, 2006). A lot of efforts to incorporate natural compounds with anti-biofilm activity in different polymers are reported in the literature. Geiger and coauthors (2004) produced a new anti-biofilm biocompatible polyester material coated with zosteric acid encapsulated in polystyrene microcapsules. Barrios and coauthors (2005) and Newby and colleagues (2006) incorporated zosteric acid into silicone coatings developing different strategies to achieve its slow release in the surrounding area**.** Release of salicylic acid from materials to inhibit biofilm formation has also been reported. Bryers and collaborators (2006) and Rosenberg and colleagues (2008) proposed a salicylic acid-releasing poly(anhydride-ester) polymers able to inhibit respectively *P. aeruginosa* and *Salmonella enterica* biofilms while Nowatsky and coauthors (2012) developed a new material by coating an urethane acrylate resin with salicylic acid. A recently studied salicylic-acid eluting coating involves ultraviolet-cured polyurethane acrylate polymer containing salicyl acrylate. Under aqueous environments, the polymer hydrolyzes and releases salicylic acid, leaving the backbone intact. The rate of salicylic acid release is dependent upon the composition of the polymer, and the release of such acid was shown to inhibit biofilm formation of *S. epidermidis*, *Bacillus subtilis*, *E. coli*, *P. aeruginosa*, as well as *S. aureus* (Lo et al., 2014). Similarly glass coverslips coated with poly(anhydride) ester with salicylic acid bound to the polymer backbone were used to study the release of salicylic acid during polymer degradation and its effect against *Salmonella typhimurium*. Continuous release of salicylic acid from coverslips resulted in a prevention of biofilm formation (Guinta et al., 2011). However also this strategy suffers from recurrent problems and limitations. The prerequisite for a good performance is the continuous and constant elution of the anti-biofilm molecules from the surface, with a sufficient release rates to deter bacterial attachment and slow enough to ensure the long service life of the coating (Barrios et al., 2005). Unluckily, the amount of the substance released is influenced by several factor, i.e. the processing parameters, the loading

dose, the applied technique, the molecular size of the molecule and the physic-chemical properties of the polymeric material that makes arduous a strict monitoring of the anti-biofilm rate from the surface. In most of cases these materials exhibit discontinuous release rate according to first-order kinetics with an initially high release and afterwards exponential decrease of the released. In addition, a too much high molecule concentration is reached close the surface, mostly reaching a concentration lethal for microorganisms (von Eiff et al., 2005). Indeed these questions limit the coatings effectiveness to only a short period of time, making this system often unfeasible for a wide range of practical applications such as medical materials and devices.

The problem about the release rates in aqueous medium is likely attributable to the fact that most polymeric matrices and anti-biofilm compounds have incompatible physical characteristics. Most of the coating matrices are hydrophobic polymers, while some anti-biofilm compounds are hydrophilic, making their miscibility with the coating matrices difficult. The result is a non-uniform distribution of the molecules inside the material that increases the tendency of the surfaces to absorb and diffuse water through the polymer matrix allowing the anti-biofilm molecules to diffuse out (Barrios et al., 2005; Newby *et al.*, 2006; Nowatzki et al., 2012). Barrios and coauthors (2005) investigated various techniques of incorporating zosteric acid into a model silicone coating to determine how the leaching can be controlled when zosteric acid is entrapped inside a coating. The authors proved that as the distribution of zosteric acid became more uniform, the leach rates reduced extending the working time of the coating. To slow the leaching of zosteric acid, more homogenous distribution of smaller zosteric acid aggregates or even individual zosteric acid molecules within the silicone coating would be desired. On the contrary large aggregates created large pathways in the thickness of the coating allowing the water to enter and dissolve them. As a results the solubilized anti-biofilm molecules quickly leaves the coating through these pathways making it inefficient. The only use of mixtures of pyridine/water and acetone/water as entrapment solvents produced homogeneous coatings with good anti-biofilm properties compared to pure silicone. Beside these efforts, no constant rate was reached since substantial high rate occurred during a first stage, and then the rate gradually leveled off, and approached an almost constant value only in the second stage. A further problem is that the release of the anti-biofilm compounds could affects the polymers integrity. In the research of Bryers and collaborators (2006) salicylic acid was released from the surface by hydrolysis of the main chain bonds of the polymer. As a consequence, materials made from these polymers lost mechanical strength and structural integrity as they degraded, a property suitable for some applications but not for others (Novatzky et al., 2012).

With this perspective it is become imperative to develop new technologies with both long anti-biofilm working life and without the problem of constant release. The covalent bind of these natural molecules to the surfaces could easily side-step the problem of constant release, guaranteeing the long life of the material since molecules are permanently attached and integrated in the scaffold structure of the polymers. However this kind of approach requires a deep knowledge of the exact structural elements required by the molecules for exerting their anti-biofilm activity since this approach supposes to identify a binding site in the molecule structure necessary for its immobilization on the surface without destroying the biological activity. However in most of the cases, this information is not available and only few studies about structure-anti-biofilm activity-relationships are reported in literature.

References

Abd El-Aziz A.A., El-Banna T., Sonbol F.I., Abo-Kamar A., Seif-Eldin D.W. (2012). Evaluation of the combination of N-acetylcysteine and or sodium salicylate with ciprofloxacin on bacterial adhesion and biofilm formation on urinary catheters. *The International Arabic Journal of Antimicrobial Agents*, 2:1-4.

Agrios G.N. (2012). Plant Pathology. Elsevier Academic Press Publication, San Diego.

Anderl J.N., Franklin M.J., Stewart P.S. (2000). Role of antibiotic penetration limitation in *Klebsiella pneumoniae* biofilm resistance to ampicillin and ciprofloxacin. *Antimicrobial Agents and Chemotherapy*, 44: 1818-24.

Anderl J.N., Zahller J., Roe F., Stewart P.S. (2003). Role of nutrient limitation and stationary-phase existence in *klebsiella pneumoniae* boifilm resistance to ampicillin and ciprofloxacin. *Antimicrobial Agents and Chemotherapy*, 47: 1251-1256.

Ashraf M., Naqvi M.H., Iqbal M.M. (2001). Microbial biofilms for environmental waste management: an overview. *The Nucleus*, 38: 131-135.ASTM E2196-12 (2012). Standard test method for quantification of *Pseudomonas aeruginosa* biofilm grown with medium shear and continuous flow using rotating disk reactor, ASTM International, West Conshohocken, PA, USA. http://www.astm.org/Stardards/E2196.htm.

Bandara M.B.K., Zhu H., Sankaridurg P.R., Willcox M.D.P. (2006). Salicylic acid reduces the production of several potential virulence factors of *Pseudomonas aeruginosa* associated with microbial keratitis. *Investigative Ophthalmology and Visual Science*, 47: 4453-4460.

Barrios C.A., Xu Q., Cutright T., Newby B.Z. (2005). Incorporating zosteric acid into silicone coatings to achieve its slow release while reducing fresh water bacterial attachment. *Colloids and Surface B: Biointerface*, 41:83-93.

Beumer R.R., Te Giffel M.C., Spoorenberg E., Rombouts F.M. (1996). *Listeria* species in domestic environments. *Epidemiology and Infection*, 117: 437-442.

Blazquez J. (2003). Hypermutation as a factor contributing to the acquisition of antimicrobial resistance. *Clinical Infectious Diseases*, 37:1201-1209.

Bryers J.D., Jarvis R.A., Lebo J., Prudencio A., Kyriakides T.R., Uhrich K. (2006). Biodegradation of poly(anhydride-esters) into non-steroidal anti-inflammatory drugs and their effect on *Pseudomonas aeruginosa* biofilms in vitro and on the foreign-body response in vivo. *Biomaterials*, 27:5039-48.

Calabrese E.J., Baldwin L.A. (2002). Defining hormesis. *Human & Experimental Toxicology*, 21:91-97.

Cappitelli F., Villa F., Sorlini C. (2011). New environmentally friendly approaches against biodeterioration of outdoor cultural heritage in biocolonization of stone: Control and Preventive Methods. In Charola A.E., McNamara C., Koestler R.J. (eds), Proceedings from the MCI Workshop Series, Smithsonian Institution Scholarly Press (SISP), Washington, pp 51-58.

Cappitelli F., Polo A., Villa F. (2014). Biofilm formation in food processing environments is still poorly understood and controlled. *Food Engineering Reviews*, 6: 29-42.

Cegelski L., Marshall G.R., Eldridge G.R., Hultgren S.J. (2008). The biology and future prospects of antivirulence therapies. *Nature Reviews Microbiology*, 6: 17-27.

Chow S., Gu K., Jiang L., Nassour A. (2011). Salicylic acid affects swimming, twitching and swarming motility in *Pseudomonas aeruginosa*, resulting in decreased biofilm formation. *Journal of Experimental Microbiology and Immunology*, 15:22-29.

Coenye T., De Prijck K., Nailis K., Nelis H.J. (2011). Prevention of *Candida albicans* biofilm formation. *The Open Mycology Journal*, 5:9-20.

Costerton J.W., Cheng K.-J., Geesey G.G., Ladd T.I., Nickel J.C., Dasgupta M., Marrie T.J. (1987). Bacterial biofilms in nature and disease. *Annual Review of Microbiology*, 41: 435-464.

Costerton J.W. (1997). Introduction to biofilm. *International Journal of Antimicrobial Agents*, 11: 217-221.

Council Recommendation (2001). Prudent use of antimicrobial agents in human medicine (2002/77/EC). http://antibiotic.ecdc.europa.eu/PDFs/l_03420020205en00130016.pdf

Crispim C.A., Gaylarde P.M., Gaylarde C.C. (2003). Algal and cyanobacterial biofilms on calcareous historic buildings. *Current Microbiology*, 46:79-82.

Daghrir R., Drogui P. (2013). Tetracycline antibiotics in the environment: a review. *Environmental Chemistry Letters*, 11:209-227.

Da M.L., Heroux A.K., Pakzad Z., Schiffmacher K. (2010). Salicylic acid attenuates biofilm formation but not swarming in *Pseudomonas aeruginosa*. *Journal of Experimental Microbiology and Immunology*, 14:69-73.

Damman C.J. (2013). Salicylates and the microbiota: a new mechanistic understanding of an ancient drug's role in dermatological and gastrointestinal disease. *Drug Development Research*, 74:344-352.

Darouiche R.O. (2007). Antimicrobial coating of devices for prevention of infection: principles and protection. *The International Journal of Artificial Organs*, 30: 820-827.

Davey M.E., O'Toole G.A. (2000). Microbial biofilms: from ecology to molecular genetics. *Microbiology and Molecular Biology Reviews*, 64: 847-867.

Davies D. (2003). Understanding biofilm resistance to antibacterial agents. *Nature Reviews Drug Discovery*, 2: 114-122.

Directive 98/8/EC of the European Parliament and of the Council of 16 February 1998 concerning the placing of biocidal products on the market. http://eurlex.europa.eu/LexUriServ/site/en/ consleg/1998/L/ 01998L000820070119-en.pdf.

Dong Y., Huang C., Park J., Wang G. (2012). Growth inhibitory levels of salicylic acid decrease *Pseudomonas aeruginosa fliC* flagellin gene expression. *Journal of Experimental Microbiology and Immunology*, 16: 73-78.

Dowd S.E., Sun Y., Smith E., Kennedy J.P., Jones C.E., Wolcott R. (2009). Effects of biofilm treatments on the multi-species Lubbock chronic wound biofilm model. *Journal of Wound Care*, 18: 508-512.

Dunne M.W. Jr. (2002). Bacterial adhesion: seen any good biofilms lately? *Clinical Microbiology Review*, 15: 155-166.

El-Banna T., Sonbol F.I., Abd El-Aziz A.A., Abo-Kamar A., Seif-Eldin D.W. (2012). Effect of the combination of salicylate with aminoglycosides on bacterial adhesion to urinary catheters. *International Research Journal of Pharmaceuticals*, 2:39-45.

Empa (2013). Standardized biofilms for assessing biofilm removal efficiency. Technological report TT-Ref. 2007-074. http://www.switt.ch/adminall2/userfiles/technologien/463_empa_technology_offer_biofilms_for_ assessing _biofilms_removal.pdf.

European Food Safety Authority and European Centre for Disease Prevention and Control (2012). The European Union summary report on antimicrobial resistance in zoonotic and indicator bacteria from humans, animals and food in 2010. EFSA J 10:2598 [233 pp]. www.efsa.europa.eu/efsajournal.

Farber B.F., Wolff A.G. (1993). Salicylic acid prevents the adherence of bacteria and yeast to silastic catheters. *Journal of Biomedical Materials Research*, 27:599-602.

Farber B.F., Hsieh H-C., Donnenfeld E.D., Perry H.D., Epstein A., Wolff A.G. (1995). A Novel antibiofilm technology for contact lens solutions. *Ophthalmology*, 102: 831-836.

Farkas A., Dragan-Bularda M., Muntean V., Ciataras D., Tigan S. (2013). Microbial activity in drinking water-associated biofilms. *Central European Journal of Biology*, 8: 201-214.

Flemming H.C., Percival S.I., Walker J.T. (2002). Contamination potential of biofilms in water distribution systems. *Water Science and Technology*, 2: 271-280.

Flemming H-C. (2005). Alternative and conventional antifouling strategies. *International Biodeterioration and Biodegradation*, 56: 121-134.

Flemming H-C. (2008). Why microorganisms live in biofilms and the problem of biofouling. In Flemming H-C., Murthy P.S., Venkatesan R., Cooksey K. eds., Marine and Industrial Biofouling. Springer, Berlin Heidelberg. pp. 3-12.

Flemming H-C., Wingender J. (2010). The biofilm matrix. *Nature Reviews Microbiology*, 8: 623-633.

Francolini I., Donelli G. (2010). Prevention and control of biofilm-based medical-device-related infections. *FEMS Immunology and Medical Microbiology*, 59: 227-238.

Fux C.A., Costerton J.W., Stewart P.S., Stoodley P. (2005). Survival strategies of infectious biofilms. *Trends in Microbiology*, 13: 34-40.

García-Fernández L., Cui J., Serrano C., Shafiq Z., Gropeanu R.A., San Miguel V., Ramos J.I., Wang M., Auernhammer G.K., Ritz S., Golriz A.A., Berger R., Wagner M., del Campo A. (2013). Antibacterial strategies from the sea: polymer-bound cl-catechols for prevention of biofilm formation. *Advanced Materials*, 25: 529-533.

Geiger T., Delavy P., Hany R., Schleuniger J., Zinn M. (2004). Encapsulated zosteric acid embedded in poly[3-hydroxyalkanoate] coatings—Protection against biofouling. *Polymer Bulletin*, 52:65-72.

Guinta R.A., Carbone L.A., Rosenberg E.L., Uhrich E.K., Tabak M., Chikindas L.M. (2011). Slow release of salicylic acid from degrading poly(anhydride ester) polymer disrupts bimodal pH and prevents biofilm formation in *Salmonella typhimurium* MAE52. In Bailey W.C. (ed), Biofilms: Formation, Development and Properties, Nova Science Publishers, New York, pp. 649-658

Hall-Stoodley L., Costerton W.J., Stoodley P. (2004). Bacterial biofilms: from the natural environment to infectious diseases. *Nature Review Microbiology*, 2: 95-108.

Hara M., Furukawa J., Sato A., Mizoguchi T., Miura K. (2012). Abiotic stress and role of salicylic acid in plants. In Ahmad P., Prasad M.N.V. (eds), Abiotic stress responses in plants: metabolism, productivity and sustainability, Springer, New York, pp 235-251.

Harder T. (2008). Marine epibiosis: concepts, ecological consequences and host defence. In Flemming H-C., Murthy S.P., Venkatesan R., Cooksey K., Marine and industrial biofouling, Springer, Heidelberg New York, pp 219-232.

Harrison J.J., Ceri H., Turner R.J. (2007). Multimetal resistance and tolerance in microbial biofilms. *Nature reviews microbiology*, 5: 928-938.

Hausner M., Wuertz S. (1999). High rates of conjugation in bacterial biofilms as determined by quantitative in situ analysis. *Applied and Environmental Microbiology*, 65: 3710-3713.

Hetrick E.M., Schoenfisch M.H. (2006). Reducing implant-related infections: active release strategies. *Chemical Society Reviews*, 35:780-789.

Hurdle J.G., O'Neill A.J., Chopra I., Lee R.E. (2011). Targeting bacterial membrane function: an underexploited mechanism for treating persistent infections. *Nature Reviews Microbiology,* 9**:** 62-75.

Issac Abraham S.V., Palani A., Khadar Syed M., Shunmugiah K.P., Arumugam V.R. (2012). Antibiofilm and quorum sensing inhibitory potential of *Cuminum cyminum* and its secondary metabolite methyl eugenol against Gram negative bacterial pathogens. *Food Research International*, 45: 85-92.

Johnson J.R., Kuskowski M.A., Wilt T.J. (2006). Systematic review: antimicrobial urinary catheters to prevent catheter-associated urinary tract infection in hospitalized patients. *Annals of Internal Medicine*, 144: 116-126.

Junker L.M., Clardy J. (2007). High-throughput screens for small-molecule inhibitors of *Pseudomonas aeruginosa* biofilm development. *Antimicrobial Agents and Chemotherapy*, 51: 3582–3590.

Karatan E., Watnick P. (2009). Signals, regulatory networks, and materials that build and break bacterial biofilms. *Microbiology and Molecular Biology Reviews*, 73: 310-347.

Khan M.S.A., Ahmad I., Sajid M., Cameotra S.S. (2014). Current and emergent control strategies for medical biofilm. In Rumbaugh K.P., Ahmad A. (eds), Antibiofilm agents: from diagnosis to treatment and prevention, Springer, Heidelberg, pp. 117-160.

Khoshkdaman M., Ebadi A.A., Kahrizi D. (2012). Evaluation of pathogencity and race classification of *Xanthomonas oryzae pv. oryzae* in Guilan province-Iran. *Agricultural Sciences*, 3: 557-561.

Lagonenko L., Lagonenko A., Evtushenkov A. (2013). Impact of salicylic acid on biofilm formation by plant pathogenic bacteria. *Journal of Biology and Earth Science*, 3: B176-B181.

Lo J., Lange D., Chew B.H. (2014). Ureteral stents and Foley catheters-associated urinary tract infections: the role of coatings and materials in infection prevention. *Antibiotics*, 3: 87-97.

Mah T.F., Pitts B., Pellock B., Walker G.C., Stewart P.S., O'Toole G.A. (2003). A genetic basis for *Pseudomonas aeruginosa* biofilm antibiotic resistance. *Nature*, 426: 306-310.

Muller E., Al-Attar J., Wolff A.G., Farber B.F. (1998). Mechanism of salicylate-mediated inhibition of biofilm in *Staphylococcus epidermidis*. *The Journal of Infectious Diseases*, 177:501-503.

Navarro G., Cheng A.T., Peach K.C., Bray W.M., Bernan V.S., Yildiz F.H., Liningtona R.G. (2014). Image-based 384-well high-throughput screening method for the discovery of skyllamycins a to c as biofilm inhibitors and inducers of biofilm detachment in *Pseudomonas aeruginosa*. *Antimicrobial agents and Chemotherapy*, 58: 1092-1099.

Newby B.Z., Cutright T., Barrios C.A., Xu Q. (2006). Zosteric acid—An effective antifoulant for reducing fresh water bacterial attachment on coatings. *The University of Akron*, 3: 69-77.

Nichols W.W., Dorrington S.M., Slack M.P.E., Walmsley H.L. (1988). Inhibition of tobramycin diffusion by binding to alginate. *Antimicrobial Agents and Chemotherapy*, 32: 518-523.

Nowatzki P.J., Koepsel R.R., Stoodley P., Min K., Harper A., Murata H., Donfack J., Hortelano E.R., Ehrlich G.D., Russell A.J. (2012). Salicylic acid-releasing polyurethane acrylate polymers as anti-biofilm urological catheter coatings. *Acta Biomaterialia*, 8: 1869-1880.

Oerke E-C. (2006). Crop losses to pests. *Journal of Agricultural Science*, 144: 31-43.

Oliver A., Canton R., Campo P., Baquero F., Blazquez J. (2000). High frequency of hypermutable *Pseudomonas aeruginosa* in cystic fibrosis lung infection. *Science*, 288: 1251-1253.

Pace J.L., Rupp M.E., Finch R.G. (2006). Biofilms, Infection, and Antimicrobial Therapy. Taylor & Francis Group, Boca Raton.

Panmanee W., Taylor D., Shea C.J.A., Tang H., Nelson S., Seibel W., Papoian R., Kramer R., Hassett D.J.,

Lamkin T.J. (2013). High-throughput screening for small molecule inhibitors of *Staphylococcus epidermidis* RP62a biofilms. *Journal of Biomolecular Screening*, 18: 820-829.

Patel I., Patel V., Thakkar A., Kothari V. (2013). Microbial biofilms: microbes in social mode. *International Journal of Biotechnology Research and Practice*, 1: 19-34.

Plyuta V.A., Lipasovaa V.A., Kuznetsovb A.E., Khmela I.A. (2013). Effect of salicylic, indole-3-acetic, gibberellic, and abscisic acids on biofilm formation by *Agrobacterium tumefaciens* C58 and *Pseudomonas aeruginosa* PAO1. *Applied Biochemistry and Microbiology*, 49: 706-710.

Polo A., Foladori P., Ponti B., Bettinetti R., Gambino M., Villa F., Cappitelli F. (2014). Evaluation of zosteric acid for mitigating biofilm formation of *Pseudomonas putida* isolated from a membrane bioreactor system *International Journal of Molecular Sciences*, 15: 9497-9518.

Polonio R.E, Mermel L.A., Paquette G.E., Sperry J.F. (2001). Eradication of biofilm-forming *Staphylococcus epidermidis* (RP62A) by a combination of sodium salicylate and vancomycin. *Antimicrobial Agents and Chemotherapy*, 45: 3262-3266.

Pratt L.A., Kolter R. (1998). Genetic analysis of *Escherichia coli* biofilm formation: roles of flagella, motility, chemotaxis and type I pili. *Molecular Microbiology*, 30: 285-293.

Prithiviraj B., Bais H.P., Weir T., Suresh B., Najarro E.H., Dayakar B.V., Schweizer H.P., Vivanco J.M. (2005). Down regulation of virulence factors of *Pseudomonas aeruginosa* by salicylic acid attenuates its virulence on *Arabidopsis thaliana* and *Caenorhabditis elegans*. *Infection and Immunity*, 73: 5319–5328.

Quave C.L., Estévez-Carmona M., Compadre C.M., Hobby G., Hendrickson H., Beenken K.E., Smeltzer M.S. (2012). Ellagic acid derivatives from *Rubus ulmifolius* inhibit *Staphylococcus aureus* biofilm formation and improve response to antibiotics. *PLoS ONE*, 7:e28737.

Raloff J. (1996). Sponges and sinks and rags, oh my! Where microbes lurk and how to rout them. *Science News*, 150: 172–174.

Rasko D.A., Sperandio V. (2010). Anti-virulence strategies to combat bacteria-mediated disease. *Nature Reviews Drug Discovery*, 9:117-128.

Rasmussen L., White E.L., Pathak A., Ayala J.C., Wang H., Wu J-H., Benitez J.A., Silva A.J. (2011). A high-throughput screening assay for inhibitors of bacterial motility identifies a novel inhibitor of the Na^+-driven flagellar motor and virulence gene expression in *Vibrio cholera*. *Antimicrobial Agents and Chemotherapy*, 55: 4134-4143.

Rayner J., Veeh R., Flood J. (2004). Prevalence of microbial biofilms on selected fresh produce and household surfaces. *International Journal of Food Microbiology*, 95: 29–39.

Ren D., Zuo R., González Barrios A.F., Bedzyk L.A., Eldridge G.R., Pasmore M.E., Wood T.K. (2005). Differential gene expression for investigation of *Escherichia coli* biofilm inhibition by plant extract ursolic acid. *Applied Environmental Microbiology*, 71: 4022-4034.

Rosenberg L.E., Carbone A.L., Römling U., Uhrich K.E., Chikindas M.L. (2008). Salicylic acid-based poly(anhydride esters) for control of biofilm formation in *Salmonella enterica* serovar Typhimurium. *Letters in Applied Microbiology*, 46: 593-599.

Sambanthamoorthy K., Gokhale A.A., Lao W., Parashar V., Neiditch M.B., Semmelhack M.F., Lee I., Waters C.M. (2011). Identification of a novel benzimidazole that inhibits bacterial biofilm formation in a broad-spectrum manner. *Antimicrobial Agents and Chemotherapy*, 55: 4369–4378.

SCENIHR (2009). The scientific committee on emerging and newly identified health risks report. http://ec.europa.eu/health/opinions/en/biocides-antibiotic-resistance/l-3/8-risk-assessment.htm.

Schachter B. (2003). Slimy business-the biotechnology of biofilms. *Nature Biotechnology*, 21: 361-365.

Schultz M.P., Bendick J.A., Holm E.R., Hertel W.M. (2014). Economic impact of biofouling on a naval surface ship. *Biofouling*, 27: 87–98.

Smith D.R., Chapman M.R. (2010). Economical evolution: microbes reduce the synthetic cost of extracellular proteins. *mBio*, 1: e00131-10.

Sousa A.C.A., Pastorinho M.R., Takahashi S., Tanabe S. (2014). History on organotin compounds, from snails to humans. *Environmental Chemistry Letters*, 12: 117-137.

Southey-Pillig C.J., Davies D.G., Sauer K. (2005). Characterization of temporal protein production in *Pseudomonas aeruginosa* biofilms. *Journal of Bacteriology*, 187: 8114–8126.

Stanley M.S., Callow M.E., Perry R., Alberte R.S., Smith R., Callow J.A. (2002). Inhibition of fungal spore adhesion by zosteric acid as the basis for a novel, non-toxic crop protection technology. *Phytopathology*, 92: 378-383.

Stewart P.S., Roe F., Rayner J., Elkins J.G., Lewandowski Z., Ochsner U.A., Hassett D.J. (2000). Effect of catalase on hydrogen peroxide penetration into *Pseudomonas aeruginosa* biofilms. *Applied and Environmental Microbiology*, 66: 836-838.

Stewart P.S., Costerton J.W. (2001). Antibiotic resistance of bacteria in biofilms. *Lancet*, 358: 135-138.

Stewart P.S., Franklin M.J. (2008). Physiological heterogeneity in biofilms. Nature Review, 6: 199-210.

Stoodley P., Sauer K., Davies D.G., Costerton J.W. (2002). Biofilms as complex differentiated communities. *Annual Review of Microbiology*, 56: 187-209.

Stowe S.D., Richards J.J., Tucker A.T., Thompson R., Melander C., Cavanagh J. (2011). Anti-biofilm compounds derived from marine sponges. *Marine Drug*, 9: 2010-2035.

Teichberg S., Farber B.F., Wolff A.G., and Roberts B. (1993). Salicylic acid decreases extracellular biofilm production by *Staphylococcus epidermidis*: electron microscopic analysis. *The Journal of Infectious Diseases*, 167: 1501-1503.

Todd J.T., Zimmerman R.C., Crews P., Alberte R.S. (1993). Isolation of p-sulfoxy cinnamic acid from *Zostera marina* L. (eelgrass) and the antifouling activity of phenolic acid sulfate esters. *Phytochemistry,* 34: 401-404.

Van Bambeke F., Glupczynski Y., Plésiat P., Pechère J.C., Tulkens P.M. (2003). Antibiotic efflux pumps in prokaryotic cells: occurrence, impact on resistance and strategies for the future of antimicrobial therapy. *Journal of Antimicrobial Chemotherapy*, 51: 1055-1065.

Van Houdt R., Michiels C.W. (2010). Biofilm formation and the food industry, a focus on the bacterial outer surface. *Journal of Applied Microbiology*, 109: 1117-1131.

Vikram A., Jayaprakasha G.K., Jesudhasan P.R., Pillai S.D., Patil B.S. (2010). Suppression of bacterial cell-cell signalling, biofilm formation and type III secretion system by citrus flavonoids. *Journal of Applied Microbiology*, 109: 515-527.

Villa F., Giacomucci L., Polo A., Principi P., Toniolo L., Levi M., Turri S., Cappitelli F. (2009). N-vanillylnonanamide tested as a non-toxic antifoulant, applied to surfaces in a polyurethane coating. *Biotechnology Letters*, 31: 1407-1413.

Villa F., Albanese D., Giussani B., Stewartd P. S., Daffonchio D., Cappitelli F. (2010). Hindering biofilm formation with zosteric acid. *Biofouling*, 26: 739-752.

Villa F., Pitts B., Stewart P.S., Giussani B., Roncoroni S., Albanese D., Giordano C., Tunesi M., Cappitelli F. (2011). Efficacy of zosteric acid sodium salt on the yeast biofilm model *Candida albicans*. *Microbial Ecology*, 62: 584-598.

Villa F., Borgonovo G., Cappitelli F., Giussani B., Bassoli A. (2012). Sub-lethal concentrations of *Muscari comosum* bulb extract suppress adhesion and induce detachment of sessile yeast cells. *Biofouling*, 28:1107-1117.

Villa F., Remelli W., Forlani F., Vitali A., Cappitelli F. (2012). Altered expression level of *Escherichia coli* proteins in response to treatment with the antifouling agent zosteric acid sodium salt. *Environmental Microbiology*, 14: 1753-1761.

Villa F., Cappitelli F. (2013). Plant-derived bioactive compounds at sub-lethal concentrations: towards smart biocide-free antibiofilm strategies. *Phytochemistry Reviews*, 12: 245-254.

Von Eiff C., Kohnen W., Becker K., Jansen B. (2005). Modern strategies in the prevention of implant-associated infections. *The International Journal of Artificial Organs*, 28: 1146-1156.

Wenderska I.B., Chong M., McNulty J., Wright G.D., Burrows L.L. (2011). Palmitoyl-DL-carnitine is a multitarget Iinhibitor of *Pseudomonas aeruginosa* biofilm development. *ChemBioChem*, 12: 2759-2766.

Wong C.C., Cheng K.W., He Q., Chen F. (2008). Unraveling the molecular targets of natural products: insights from genomic and proteomic analyses. *Proteomics Clinical Application*, 2: 338-354.

Wood T.K., Knabel S.J., Kwana B.W. (2013). Bacterial persister cell formation and dormancy. *Applied and Environmental Microbiology*, 79: 7116-7121.

Worthington R.J., Richards J.J., Melander C. (2012). Small molecule control of bacterial biofilms. *Organic and Biomolecular Chemistry*, 10: 7457-7474.

Wright G.D., Sutherland A.D. (2007). New strategies for combating multidrug-resistant bacteria. *TRENDS in Molecular Medicine*, 13: 260-267.

Wu H., Song Z., Hentzer M., Andersen J.B., Molin S., Givskov M., Høiby N. (2004). Synthetic furanones inhibit quorum-sensing and enhance bacterial clearance in *Pseudomonas aeruginosa* lung infection in mice. *Journal of Antimicrobial Chemotherapy*, 53: 1054-1061.

Xu Q., Barrios C.A., Cutright T., Newby B.Z. (2005a). Assessment of antifouling effectiveness of two natural product antifoulants by attachment study with freshwater bacteria. *Environmental Science and Pollutant Research*, 12: 278-284.

Xu Q., Barrios C.A., Cutright T., Newby B.Z. (2005b). Evaluation of toxicity of capsaicin and zosteric acid and their potential application as antifoulants. *Environmental Toxicology*, 20: 467-474.

Yang L., Rybtke M.T., Jakobsen T.H., Hentzer M., Bjarnsholt T., Givskov M., Tim Tolker-Nielsen (2009). Computer-aided identification of recognized drugs as *Pseudomonas aeruginosa* quorum-sensing inhibitors. *Antimicrobial Agents and Chemotherapy*, 53: 2432-2443**.**

Young M.E., Alakomi H-L., Gorbushina A.A., Krumbein W.E., Maxwell I., McCullagh C., Robertson P., Saarela M., Valero J., Vendrell M. (2008). Development of a biocidal treatment regime to inhibit biological growths on cultural heritage: BIODAM. *Environmental Geology*, 56: 631-641.

Zeng Z., Qian L., Cao L., Tan H., Huang Y., Xue X., Shen Y., Zhou S. (2008). Virtual screening for novel quorum sensing inhibitors to eradicate biofilm formation of *Pseudomonas aeruginosa**. Applied Microbiology and Biotechnology*, 79: 119-126.

Zimmerman R.C, Alberte R.S., Todd J.S. (1995). Phenolic acid sulfate esters for prevention of marine biofouling. United States Patent US005384176A.

Aim of the research

It is proved that microorganisms in form of biofilm communities are able to colonize every surface that offer minimal condition for life. All human artefact surfaces like industrial installations, work benches, harbor systems and also medical devices are susceptible to biofilm colonization with devastating consequences in term of social and economic impact. Unfortunately, the traditional approaches including biocides and antibiotics are not consistently and universally effective against deleterious biofilms since adopting the sessile mode of life, microorganisms improve their resistance to antimicrobial agents up to several orders of magnitude. In addition, increasingly restrictive regulations limiting the use of substances hazardous to human health and the environment have resulted in several biocides being banned. In this contest the development of new improved effective solutions able to replace the presently dominating drug/device products is becoming imperative.
The new technology would be able to interfere with the key-steps that orchestrate surface-pathogen interactions in order to hamper infection cascade. Depriving microorganisms of their ability to develop biofilm without affecting their existence may decrease selection pressure for drug-resistant mutations, restoring the efficacy of traditional antimicrobial agents. The ideal approach would create permanently non-leaching, long-lasting bio-hybrid materials by covalent functionalization of polymeric materials with bio-inspired non-toxic and biocide-free anti-biofilm compounds with novel targets, unique modes of action and properties that are different from those of the currently used antimicrobials. The natural compounds zosteric acid (*p*-(sulfoxy) cinnamic acid) and salicylic acid were previously proved to be powerful anti-biofilm agents able to successfully reduce bacterial and fungal biofilm at concentrations that not affect microorganism viability.

The aim of the PhD project is to develop new effective biocide-free materials able to resist to biofilm over a working timescale. In this project zosteric acid and salicylic acid are selected as suitable anti-biofilm compounds for new preventive or integrative approaches against bacterial and fungal biofilm formation. Specifically **the aim of the project is to develop new anti-biofilm materials by covalently anchoring zosteric acid and salicylic acid to commercial polymeric materials in a procedure that allow the anti-biofilm compounds to preserve the biological function upon the conjugation process and over a working timescale.** This research is addressed in providing a new improved solution able to reduce the incidence of biofilm formation with a mode of action distinct to the traditional antimicrobial strategies. In this approach, no molecules are leached from the surface, sidestepping the problem of the compound release kinetics and providing long term protection against bacterial colonization since the molecule is permanently attached to the surface. In addition the risk of developing resistant microbial strains is reduced, as the concentration of the anti-biofilm agent is constantly below the lethal concentration. The proved low toxicity of both zosteric acid and salicylic acid has the potential to spread this technology to different sectors resulting in new safe and eco-friendly types of products available for a wide range of applications included medical devices and food packaging. The understanding of the precise mode of action of these anti-biofilm compounds will also bring toward the design of more efficient and manufacturable technologies.

In detail the research will be structured as follows.
PART A: Determination of zosteric acid and salicylic acid chemical structure determinants of their anti-biofilm activity and identification of their molecular target.

- The chemical structural elements of zosteric acid and salicylic acid required for their anti-biofilm activity will be investigated. A small library of molecules related to the scaffold of zosteric acid and salicylic acid will be synthesized and their anti-biofilm activity against the

bacterium model *Escherichia coli* will be verified through a quantitative biofilm assay. The ability of each compound to be a carbon and energy source and to affect planktonic growth will be also evaluated. Obtained data will be used to identify possible modifications in zosteric acid and salicylic acid structure necessary for their binding with the reactive positions on the polymers without attempting their anti-biofilm activity.

- Molecular targets and pathways involved in zosteric acid and salicylic acid anti-biofilm activity will be investigated by proteomic approaches. A small-scale affinity purification of proteins from *E. coli* extracts on immobilized zosteric acid and salicylic acid moieties will be performed. *E. coli* proteins bound to a functionalized matrix will be eluted by competition, analyzed by SDS-PAGE and identified by mass spectrometry techniques.

PART B: Functionalization of surfaces with zosteric acid and salicylic acid and investigation of their anti-biofilm performance.

- In collaboration with chemists, methods to efficiently functionalize a polyethylene surface with zosteric acid and salicylic acid will be developed. Physical and chemical treatments will be performed to activate the polymeric surface making it suitable for the covalent attachment of zosteric acid and salicylic acid. Surface functionalization and the anti-biofilm compounds stability and retention will be verified on both new and used material.
- The anti-biofilm efficacy of the innovative materials will be investigated against *E. coli* biofilm using CDC reactor to simulate flow conditions normally encountered in vivo. The number of adhered cells on both traditional and functionalized polyethylene surface will be established by plate count assays. Biofilm grown on both treated and control material will be also submitted to microscopic analysis. The ability of biofunctionalized materials to enhance the susceptibility of established biofilms to traditional antimicrobial agents will be also evaluated. To test this, a mature biofilm grown in the cell flow chamber with and without the bio-hybrid material, will be stained with a fluorogenic probe and exposed to commercially available antimicrobial agents. The effect of biocide exposure will be visualized in vivo measuring fluorescence lost by direct time-lapse confocal laser scanning microscopy and quantifying the antimicrobial attack through image analysis. In addition simple plate count method will be performed after the antimicrobial treatment.

A scaffold-based library survey shows the structural features responsible of the anti-biofilm activity of zosteric acid against *Escherichia coli*

Abstract

The natural compound zosteric acid or *p*-(sulfooxy)cinnamic acid (ZA) has been proposed as a preventive or integrative approach against biofilm formation. Advantages would be conferred by covalently coupling the molecule to the surface of a material in a way to deliver the active moiety to the cellular target. The development of this preventive strategy is limited by the lack of information about the structural chemical determinants required for ZA anti-biofilm activity. In this study 43-member library of small molecules based on ZA scaffold diversity was designed and screened against *Escherichia coli* to understand the structural reason for biofilm inhibition at sub-lethal concentration and identify functional groups that could be exploited for the covalent linkage to an abiotic surface. Structure-activity relationship considerations revealed that the carboxylic acid moiety conjugated to the double bond in *trans* configuration was an essential requirement in ZA chemical structure to guarantee a good anti-biofilm performance, while the deletion of the sulphate ester group seems not to compromise the ZA anti-biofilm activity. Moreover the biological results revealed that the *para* position on the phenyl ring is a good point for the coupling to a polymer.

Introduction

Direct observations of a wide variety of natural habitats have established that 99% of microorganisms grow in form of biofilms, complex structured communities of microorganisms associated with surfaces and embedded in a self-produced extracellular polymeric substances. It is reported that biofilms are able to colonize every surface that offers minimal condition for the life included all human artefact surfaces like industrial installations, work benches, water distribution systems and also medical sector with devastating consequences in term of social and economic impact (Costerton et al., 1987). Especially in the clinical area, the role of biofilms in the contamination of medical implants has been well established. Unluckily, these implants are major contributors to morbidity and mortality among hospitalized patients as they are associated with high risk of biofilm infections (von Eiff et al., 2005; Hall-Stoodley et al., 2004).

The most detrimental property of biofilms is that conventional antimicrobial practices have been proved inadequate since, by adopting the sessile mode of life, microorganisms improve their resistance to antimicrobial agents up to several orders of magnitude (Smith, 2005; Darouiche, 2007; Donlan, 2011). In addition, the long term and intensive use of antibiotics and biocides has dramatically supported the development of resistant microbial strains reducing the possibility of treating biofilm effectively (Andersson et al., 2010). Increasingly restrictive regulations limiting the use of substances hazardous to human health and the environment, have also resulted in several biocides being banned. With this perspective the development of new improved therapeutic solutions able to reduce the incidence of biofilm-associated contaminations has become imperative. An innovative approach could be the use of biocide-free anti-biofilm agents with novel targets, unique modes of action and properties that are different from those of the currently used antimicrobials (Kaplan, 2009). The use

of sub-lethal doses of bio-inspired molecules able to interfere with specific key steps that are involved in biofilm formation could be an interesting strategy (Villa et al., 2012a; Cappitelli et al., 2014). In this context, nature represents an immense source of new bioactive substances with unrivalled structural diversity and complexity (Wong et al., 2008; Villa et al., 2009). Plants have adaptively developed fascinating strategies over millions of years to prevent harmful bacterial colonization on their living tissues in response to an ever-present pathogen pressure. These natural strategies have inspired anti-biofilm strategies and could be a promising starting point for novel therapeutic approaches (Villa et al., 2013). Zosteric acid or *p*-(sulfoxy) cinnamic acid (ZA), a secondary metabolite produced by the seagrass *Zostera marina*, might be suitable for implementation as a preventive or integrative approach against biofilm formation. At sub-lethal concentrations, ZA is able to reduce both bacterial and fungal adhesion, and plays a pivotal role in shaping biofilm architecture, in reducing biofilm biomass and thickness, in thwarting budded-to-hyphal-form transition, in extending the performance of antimicrobial agents, showing cytocompatibility towards soft and hard tissue (Villa et al., 2010; Villa et al., 2011; Polo et al., 2014). The comparative proteomic study on *E. coli* cells exposed to ZA showed that the compound acts as an environmental cue leading to global stress on bacterial cells, which promotes the expression of various protective proteins, the signal molecule autoinducer-2 production, and the synthesis of flagella, to escape from adverse conditions (Villa et al., 2012b).

Despite the promising results, ZA-based technology is far from real applications as the immobilization of the bioactive compound on a polymeric material is still in its infancy. Barrios et al. (2005) and Newby et al. (2006) incorporated ZA into silicone coatings to achieve its slow release in the surrounding area**.** Geiger and coauthors (2004) produced a new anti-biofilm biocompatible polyester material with encapsulated ZA. However, this approach posed several problems such as the non-uniform distribution of ZA inside the material and the formation of aggregates due to the incomplete miscibility of ZA in the polymers (Newby et al., 2006). In addition, a constant release rate of the active compound has neither been achieved nor monitored, facts that might make the system less attractive for a medical application (Geiger et al., 2004).

Advantages would be conferred if we could covalently couple the bioactive molecule to the surface of a material in a way to deliver the active moiety to the cellular target. In this approach, no molecule would be leached from the surface, sidestepping the problem of the compound kinetics release, providing long-term protection against bacterial colonization, and reducing the risk of developing resistant microbial strains, as the concentration of the anti-biofilm agent would be constantly below the lethal concentration while maintaining the molecule bioactive. At present the main bottlenecks that limits the development of the aforementioned ZA-based materials is the lack of information about the exact chemical structural elements required for its anti-biofilm activity.

In this follow-up study, a 43-member library of small molecules based on ZA scaffold diversity (Table 1) was designed and screened against *E. coli* to understand the structural reason for biofilm inhibition at sub-lethal concentration and identify functional groups that could be exploited for the covalent linkage to an abiotic surface. The compounds were characterized by the introduction of substituents at different positions on phenyl ring and several side-chain modifications, such as the removal of the insaturation and the substitution of the carboxylic acid with an alcohol, an aldehyde and ester functionalities in order to maximize diversification of the structure along with their physicochemical and biological properties. Moreover, both E/Z isomers were prepared in order to explore the role of the double bond (Figure 1).

Thus, the first aim of this study was to identify important structural determinants for ZA anti-biofilm activity as a basis to mapping potential binding sites for both the polymeric surface and the cellular target, and eventually develops ZA analogues with improved anti-biofilm activity.

Code	Cmpd	R	R_1	R_2	R_3	*E/Z*
ZA	Zosteric acid	4-OSO_3H	H	H	COOH	*E*
1	Coumaric acid *	4-OH	H	H	COOH	*E*
2	4-Methylcinnamic acid	4-CH_3	H	H	COOH	*E*
3	4-Formylcinnamic acid *	4-COH	H	H	COOH	*E*
4	Cinnamic acid *	-	H	H	COOH	*E*
5	4-Methoxycinnamic acid *	4-OCH_3	H	H	COOH	*E*
6	4-Fluorocinnamic acid *	4-F	H	H	COOH	*E*
7	4-Cyanocinnamic acid	4-CN	H	H	COOH	*E*
8	4-Carboxycinnamic acid	4-COOH	H	H	COOH	*E*
9	4-Chlorocinnamic acid *	4-Cl	H	H	COOH	*E*
10	4-Aminocinnamic acid *	4-NH_2	H	H	COOH	*E*
11	4-(Trifluoromethyl)cinnamic acid	4-CF_3	H	H	COOH	*E*
12	4-Nitrocinnamic acid *	4-NO_2	H	H	COOH	*E*
13	3-Chlorocinnamic acid *	3-Cl	H	H	COOH	*E*
14	3-Hydroxycinnamic acid *	3-OH	H	H	COOH	*E*
15	3,4-Dichlorocinnamic acid *	3-Cl; 4-Cl	H	H	COOH	*E*
16	2,4-Dichlorocinnamic acid *	2-Cl; 4-Cl	H	H	COOH	*E*
17	2-Chlorocinnamic acid	2-Cl	H	H	COOH	*E*
18	2-Methoxycinnamic acid *	2-OCH_3	H	H	COOH	*E*
19	2-Chloro-4-fluorocinnamic acid *	4-F; 2-Cl	H	H	COOH	*E*
20	Caffeic acid *	3-OH; 4-OH	H	H	COOH	*E*
21	2-Hydroxycinnamic acid *	2-OH	H	H	COOH	*E*
22	3-Hydroxy-4-aminocinnamic acid *	4-NH_2; 3-OH	H	H	COOH	*E*
23	Methyl coumarate	4-OH	H	H	$COOCH_3$	*E*
24	Methyl 4-methoxycinnamate	4-OCH_3	H	H	$COOCH_3$	*E*
25	Ethyl 2-hydroxycinnamate *	2-OH	H	H	$COOCH_2CH_3$	*E*
26	Methyl cinnamate *	-	H	H	$COOCH_3$	*E*
27	Ethyl β-methylcinnamate *	-	CH_3	H	$COOCH_2CH_3$	*E*
28	Ethyl cinnamate *	-	H	H	$COOCH_2CH_3$	*E*
29	Cinnamaldehyde *	-	H	H	COH	*E*
30	α-Methyl cinnamaldehyde *	-	H	CH_3	COH	*E*
31	Cinnamyl alcohol *	-	H	H	CH_2OH	*E*
32	*Cis* coumaric acid *	4-OH	H	H	COOH	*Z*
33	*Cis* methyl coumarate	4-OH	H	H	$COOCH_3$	*Z*
34	*Cis* 4-methoxycinnamic acid	4-OCH_3	H	H	COOH	*Z*
35	*Cis* methyl 4-methoxycinnamic acid	4-OCH_3	H	H	$COOCH_3$	*Z*
36	*Cis* ethyl cinnamate	-	H	H	$COOCH_2CH_3$	*Z*
37	*Cis* cinnamic acid	-	H	H	COOH	*Z*
38	*Cis* zosteric acid	4-OSO_3H	H	H	COOH	*Z*
39	3-(4-Methoxy)phenylpropionic acid *	4-OCH_3	H	H	COOH	-
40	3-Phenylpropionic acid *	-	H	H	COOH	-
41	3-(3,4-Dihydroxy)phenylpropionic acid *	3-OH; 4-OH	H	H	COOH	-
42	3-(4-Hydroxy)phenylpropionic acid *	4-OH	H	H	COOH	-
43	Coumarin *	-	H	H	-	-

Table 1. Cinnamic acid analogues used in the present study. * Commercially available compounds.

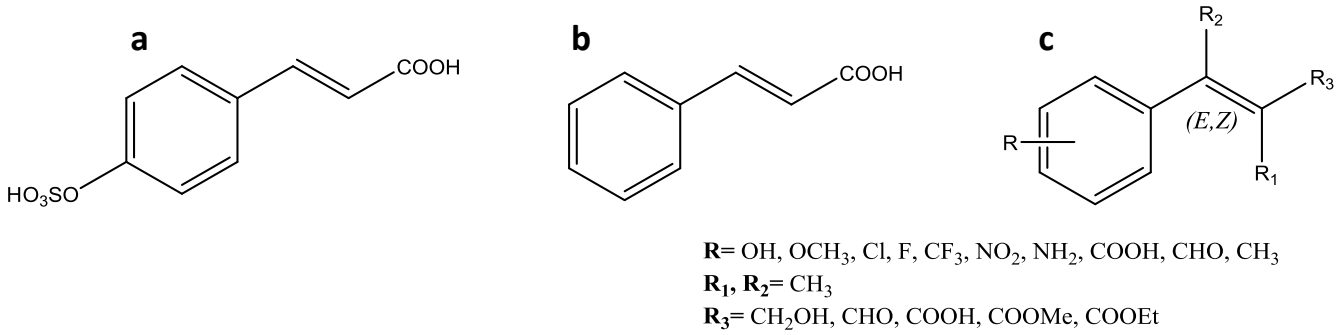

R= OH, OCH_3, Cl, F, CF_3, NO_2, NH_2, COOH, CHO, CH_3
R_1, R_2= CH_3
R_3= CH_2OH, CHO, COOH, COOMe, COOEt

Figure 1. Structural formula of chemical compounds used in this study: a) zosteric acid, b) cinnamic acid (4), c) cinnamic acid derivatives.

Materials and Methods

Synthesis of a small library of zosteric acid related compounds

All the reagents including solvents were purchased from Sigma-Aldrich and were used without any further purification. All reactions involving air-sensitive reagents were performed under nitrogen atmosphere and anhydrous solvents were used when necessary. The Biotage-Initiator microwave synthesizer was used. Reactions were monitored by thin layer chromatography (TLC) analysis on aluminium-backed Silica Gel 60 plates (0.2 mm, Merck) and were visualized under a UV lamp operating at wavelengths of 254 and 365 nm. Visualization was aided by opportune staining reagents. Intermediates and final compounds were purified by flash chromatography using Merck Silica Gel 60 (70-230 mesh). The purity of final compounds were determined by HPLC analysis and were > 95 %. ^{1}H and ^{13}C NMR spectra were recorded at room temperature on a Varian 300 MHz Oxford instrument. $CDCl_3$, CD_3OD, acetone-d6 and DMSO-d6 were used as deuterated solvents for all spectra run. Chemical shifts are expressed in ppm from tetramethylsilane resonance in the indicated solvent (TMS: 0.0 ppm) and coupling constants (J-values) are given in Hertz (Hz). ^{1}H NMR data are reported in the following order: ppm, multiplicity (s, singlet; d, doublet; t, triplet; q, quartet; m, multiplet; br, broad), and number of protons. Melting points and NMR data are consistent with literature data.

Synthesis of cinnamic acid derivatives

Zosteric acid was synthesized as already described in a previous work (Villa et al., 2010). The *cis* isomer **38** was obtained starting from *cis* 4-hydroxycinnamic acid **32** under microwave irradiation in the presence of sulphur trioxide pyridine complex in acetonitrile (Figure 2). The final product was isolated as sodium salt. The majority of the substituted cinnamic acid derivatives were prepared in high yield (>90%) by the Knoevenagel-Doebner procedure. In detail, compounds **2, 7, 8**, **11** and **17** were obtained through a one-pot reaction between the suitable substituted benzaldehyde and malonic acid in refluxing pyridine to induce decarboxylation (Szymanski et al., 2009) (Figure 3). The *trans* geometries of the ethenyl π-bonds were confirmed by proton-proton coupling constants. *Cis* cinnamic acid **37** was synthesized from the commercially available ethyl phenylpropiolate. The subsequent hydrogenation of alkyne in the presence of Lindlar catalyst and pyridine in methanol led to the corresponding *cis*-alkene **36**. Then ester group was hydrolyzed under alkaline condition to provide the final compound **37** (Figure 4). Esters of cinnamic acid in *cis* (**33**) or in *trans* configuration (**23**, **24**) were prepared by Fischer esterification of the carboxylic group (De et al., 2011). The protection of the hydroxyl group as methyl ether in the presence of iodomethane in dry *N,N*-dimethylformamide provided the compounds **35**. Hydrolysis of ester was performed in alkaline conditions to obtain the compound **34** (Figure 2).

***Escherichia coli* strain and growth condition**

The well characterized *Escherichia coli* ATCC 25404 was used as a model system for bacterial biofilms. The strain was stored at –80 °C in suspensions containing 20 % glycerol and 2 % peptone, and was routinely grown in Luria-Bertani broth (LB, Sigma-Aldrich) at 30 °C for 16 h.

Planktonic growth in presence of ZA related compounds

Planktonic growth of *E. coli* in LB medium supplemented with 0 (negative control), 0.183, 1.83, 18.3, 183 and 1830 µM of the synthesized molecules and 3 % of dimethyl sulphoxyde (DMSO) were carried out in 384-well microtiter plates. Growth curves at 30°C were generated using the PowerWave XS2 microplate reader (Biotek). Growth was followed by measuring the optical density at 600 nm (OD600) every 10 min for over 24 h in wells inoculated with 3 µl (3 % vol/vol) of an overnight culture (final concentration 10^7 cells/mL). OD-based growth kinetics were constructed by plotting the OD of suspensions minus the OD of the non-inoculated medium against incubation time. The polynomial Gompertz model (Zwietering et al, 1990) was used to fit the growth curves to calculate the maximum specific growth rate (OD600/min), using GraphPad Prism software (version 5.0, San Diego, CA, USA). Six biological replicates of each treatment were performed. Obtained data were normalized to the negative control and reported as the mean of these. Percentage reduction in comparison with the control was also calculated.

Cellular growth with the ZA related compounds as the sole carbon and energy source

The ability of bacteria to grow with each compound as the sole carbon and energy source was tested using a mineral medium (KH_2PO_4 30 g/L, Na_2HPO_4 70 g/L, NH_4Cl 10 g/L, pH 7) supplemented with 1830 µM of each synthesized molecule and 3% of DMSO. Bacteria were added to a final concentration of 10^7 cells/mL and grown at 30 °C for 72 h. The positive control was the mineral medium supplemented with glucose at both 1830 µM and 10,000 µM concentration. Microbial growth was followed by measuring OD600. All the experiments were repeated three times.

Microplate-based biofilm assay in presence of ZA related compounds

Biofilm was assessed quantitatively using fluorochrome labeled cells in hydrophobic 96-well black sided plates as previously reported by Villa et al. (2010). Briefly, 200 µL of phosphate buffered saline (PBS, 0.01 M phosphate buffer, 0.0027 M potassium chloride pH 7.4, Sigma-Aldrich) containing 10^7 cells supplemented with 0 (negative control), 0.183, 1.83, 18.3, 183 and 1830 µM of each synthesized molecule and 3 % of DMSO were placed in microtiter plate wells. Cells were incubated 18 h at 30°C. The microtiter plate wells were washed two times with 200 µL PBS and adhered cells were stained using 10 µg/mL 4,6-diamidino-2-phenylindole (Sigma-Aldrich) in PBS for 20 min in the dark at room temperature. Fluorescence intensity was measured using the fluorometer VICTOR™ X Multilabel Plate Readers (Perkin Elmer) at excitation wavelength of 335 nm and emission wavelength of 433 nm. A standard curve of fluorescence intensity versus cell number was determined and used to quantify the anti-biofilm performance of the ZA related compounds. Four measurements were performed for each condition. Obtained data were normalized to the negative control and reported as the mean of these data. Percentage reduction in comparison to the control was also calculated.

Statistical analysis

Analysis of variance (ANOVA) via a software run in MATLAB (Version 7.0, The MathWorksInc, Natick, USA) was applied to statistically evaluate any significant differences among the samples. Tukey's honestly significant different test (HSD) was used for pairwise comparison to determine the significance of the data. Differences were considered significant for $p < 0.05$.

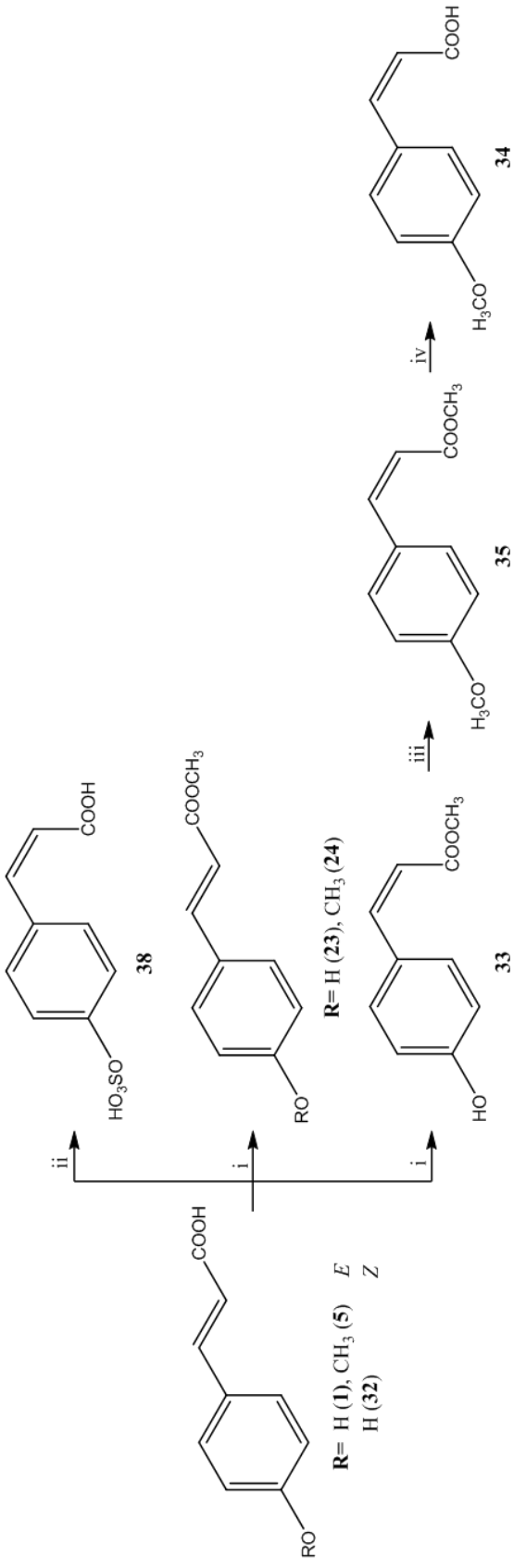

Figure 2. Reactions to obtain *cis* zosteric acid, *cis* 4-methoxy cinnamic acid and methyl ester derivatives. Reagents and conditions: i) from **1** for **23**, from **5** for **24**, from **32** for **33**: H_2SO_4, MeOH, reflux, 1 h; ii) from **32**: Py · SO_3, DMF dry, 120 °C, 25 min; iii) CH_3I, anhydrous K_2CO_3, dry DMF, reflux, 1.5 h; iv) 1N NaOH, EtOH, reflux, 2h.

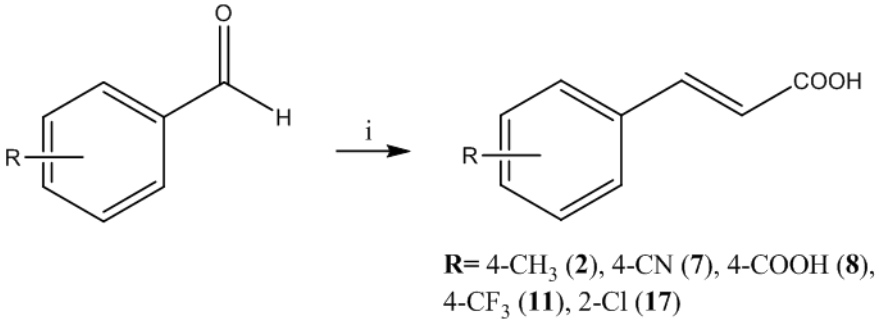

R= 4-CH_3 (**2**), 4-CN (**7**), 4-COOH (**8**), 4-CF_3 (**11**), 2-Cl (**17**)

Figure 3. Reaction to obtain substituted cinnamic acid derivatives. Reagents and conditions: i) malonic acid, Py, piperidine, reflux, 80-180 min.

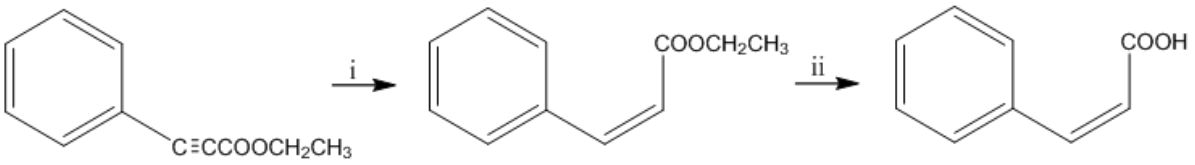

36 **37**

Figure 4. Reactions to obtain *cis* cinnamic acid. Reagents and conditions: i) Lindlar catalyst, H2, pyridine, MeOH, rt, 16h; ii) 1N NaOH, EtOH/THF (1:1), rt, 12 h.

Results

DMSO did not affect *E. coli* planktonic growth and cells adhesion

DMSO was necessary to dissolve the molecules in the aqueous medium but, firstly, its possible impact on *E. coli* as carbon and energy source and on the growth and cell adhesion was assessed. Three % DMSO was not a carbon and energy source for the microorganisms. In addition, no significant differences among the number of planktonic and adhered cells with or without 3% DMSO were observed (Table 2).

DMSO concentration	Planktonic growth (OD600/min) (x10^3)	Cells adhesion (No. adhered cells) (x10^7)
0 %	1.33±0.01[a]	2.02±0.39[a]
3 %	1.28±0.03[a]	1.92±0.18[a]

Table 2. Planktonic growth and cells adhesion with and without 3 % DMSO. According to post hoc analysis (Tukey's HSD, $p < 0.05$), data sharing the same letter indicates no significant difference.

ZA related compounds were not a carbon and energy source for *E. coli*

The ability of *E. coli* to grow with 43 ZA-related compounds at 1830 µM as the sole carbon and energy source was tested and compared with a positive control with glucose at the same concentration.

E. coli in the positive control did not grow and showed an OD600 lower than 0.05 after 48 h incubation. The minimum glucose concentration in a mineral medium that supported *E. coli* growth was 10 mM (OD600: 0.201±0.007). Consequently, *E. coli* with glucose 10 mM was used as a positive control.
E. coli did not grow in the presence of each ZA related compound as the sole carbon and energy source and showed an OD600 lower than 0.05 after 48 h incubation with each molecule. All derivatives were submitted to further biological assays in order to evaluate their ability to affect both planktonic growth and surface cell adhesion.

ZA related compounds affect E. coli planktonic growth depending on their concentration
E. coli maximum specific growth rates in the presence of each ZA related compound at 0.183, 1.83, 18.3, 183 and 1830 µM were calculated and compared to a negative control grown without the molecule using the ANOVA statistic test (Table 3). Molecules able to reduce the maximum specific growth rate of *E. coli* planktonic cells respect to the negative control less than 10 % were coded as 0, between 10 % and 20 % were coded - 1, between 20 % and 30 % were coded - 2, and more than 30 % were coded - 3.

ZA related compounds affected *E. coli* cells adhesion depending on their concentration
The number of adhered cells in the presence of each ZA related compound at 0.183, 1.83, 18.3, 183 and 1830 µM was assessed quantitatively using fluorochrome labelled cells and compared to a negative control in the absence of the molecule using the ANOVA statistic test (Table 3). Molecules able to reduce the number of *E.coli* adhered cells respect to the negative control less than 20 % were coded 0, between 20 % and 30 % were coded - 1, between 30 % and 40 % were coded - 2 and more than 40 % were coded - 3. Molecules able to increase the number of adhered cells respect to the negative control more than 20 % were coded + 1.

ZA related compounds presented different biological trends
With the aim to identify trends, planktonic growth and cells adhesion data were grouped to obtain a global picture of the biological activity of each ZA related compound at the different concentrations (Figure 5). Compounds showed: i) no biological activity (no reduction of the number of adhered cells and no planktonic growth effect), ii) anti-biofilm activity (reduction of the number of adhered cells and no planktonic growth effect), iii) increased biofilm formation (increase of the number of adhered cells and no planktonic growth effect), iv) planktonic to biofilm mode of life transition (no reduction or increase of the number of adhered cells and planktonic growth effect) and v) biocidal effect (reduction of the number of adhered cells and planktonic growth effect).
Five molecules (**7**, **12**, **18**, **19**, **39**) induced no biological activity at low and middle concentrations and planktonic to biofilm mode of life transition or biocidal effect at the maximum concentration (Trend 1). Eight molecules (**24**, **27**, **29-31**, **40**, **42**, **43**) showed the same trend but they promoted biofilm formation at the lowest concentration (Trend 2). Nineteen molecules (**1-6**, **8-11**, **13-15**, **20**, **21**, **23**, **26**, **28**, **41**) had no biological activity at low concentration, showed an anti-biofilm activity at middle concentrations and induced biocidal effect or planktonic to biofilm mode of life transition at the maximum concentration (Trend 3). Nine molecules (**ZA**, **16**, **17**, **22**, **25**, **33-36**) showed the same trend but they promoted biofilm formation at the lowest concentration (Trend 4). Finally, molecules **32**, **37** and **38** showed a peculiar trend (Trend 5).

ZA related compounds presented different global anti-biofilm performance
For each ZA related compound a global anti-biofilm performance value was calculated as (sum of cell adhesion codes of all concentrations)-(sum of planktonic growth code of all concentrations) (Figure 6). This value took into account i) the occurrence that ZA related compound induced a different bacterial response depending on the concentration, ii) the positive contribution of concentrations that reduce

the number of adhered cells; iii) the negative contributions of concentrations that enhance the number of adhered cells; iv) the negative contribution of concentrations that reduce planktonic growth.
Molecules with an anti-biofilm performance value i) equal 0 were considered globally without anti-biofilm performance; ii) below 0 were considered globally able to exert an anti-biofilm activity (-1: low anti-biofilm performance; -2: moderate anti-biofilm performance; ≤ -3: optimal anti-biofilm performance), iii) above 0 were considered globally able to improve biofilm performance (+1: low improvement of biofilm performance; +2: moderate improvement of biofilm performance; ≥ +3: optimal improvement of biofilm performance).
Four molecules (**7, 12, 14, 32**) presented anti-biofilm performance equal 0. Twenty molecules presented anti-biofilm performance below 0 (-1: **16**; -2: **5**, **6**, **13**, **21**, **23**, **28**; ≤ -3: **ZA**, **1-4**, **8-11**, **17**, **20**, **22**, **41**). Twenty molecules presented anti-biofilm performance above 0 (+1: **19**, **26**, **31**, **33**, **36**; +2: **15**, **25**, **27**, **39**, **42**, **43**; +2: **15**, **25**, **27**, **39**, **42**, **43**; ≥ +3: **18**, **24**, **29**, **30**, **34**, **35**, **37**, **38**, **40**).

Carboxylic acid moiety conjugated to the double bond in *trans* configuration was important for ZA anti-biofilm activity

The study involved the preparation and biological evaluation of analogues characterized by substitutions at different positions on the phenyl ring as well as a variety of side chains. This investigation highlighted features that could be useful for the design of new derivatives, with the aim to find compounds endowed with a better anti-biofilm activity compared to ZA. Interestingly, as reported in Table 3, cinnamic acid **4**, a natural compound obtained by cinnamon lacking the sulfate monoester group, has shown an interesting anti-biofilm activity at a 1000-fold lower inhibitory concentration than ZA (0.183 vs 183 μM).
The substitution pattern of the phenyl ring and the nature of the substituents were found to have a significant effect on the biofilm inhibitory activity. In the first instance, a broad variety of substituents with different electronic and steric properties were introduced at position 4 on the phenyl ring. Compounds (**1-3**, **5**, **6**, **8-11**) showed an interesting activity (Trend 3) compared to the unsubstituted cinnamic acid **4**, meanwhile the presence of cyano (**7**) and nitro (**12**) groups caused a loss in activity (Trend 1).
Comparing the derivatives bearing a hydroxyl group (**1**, **14**), as well as the chlorine atom (**9**, **13**), respectively in position 4 and 3 on the phenyl ring, highlighted that the substitution at the *para* position was preferred (**1** and **9** more active than **14** and **13**), although the same trend was still present. On the contrary the substitution at position 2 was not well tolerated. Indeed, as for compound **17** the activity was reduced 10-fold compared to **9**, while in the other cases the activity was almost completely abolished. To determine whether the introduction of a second substituent on the phenyl ring would enhance activity, a series of disubstituted derivatives (**15**, **16**, **19**, **20**, **22**) were synthesized. In general, each disubstituted compound was found to have a different behavior and a lower anti-biofilm activity compared to the corresponding monosubstituted compound. This effect was most evident for the 3,4-dichlorocinnamic acid **15**, whose activity was 10-fold lower than the monosubstituted counterpart **9**.
Following on from this, the side chain modifications were also explored. In general, the unsubstituted compounds having the carboxylic function protected as esters (**26**, **28**) showed lower activity in comparison with cinnamic acid **4**, and in particular the ethyl ester **28** was less active than methyl ester **26**. Besides, among the *para*-substituted cinnamic acid esters (**23-24**), the presence of a hydroxyl group **23** seemed to be important for the anti-biofilm activity, since the corresponding 4-methoxy derivative **24** was inactive. Moreover, derivatives bearing an aldehyde (**29**, **30**) or an alcohol (**31**) in replacement of the carboxylic acid functionality were inactive (Trend 2), confirmed that the carboxylic moiety was essential for good anti-biofilm activity. To investigate the importance of the configuration of the double bond, the majority of *cis* derivatives (**32-38**) were synthesized and found to have a different behavior (Trends 4, 5) compared to the *trans* counterparts. Interestingly, exceptions to this rule were the *cis* isomer of zosteric acid **38** and cinnamic acid **37,** that had lost their anti-biofilm activity (Trend 5). Additionally, specific concentrations of **37** and **38** seemed to enhance the biofilm formation.

Similarly, some saturated derivatives (**39-42**) were chosen to investigate the role of the double bond. All the compounds exhibited the same trend (Trend 2) except for compound **41**, a catechol derivative, that did not follow this general behaviour (Trend 3) probably due to a different mechanism of interaction (as compound **20**).
Finally, coumarin **43**, which could be considered the cyclic derivative of **4**, was unable to inhibit the biofilm growth, confirming the essential role of the side chain.
As for the anti-biofilm performance, some additional observations could be drawn. Generally, zosteric acid derivatives followed the same behaviors described for the anti-biofilm activity, with some exceptions: i) derivatives **5** and **6**, which have a methoxy group and a fluorine atom in the *para* position on the phenyl ring respectively, showed an anti-biofilm performance slightly lower than that of the cinnamic acid **4**, which was still a positive result; ii) compound **17** anti-biofilm performance turned out to be better than that of the corresponding analogue **9**, in which the chlorine atom was at position 4 on the phenyl ring; however, the general trend, according to which the substitution at position 2 was not well tolerated, was confirmed; iii) the anti-biofilm performance of the disubstituted halogen derivatives (**15**, **16**, **19**) was in general lower than that of the monosubstituted counterparts as well as the anti-biofilm activity. The same was not observed for compounds (**20**, **22**), which were characterized by electron donating substituents, whose monosubstituted analogues showed a decreased anti-biofilm performance; iv) the esters **26** and **28** showed the opposite behaviour, since the methyl ester **26** exhibited an anti-biofilm performance lower than that of the ethyl ester **28**; v) the majority of *cis* derivatives (**32-38**) were found to have a global anti-biofilm performance promoting biofilm formation.
Among the tested molecules, six molecules (**1**, **4**, **8**, **11**, **20**) have the most interesting anti-biofilm performance by showing anti-biofilm activity in a wide range of concentrations with maximum at micromolar level and with no effect on planktonic growt

		Planktonic growth			Cells adhesion		
Cmpd	**Conc. (μM)**	**OD600/min ($x10^{-3}$)**	**% reduction**	**Code (a)**	**No. adhered cells ($x10^{7}$)**	**% reduction**	**Code (b)**
ZA	0	1.28±0.03^{a}	0.00	0	1.92±0.18^{b}	0.00	0
	0.183	1.32±0.06^{a}	2.86	0	2.77±0.17^{d}	44.59	1
	1.83	1.31±0.04^{a}	1.76	0	1.54±0.29^{c}	-19.76	0
	18.3	1.29±0.04^{a}	0.11	0	1.55±0.19^{c}	-19.34	0
	183	1.30±0.04^{a}	1.07	0	1.39±0.13^{c}	-27.67	-1
	1830	1.30±0.04^{a}	1.21	0	0.56±0.12^{a}	-70.56	-3
1	0	1.28±0.03^{abc}	0.00	0	1.92±0.18^{b}	0.00	0
	0.183	1.31±0.03^{ab}	2.06	0	2.29±0.16^{b}	19.37	0
	1.83	1.26±0.04^{abc}	-1.72	0	1.03±0.14^{ce}	-46.05	-3
	18.3	1.23±0.02^{abc}	-3.99	0	1.42±0.24^{de}	-25.80	-1
	183	1.23±0.06^{abc}	-3.87	0	1.49±0.14^{de}	-22.36	-1
	1830	0.97±0.04^{e}	-24.17	-2	1.22±0.27^{cde}	-36.38	-2
2	0	1.28±0.03^{a}	0.00	0	1.92±0.18^{bc}	0.00	0
	0.183	1.33±0.03^{a}	3.41	0	1.86±0.23^{bcd}	-3.15	0
	1.83	1.32±0.03^{a}	2.66	0	0.47±0.09^{a}	-75.40	-3
	18.3	1.26±0.07^{a}	-2.23	0	1.50±0.18^{cde}	-21.94	-1
	183	1.28±0.07^{a}	-0.48	0	1.39±0.32^{de}	-27.44	-1
	1830	0.87±0.03^{b}	-32.54	-3	1.40±0.28^{de}	-27.01	-1
3	0	1.28±0.03^{abc}	0.00	0	1.92±0.18^{b}	0.00	0
	0.183	1.23±0.06^{abd}	-4.42	0	1.26±0.15^{ce}	-34.41	-1
	1.83	1.33±0.03^{ac}	3.46	0	0.73±0.07^{ade}	-61.92	-3
	18.3	1.32±0.03^{ac}	3.08	0	1.04±0.23^{cde}	-45.97	-3
	183	1.28±0.05^{abc}	-0.03	0	1.17±0.28^{ce}	-39.12	-2
	1830	1.02±0.01^{e}	-20.44	-2	1.33±0.08^{ce}	-30.69	-2
4	0	1.28±0.03^{abc}	0.00	0	1.92±0.18^{bef}	0.00	0
	0.183	1.24±0.04^{abcd}	-3.32	0	1.25±0.43^{cdef}	-34.95	-2
	1.83	1.22±0.01^{abcdf}	-4.74	0	1.17±0.17^{cdf}	-38.77	-2
	18.3	1.19±0.04^{bcdef}	-7.58	0	1.78±0.10^{bcef}	-7.37	0
	183	1.14±0.05^{def}	-11.37	-1	1.44±0.15^{bcdef}	-25.03	-1
	1830	0.83±0.02^{h}	-35.10	-3	1.32±0.28^{cdef}	-31.11	-2
5	0	1.28±0.03^{abc}	0.00	0	1.92±0.18^{bceh}	0.00	0
	0.183	1.24±0.02^{ac}	-3.14	0	1.92±0.26^{bcefgh}	0.37	0
	1.83	1.23±0.03^{ac}	-4.12	0	1.17±0.11^{defl}	-39.15	-2
	18.3	1.14±0.01^{df}	-11.53	-1	1.58±0.13^{bcdefghl}	-17.47	0
	183	1.15±0.06^{de}	-10.43	-1	1.36±0.24^{bcdefghl}	-28.79	-1
	1830	0.94±0.04^{g}	-26.65	-2	1.14±0.25^{df}	-40.52	-3
6	0	1.28±0.03^{a}	0.00	0	1.92±0.18^{b}	0.00	0
	0.183	1.30±0.07^{a}	1.21	0	2.30±0.62^{b}	19.90	0
	1.83	1.25±0.05^{a}	-2.36	0	2.05±0.20^{b}	7.00	0
	18.3	1.31±0.01^{a}	2.38	0	1.12±0.21^{c}	-41.44	-3
	183	1.16±0.03^{b}	-10.03	-1	1.25±0.25^{c}	-34.97	-2
	1830	0.85±0.03^{d}	-33.69	-3	1.39±0.23^{c}	-27.46	-1

Table 3, part a. Planktonic growth and cells adhesion in the presence of each ZA related compound. Percentage reduction respect to the negative control is reported. a) Percentage reduction of the maximum specific growth rate: code (0) x > -10 %; code (-1) -10 % ≤ x < -20 %; code (-2) -20 % ≤ x < -30 %; code (-3) x ≤ -30 %; b) Percentage reduction of the number of adhered cells: code (+1) x > +20 %; code (0) +20 % ≤ x < -20 %; code (-1) -20 % ≤ x < -30 %; code (-2) -30 % ≤ x < -40 %; code (-3) x ≤ -40 %. According to post hoc analysis (Tukey's HSD, $p < 0.05$), data sharing the same letter indicates no significant difference.

		Planktonic growth			Cells adhesion		
Cmpd	**Conc. (μM)**	**OD600/min ($x10^{-3}$)**	**% reduction**	**Code (a)**	**No. adhered cells ($x10^{7}$)**	**% reduction**	**Code (b)**
7	0	1.28±0.03^{a}	0.00	0	1.92±0.18^{bc}	0.00	0
	0.183	1.29±0.03^{a}	0.12	0	1.73±0.32^{bcd}	-9.57	0
	1.83	1.26±0.02^{a}	-1.99	0	1.75±0.37^{bc}	-8.60	0
	18.3	1.31±0.00^{a}	1.90	0	1.88±0.41^{bc}	-1.95	0
	183	1.28±0.05^{a}	-0.41	0	1.56±0.20^{bcd}	-18.67	0
	1830	0.96±0.04^{c}	-24.88	-2	1.18±0.23^{cd}	-38.63	-2
8	0	1.28±0.03^{a}	0.00	0	1.92±0.18^{b}	0.00	0
	0.183	1.30±0.04^{a}	1.13	0	1.63±0.37^{b}	-14.90	0
	1.83	1.26±0.05^{a}	-1.68	0	1.14±0.19^{c}	-40.28	-3
	18.3	1.27±0.03^{a}	-1.14	0	1.06±0.18^{c}	-44.92	-3
	183	1.28±0.05^{a}	-0.51	0	1.14±0.11^{c}	-40.73	-3
	1830	1.11±0.01^{b}	-13.24	-1	2.19±0.28^{d}	14.29	0
9	0	1.28±0.03^{a}	0.00	0	1.92±0.18^{bc}	0.00	0
	0.183	1.25±0.04^{a}	-2.79	0	1.75±0.21^{bcd}	-8.89	0
	1.83	1.27±0.03^{a}	-0.79	0	1.43±0.25^{cde}	-25.63	-1
	18.3	1.30±0.05^{a}	1.06	0	1.18±0.31^{de}	-38.64	-2
	183	1.12±0.00^{b}	-12.86	-1	1.40±0.31^{cde}	-27.19	-1
	1830	0.83±0.02^{c}	-35.27	-3	1.14±0.22^{de}	-40.36	-3
10	0	1.28±0.03^{a}	0.00	0	1.92±0.18^{bc}	0.00	0
	0.183	1.26±0.04^{a}	-1.86	0	1.81±0.18^{bcdf}	-5.41	0
	1.83	1.24±0.02^{a}	-3.08	0	1.47±0.17^{cdef}	-23.51	-1
	18.3	1.24±0.02^{a}	-3.14	0	1.19±0.22^{deg}	-37.94	-2
	183	1.25±0.06^{a}	-2.43	0	1.57±0.18^{cdf}	-18.09	0
	1830	0.87±0.02^{d}	-32.40	-3	1.10±0.28^{deg}	-42.38	-3
11	0	1.28±0.03^{abc}	0.00	0	1.92±0.18^{b}	0.00	0
	0.183	1.25±0.04^{abc}	-2.93	0	2.26±0.16^{c}	18.06	0
	1.83	1.24±0.02^{abc}	-3.19	0	1.53±0.17^{d}	-20.05	-1
	18.3	1.31±0.01^{ab}	2.04	0	1.43±0.28^{d}	-25.44	-1
	183	1.24±0.04^{ac}	-3.38	0	0.40±0.06^{a}	-79.23	-3
	1830	0.87±0.01^{f}	-32.56	-3	0.48±0.03^{a}	-74.86	-3
12	0	1.28±0.03^{ab}	0.00	0	1.92±0.18^{bc}	0.00	0
	0.183	1.34±0.07^{ab}	4.38	0	1.82±0.44^{bcd}	-4.88	0
	1.83	1.29±0.05^{abc}	0.19	0	1.82±0.11^{bcd}	-5.16	0
	18.3	1.22±0.05^{bc}	-4.95	0	1.63±0.29^{bcd}	-14.70	0
	183	1.21±0.03^{c}	-5.56	0	1.54±0.30^{cd}	-19.83	0
	1830	0.99±0.03^{d}	-23.12	-2	1.30±0.33^{d}	-32.21	-2
13	0	1.28±0.03^{ac}	0.00	0	1.92±0.18^{bc}	0.00	0
	0.183	1.29±0.02^{ac}	0.41	0	1.78±0.05^{bce}	-7.13	0
	1.83	1.22±0.08^{ab}	-4.66	0	1.75±0.19^{bce}	-8.79	0
	18.3	1.31±0.02^{ac}	2.40	0	1.31±0.24^{cdef}	-31.41	-2
	183	1.25±0.03^{abc}	-2.47	0	1.59±0.18^{de}	-17.14	0
	1830	1.00±0.02^{d}	-22.39	-2	1.19±0.24^{df}	-37.93	-2

Table 3, part b. Planktonic growth and cells adhesion in the presence of each ZA related compound. Percentage reduction respect to the negative control is reported. a) Percentage reduction of the maximum specific growth rate: code (0) x > -10 %; code (-1) -10 % ≤ x < -20 %; code (-2) -20 % ≤ x < -30 %; code (-3) x ≤ -30 %; b) Percentage reduction of the number of adhered cells: code (+1) x > +20 %; code (0) +20 % ≤ x < -20 %; code (-1) -20 % ≤ x < -30 %; code (-2) -30 % ≤ x < -40 %; code (-3) x ≤ -40 %. According to post hoc analysis (Tukey's HSD, $p < 0.05$), data sharing the same letter indicates no significant difference.

		Planktonic growth			Cells adhesion		
Cmpd	**Conc. (μM)**	**OD600/min ($x10^{-3}$)**	**% reduction**	**Code (a)**	**No. adhered cells ($x10^{7}$)**	**% reduction**	**Code (b)**
14	0	1.28 ± 0.03^{abc}	0.00	0	1.92 ± 0.18^{bcef}	0.00	0
	0.183	1.21 ± 0.02^{abcde}	-5.68	0	1.93 ± 0.06^{bcefg}	0.68	0
	1.83	1.27 ± 0.01^{abc}	-1.20	0	1.70 ± 0.14^{bcef}	-11.20	0
	18.3	1.23 ± 0.04^{abcd}	-3.89	0	1.33 ± 0.21^{abcef}	-30.56	-2
	183	1.30 ± 0.02^{abc}	1.57	0	2.29 ± 0.50^{bcef}	19.62	0
	1830	1.14 ± 0.03^{bde}	-10.95	-1	4.25 ± 1.35^{hi}	121.57	+
15	0	1.28 ± 0.03^{a}	0.00	0	1.92 ± 0.18^{bc}	0.00	0
	0.183	1.31 ± 0.05^{a}	1.90	0	1.76 ± 0.08^{bce}	-7.98	0
	1.83	1.27 ± 0.05^{a}	-1.23	0	1.72 ± 0.18^{bce}	-10.36	0
	18.3	1.30 ± 0.01^{a}	1.46	0	1.41 ± 0.14^{de}	-26.16	-1
	183	1.29 ± 0.03^{a}	0.63	0	1.53 ± 0.23^{cde}	-19.96	0
	1830	0.86 ± 0.02^{b}	-32.67	-3	1.58 ± 0.26^{cde}	-17.47	0
16	0	1.28 ± 0.03^{a}	0.00	0	1.92 ± 0.18^{bf}	0.00	0
	0.183	1.29 ± 0.04^{a}	0.21	0	3.59 ± 0.37^{c}	87.42	+
	1.83	1.31 ± 0.05^{a}	2.05	0	1.46 ± 0.19^{def}	-23.68	-1
	18.3	1.28 ± 0.04^{a}	-0.29	0	1.36 ± 0.19^{de}	-28.82	-1
	183	1.29 ± 0.05^{a}	0.13	0	1.74 ± 0.11^{bdf}	-8.95	0
	1830	1.03 ± 0.05^{d}	-20.16	-2	1.33 ± 0.17^{de}	-30.57	-2
17	0	1.28 ± 0.03^{abc}	0.00	0	1.92 ± 0.18^{bd}	0.00	0
	0.183	1.28 ± 0.03^{abcd}	-0.29	0	3.62 ± 0.37^{c}	88.79	+
	1.83	1.30 ± 0.07^{abcd}	0.87	0	1.76 ± 0.08^{bdf}	-8.09	0
	18.3	1.33 ± 0.04^{ab}	3.62	0	1.37 ± 0.14^{ef}	-28.33	-1
	183	1.29 ± 0.02^{abc}	0.68	0	1.49 ± 0.19^{def}	-22.26	-1
	1830	1.05 ± 0.04^{ef}	-17.95	-1	1.08 ± 0.15^{h}	-43.68	-3
18	0	1.28 ± 0.03^{ab}	0.00	0	1.92 ± 0.18^{bcd}	0.00	0
	0.183	1.28 ± 0.02^{ab}	0.07	0	2.16 ± 0.15^{bc}	12.75	0
	1.83	1.26 ± 0.04^{abc}	-1.68	0	1.89 ± 0.19^{bcd}	-1.22	0
	18.3	1.31 ± 0.04^{ab}	1.79	0	1.61 ± 0.23^{bd}	-16.05	0
	183	1.20 ± 0.03^{bc}	-6.82	0	1.95 ± 0.25^{bcd}	1.50	0
	1830	1.00 ± 0.05^{c}	-22.04	-2	2.79 ± 0.46^{e}	45.65	+
19	0	1.28 ± 0.03^{a}	0.00	0	1.92 ± 0.18^{bc}	0.00	0
	0.183	1.30 ± 0.06^{a}	0.88	0	1.93 ± 0.44^{bcd}	0.81	0
	1.83	1.29 ± 0.05^{a}	0.50	0	1.67 ± 0.12^{bcd}	-12.94	0
	18.3	1.30 ± 0.01^{a}	1.58	0	1.65 ± 0.19^{cd}	-13.94	0
	183	1.32 ± 0.04^{a}	2.69	0	1.80 ± 0.28^{bcd}	-6.18	0
	1830	1.05 ± 0.04^{b}	-18.13	-1	1.61 ± 0.14^{cd}	-15.75	0
20	0	1.28 ± 0.03^{a}	0.00	0	1.92 ± 0.18^{bc}	0.00	0
	0.183	1.30 ± 0.03^{a}	1.40	0	1.91 ± 0.33^{bcd}	-0.13	0
	1.83	1.31 ± 0.03^{a}	2.18	0	1.58 ± 0.10^{cde}	-17.44	0
	18.3	1.30 ± 0.04^{a}	1.14	0	1.52 ± 0.23^{de}	-20.60	-1
	183	1.29 ± 0.04^{a}	0.12	0	0.60 ± 0.04^{a}	-68.90	-3
	1830	1.13 ± 0.02^{b}	-11.61	-1	0.72 ± 0.13^{a}	-62.34	-3

Table 3, part c. Planktonic growth and cells adhesion in the presence of each ZA related compound. Percentage reduction respect to the negative control is reported. a) Percentage reduction of the maximum specific growth rate: code (0) $x > -10$ %; code (-1) $-10\ \% \leq x < -20$ %; code (-2) $-20\ \% \leq x < -30$ %; code (-3) $x \leq -30$ %; b) Percentage reduction of the number of adhered cells: code (+1) $x > +20$ %; code (0) $+20\ \% \leq x < -20$ %; code (-1) $-20\ \% \leq x < -30$ %; code (-2) $-30\ \% \leq x < -40$ %; code (-3) $x \leq -40$ %. According to post hoc analysis (Tukey's HSD, $p < 0.05$), data sharing the same letter indicates no significant difference.

		Planktonic growth			Cells adhesion		
Cmpd	**Conc. (μM)**	**OD600/min ($x10^{-3}$)**	**% reduction**	**Code (a)**	**No. adhered cells ($x10^{7}$)**	**% reduction**	**Code (b)**
21	0	1.28 ± 0.03^{a}	0.00	0	1.92 ± 0.18^{bc}	0.00	0
	0.183	1.32 ± 0.04^{a}	2.92	0	1.71 ± 0.16^{bcd}	-10.57	0
	1.83	1.30 ± 0.01^{a}	0.95	0	1.60 ± 0.18^{cde}	-16.42	0
	18.3	1.30 ± 0.05^{a}	1.62	0	1.72 ± 0.23^{bcd}	-10.51	0
	183	1.32 ± 0.00^{a}	2.52	0	1.34 ± 0.18^{def}	-30.22	-2
	1830	1.03 ± 0.04^{b}	-20.07	-2	1.24 ± 0.16^{def}	-35.24	-2
22	0	1.28 ± 0.03^{acd}	0.00	0	1.92 ± 0.18^{b}	0.00	0
	0.183	1.21 ± 0.01^{bcdf}	-5.58	0	3.07 ± 0.17^{c}	60.29	+
	1.83	1.29 ± 0.03^{acd}	0.75	0	2.66 ± 0.23^{ce}	38.91	+
	18.3	1.29 ± 0.02^{acd}	0.43	0	1.37 ± 0.06^{deg}	-28.42	-1
	183	1.24 ± 0.01^{abcdf}	-3.61	0	1.18 ± 0.33^{df}	-38.53	-2
	1830	1.17 ± 0.06^{bcf}	-9.14	0	0.99 ± 0.04^{degh}	-48.14	-3
23	0	1.28 ± 0.03^{a}	0.00	0	1.92 ± 0.18^{b}	0.00	0
	0.183	1.32 ± 0.02^{a}	2.93	0	2.26 ± 0.22^{c}	17.80	0
	1.83	1.29 ± 0.07^{a}	0.37	0	1.22 ± 0.15^{d}	-36.25	-2
	18.3	1.31 ± 0.06^{a}	2.26	0	1.50 ± 0.16^{d}	-21.75	-1
	183	1.12 ± 0.03^{b}	-12.66	-1	1.24 ± 0.15^{d}	-35.24	-2
	1830	0.56 ± 0.02^{c}	-56.28	-3	1.47 ± 0.23^{d}	-23.17	-1
24	0	1.28 ± 0.03^{a}	0.00	0	1.92 ± 0.18^{b}	0.00	0
	0.183	1.26 ± 0.03^{a}	-1.69	0	4.77 ± 0.47^{c}	148.78	+
	1.83	1.29 ± 0.01^{a}	0.37	0	1.83 ± 0.22^{b}	-4.76	0
	18.3	1.31 ± 0.01^{a}	2.32	0	1.96 ± 0.12^{b}	2.38	0
	183	1.15 ± 0.03^{b}	-10.36	-1	4.16 ± 0.54^{c}	117.10	+
	1830	1.09 ± 0.01^{b}	-15.26	-1	9.52 ± 1.19^{e}	396.86	+
25	0	1.28 ± 0.03^{a}	0.00	0	1.92 ± 0.18^{b}	0.00	0
	0.183	1.27 ± 0.01^{a}	-0.72	0	2.60 ± 0.15^{c}	35.59	+
	1.83	1.29 ± 0.02^{a}	0.83	0	1.73 ± 0.16^{b}	-9.71	0
	18.3	1.24 ± 0.05^{a}	-3.48	0	1.67 ± 0.08^{b}	-12.95	0
	183	1.12 ± 0.04^{b}	-12.58	-1	1.64 ± 0.24^{b}	-14.33	0
	1830	0.55 ± 0.01^{c}	-56.89	-3	1.12 ± 0.15^{d}	-41.78	-3
26	0	1.28 ± 0.03^{ab}	0.00	0	1.92 ± 0.18^{bc}	0.00	0
	0.183	1.31 ± 0.02^{ab}	2.18	0	1.63 ± 0.13^{bcd}	-15.20	0
	1.83	1.27 ± 0.04^{abc}	-1.37	0	1.58 ± 0.17^{cd}	-17.76	0
	18.3	1.26 ± 0.06^{abc}	-1.92	0	1.52 ± 0.25^{cd}	-20.80	-1
	183	1.25 ± 0.03^{abc}	-2.92	0	1.47 ± 0.11^{cd}	-23.44	-1
	1830	0.81 ± 0.03^{e}	-37.06	-3	1.62 ± 0.20^{cd}	-15.63	0
27	0	1.28 ± 0.03^{a}	0.00	0	1.92 ± 0.18^{bde}	0.00	0
	0.183	1.28 ± 0.04^{a}	-0.57	0	2.52 ± 0.45^{c}	31.74	+
	1.83	1.29 ± 0.06^{a}	0.23	0	1.99 ± 0.23^{bd}	4.07	0
	18.3	1.29 ± 0.05^{a}	0.20	0	1.95 ± 0.11^{bd}	1.79	0
	183	1.29 ± 0.02^{a}	0.60	0	1.67 ± 0.18^{be}	-12.90	0
	1830	1.15 ± 0.03^{b}	-10.65	-1	1.71 ± 0.16^{be}	-10.97	0

Table 3, part d. Planktonic growth and cells adhesion in the presence of each ZA related compound. Percentage reduction respect to the negative control is reported. a) Percentage reduction of the maximum specific growth rate: code (0) $x > -10$ %; code (-1) $-10\ \% \leq x < -20$ %; code (-2) $-20\ \% \leq x < -30$ %; code (-3) $x \leq -30$ %; b) Percentage reduction of the number of adhered cells: code (+1) $x > +20$ %; code (0) $+20\ \% \leq x < -20$ %; code (-1) $-20\ \% \leq x < -30$ %; code (-2) $-30\ \% \leq x < -40$ %; code (-3) $x \leq -40$ %. According to post hoc analysis (Tukey's HSD, $p < 0.05$), data sharing the same letter indicates no significant difference.

		Planktonic growth			Cells adhesion		
Cmpd	**Conc. (μM)**	**OD600/min ($x10^{-3}$)**	**% reduction**	**Code (a)**	**No. adhered cells ($x10^{7}$)**	**% reduction**	**Code (b)**
28	0	1.28±0.03^{a}	0.00	0	1.92±0.18^{b}	0.00	0
	0.183	1.31±0.02^{a}	1.67	0	1.94±0.01^{b}	1.10	0
	1.83	1.28±0.02^{a}	-0.20	0	1.99±0.15^{b}	3.77	0
	18.3	1.28±0.03^{a}	-0.61	0	1.76±0.10^{b}	-8.15	0
	183	1.28±0.05^{a}	0.01	0	1.26±0.18^{c}	-34.39	-2
	1830	0.86±0.02^{c}	-33.01	-3	0.92±0.14^{d}	-52.00	-3
29	0	1.28±0.03^{a}	0.00	0	1.92±0.18^{bd}	0.00	0
	0.183	1.29±0.05^{a}	0.29	0	2.56±0.26^{c}	33.75	1
	1.83	1.29±0.04^{a}	0.23	0	1.79±0.11^{bd}	-6.83	0
	18.3	1.31±0.06^{a}	1.72	0	1.93±0.24^{bd}	0.73	0
	183	1.28±0.05^{a}	-0.43	0	2.14±0.15^{bcd}	11.51	0
	1830	0.76±0.02^{b}	-40.52	-3	1.42±0.27^{d}	-25.78	-1
30	0	1.28±0.03^{a}	0.00	0	1.92±0.18^{be}	0.00	0
	0.183	1.23±0.01^{a}	-3.95	0	2.38±0.21^{ce}	24.26	1
	1.83	1.29±0.02^{a}	0.31	0	1.82±0.18^{be}	-5.29	0
	18.3	1.32±0.03^{a}	2.86	0	1.97±0.19^{be}	2.99	0
	183	1.26±0.05^{a}	-2.10	0	2.06±0.22^{bce}	7.33	0
	1830	0.83±0.03^{b}	-35.51	-3	1.40±0.16^{f}	-26.98	-1
31	0	1.28±0.03^{a}	0.00	0	1.92±0.18^{b}	0.00	0
	0.183	1.23±0.03^{a}	-3.94	0	2.85±0.43^{c}	48.69	1
	1.83	1.26±0.00^{a}	-2.14	0	1.58±0.29^{b}	-17.68	0
	18.3	1.29±0.01^{a}	0.61	0	1.99±0.43^{b}	4.02	0
	183	1.24±0.04^{a}	-3.25	0	1.85±0.22^{b}	-3.23	0
	1830	0.82±0.02^{d}	-36.19	-3	0.94±0.19^{e}	-50.79	-3
32	0	1.28±0.03^{a}	0.00	0	1.92±0.18^{bc}	0.00	0
	0.183	1.29±0.07^{a}	0.30	0	1.39±0.15^{abc}	-27.34	-1
	1.83	1.27±0.05^{a}	-0.88	0	1.64±0.11^{bc}	-14.39	0
	18.3	1.27±0.04^{a}	-1.26	0	1.83±0.14^{bc}	-4.30	0
	183	1.28±0.06^{a}	-0.16	0	1.62±0.19^{bc}	-15.26	0
	1830	1.25±0.02^{a}	-2.25	0	5.45±1.00^{e}	184.36	1
33	0	1.28±0.03^{a}	0.00	0	1.92±0.18^{b}	0.00	0
	0.183	1.25±0.06^{a}	-2.75	0	3.90±0.27^{c}	103.54	1
	1.83	1.26±0.03^{a}	-1.49	0	1.88±0.09^{b}	-1.99	0
	18.3	1.32±0.02^{a}	2.61	0	1.45±0.19^{d}	-24.08	-1
	183	1.13±0.03^{b}	-12.31	-1	1.31±0.24^{d}	-31.43	-2
	1830	0.74±0.02^{de}	-42.25	-3	1.51±0.16^{d}	-21.25	-1
34	0	1.28±0.03^{a}	0.00	0	1.92±0.18^{b}	0.00	0
	0.183	1.26±0.03^{a}	-2.19	0	5.75±0.32^{e}	199.95	1
	1.83	1.28±0.05^{a}	0.08	0	1.93±0.16^{bc}	0.83	0
	18.3	1.29±0.04^{a}	0.64	0	1.14±0.09^{bc}	-40.43	-3
	183	1.10±0.02^{b}	-14.41	-1	3.02±0.12^{d}	57.49	1
	1830	1.00±0.04^{c}	-22.27	-2	2.64±0.31^{d}	37.76	1

Table 3, part e. Planktonic growth and cells adhesion in the presence of each ZA related compound. Percentage reduction respect to the negative control is reported. a) Percentage reduction of the maximum specific growth rate: code (0) $x > -10$ %; code (-1) $-10\ \% \leq x < -20$ %; code (-2) $-20\ \% \leq x < -30$ %; code (-3) $x \leq -30$ %; b) Percentage reduction of the number of adhered cells: code (+1) $x > +20$ %; code (0) $+20\ \% \leq x < -20$ %; code (-1) $-20\ \% \leq x < -30$ %; code (-2) $-30\ \% \leq x < -40$ %; code (-3) $x \leq -40$ %. According to post hoc analysis (Tukey's HSD, $p < 0.05$), data sharing the same letter indicates no significant difference.

		Planktonic growth			Cells adhesion		
Cmpd	**Conc. (μM)**	**OD600/min ($x10^{-3}$)**	**% reduction**	**Code (a)**	**No. adhered cells ($x10^{7}$)**	**% reduction**	**Code (b)**
35	0	1.28±0.03^{a}	0.00	0	1.92±0.18^{bcd}	0.00	0
	0.183	1.26±0.05^{a}	-2.19	0	2.87±0.56^{bc}	49.69	1
	1.83	1.25±0.07^{a}	-2.61	0	1.72±0.19^{bd}	-10.13	0
	18.3	1.16±0.03^{b}	-9.96	0	1.12±0.14^{e}	-41.80	-3
	183	0.92±0.05^{c}	-28.33	-2	2.85±0.31^{f}	48.83	1
	1830	0.55±0.02^{d}	-56.93	-3	5.72±0.25^{h}	198.51	1
36	0	1.28±0.03^{ab}	0.00	0	1.92±0.18^{bdf}	0.00	0
	0.183	1.23±0.02^{abc}	-4.03	0	2.87±0.56^{c}	49.69	1
	1.83	1.24±0.02^{abc}	-3.79	0	1.78±0.24^{bd}	-7.38	0
	18.3	1.21±0.03^{bcd}	-5.71	0	1.13±0.17^{e}	-40.87	-3
	183	1.15±0.04^{cd}	-10.75	-1	2.27±0.17^{bf}	18.70	0
	1830	1.08±0.02^{d}	-15.57	-1	5.60±0.65^{h}	192.07	1
37	0	1.28±0.03^{ab}	0.00	0	1.92±0.18^{b}	0.00	0
	0.183	1.32±0.04^{ab}	2.71	0	2.46±0.17^{b}	28.52	1
	1.83	1.28±0.07^{ab}	-0.56	0	2.36±0.26^{b}	23.00	1
	18.3	1.30±0.03^{ab}	1.27	0	1.35±0.28^{b}	-29.61	-1
	183	1.24±0.05^{a}	-3.17	0	5.08±0.53^{c}	164.82	1
	1830	0.88±0.02^{c}	-31.64	-3	5.43±0.76^{c}	183.29	1
38	0	1.28±0.03^{a}	0.00	0	1.92±0.18^{bd}	0.00	0
	0.183	1.31±0.13^{a}	2.28	0	3.79±0.61^{c}	98.02	1
	1.83	1.31±0.01^{a}	1.66	0	3.69±0.41^{c}	92.49	1
	18.3	1.31±0.03^{a}	2.24	0	3.54±0.20^{c}	84.50	1
	183	1.24±0.03^{a}	-3.39	0	2.11±0.14^{bd}	9.90	0
	1830	1.22±0.03^{a}	-4.98	0	4.30±1.01^{c}	124.16	1
39	0	1.28±0.03^{a}	0.00	0	1.92±0.18^{b}	0.00	0
	0.183	1.29±0.03^{a}	0.31	0	1.86±0.35^{b}	-3.07	0
	1.83	1.27±0.04^{a}	-0.89	0	1.94±0.34^{b}	1.04	0
	18.3	1.26±0.06^{a}	-2.16	0	1.98±0.24^{b}	3.58	0
	183	1.27±0.02^{a}	-1.39	0	2.10±0.50^{b}	9.41	0
	1830	0.95±0.05^{b}	-25.66	-2	1.83±0.19^{b}	-4.37	0
40	0	1.28±0.03^{a}	0.00	0	1.92±0.18^{bd}	0.00	0
	0.183	1.26±0.04^{a}	-2.04	0	3.21±0.39^{cd}	67.46	1
	1.83	1.24±0.03^{a}	-3.05	0	1.90±0.20^{bcd}	-0.85	0
	18.3	1.29±0.05^{a}	0.56	0	1.92±0.16^{bcd}	0.24	0
	183	1.31±0.03^{a}	2.23	0	1.93±0.28^{bcd}	0.60	0
	1830	0.82±0.03^{b}	-36.31	-3	1.39±0.24^{bd}	-27.57	-1
41	0	1.28±0.03^{ac}	0.00	0	1.92±0.18^{b}	0.00	0
	0.183	1.27±0.04^{abc}	-0.89	0	2.09±0.40^{b}	9.15	0
	1.83	1.24±0.04^{ab}	-3.19	0	1.63±0.21^{d}	-15.16	0
	18.3	1.24±0.03^{ab}	-3.45	0	1.87±0.20^{bd}	-2.50	0
	183	1.33±0.03^{ac}	3.88	0	1.13±0.38^{ae}	-41.15	-3
	1830	1.16±0.03^{d}	-9.88	0	0.70±0.08^{ae}	-63.30	-3

Table 3, part f. Planktonic growth and cells adhesion in the presence of each ZA related compound. Percentage reduction respect to the negative control is reported. a) Percentage reduction of the maximum specific growth rate: code (0) x > -10 %; code (-1) -10 % ≤ x < -20 %; code (-2) -20 % ≤ x < -30 %; code (-3) x ≤ -30 %; b) Percentage reduction of the number of adhered cells: code (+1) x > +20 %; code (0) +20 % ≤ x < -20 %; code (-1) -20 % ≤ x < -30 %; code (-2) -30 % ≤ x < -40 %; code (-3) x ≤ -40 %. According to post hoc analysis (Tukey's HSD, $p < 0.05$), data sharing the same letter indicates no significant difference.

		Planktonic growth			Cells adhesion		
Cmpd	**Conc. (μM)**	**OD600/min ($x10^{-3}$)**	**% reduction**	**Code (a)**	**No. adhered cells ($x10^{7}$)**	**% reduction**	**Code (b)**
42	0	1.28 ± 0.03^{ab}	0.00	0	1.92 ± 0.18^{b}	0.00	0
	0.183	1.29 ± 0.01^{abc}	0.16	0	3.30 ± 0.53^{c}	72.26	1
	1.83	1.31 ± 0.05^{abc}	1.96	0	1.84 ± 0.15^{b}	-3.76	0
	18.3	1.33 ± 0.01^{bc}	3.53	0	1.78 ± 0.18^{b}	-7.28	0
	183	1.30 ± 0.01^{abc}	1.04	0	1.68 ± 0.29^{b}	-12.13	0
	1830	1.03 ± 0.02^{d}	-19.39	-1	2.23 ± 0.38^{d}	16.50	0
43	0	1.28 ± 0.03^{a}	0.00	0	1.92 ± 0.18^{bd}	0.00	0
	0.183	1.28 ± 0.04^{a}	-0.38	0	2.67 ± 0.45^{cd}	39.31	1
	1.83	1.29 ± 0.05^{a}	0.55	0	2.00 ± 0.28^{bcd}	4.48	0
	18.3	1.30 ± 0.02^{a}	1.61	0	1.99 ± 0.33^{bd}	4.03	0
	183	1.27 ± 0.03^{a}	-1.19	0	1.95 ± 0.34^{bcd}	1.86	0
	1830	1.03 ± 0.04^{b}	-19.67	-1	1.66 ± 0.33^{bd}	-13.31	0

Table 3, part g. Planktonic growth and cells adhesion in the presence of each ZA related compound. Percentage reduction respect to the negative control is reported. a) Percentage reduction of the maximum specific growth rate: code (0) $x > -10$ %; code (-1) $-10\ \% \leq x < -20$ %; code (-2) $-20\ \% \leq x < -30$ %; code (-3) $x \leq -30$ %; b) Percentage reduction of the number of adhered cells: code (+1) $x > +20$ %; code (0) $+20\ \% \leq x < -20$ %; code (-1) $-20\ \% \leq x < -30$ %; code (-2) $-30\ \% \leq x < -40$ %; code (-3) $x \leq -40$ %. According to post hoc analysis (Tukey's HSD, $p < 0.05$), data sharing the same letter indicates no significant difference.

Molecule	0 µM	0.183 µM	1.83 µM	18.3 µM	183µM	1830 µM	Trend
7							1
12							
18							
19							
39							
27							2
24							
42							
43							
29							
30							
31							
40							
41							3
14							
15							
26							
8							
21							
28							
13							
20							
6							
10							
1							
2							
11							
5							
9							
23							
4							
3							
ZA							4
22							
35							
34							
36							
25							
16							
17							
33							
32							5
38							
37							

Figure 5. Biological activity of each ZA related compound at the different tested concentrations. No biological activity; Anti-biofilm activity; Increased biofilm formation; Planktonic to biofilm mode of life transition; Biocidal effect.

Molecule	0 µM	0.183 µM	1.83 µM	18.3 µM	183µM	1830 µM	Total value
37							6
24							5
35							5
38							4
29							3
30							3
40							3
34							3
18							3
25							2
27							2
42							2
43							2
39							2
15							2
31							1
33							1
36							1
19							1
26							1
12							0
7							0
14							0
32							0
16							-1
21							-2
28							-2
13							-2
6							-2
5							-2
23							-2
ZA							-3
17							-3
9							-3
10							-3
2							-3
4							-3
22							-4
11							-5
1							-5
41							-6
20							-6
8							-8
3							-9

Figure 6. Anti-biofilm performance of each ZA related compound. Total and related to each concentration value is reported. Anti-biofilm performance: ≥ 3, = 2; = 1; = 0; = -1; = -2; ≤ -3.

Discussion

Zosteric acid (ZA) has been proposed as a new anti-biofilm compound able to counteract both bacterial and fungal biofilm formation (Villa et al., 2010; Villa et al., 2011). Advantages would be conferred by covalently coupling this molecule to the surface of a material in a way to preserve the biological function. The development of this preventive strategy is limited by the lack of information about the structural chemical determinants responsible of its anti-biofilm activity. Previously Stanley and colleagues (2002) hypothesized that the antifouling effect of ZA lies in the high affinity for water shown by its sulfate groups that increase the cell surface hydrophility. In contrast, Villa and co-authors (2011) demonstrated that the activity of methyl zosterate, which carboxylate moiety was replaced by a methyl ester group, had no anti-biofilm ability, suggesting that the activity of ZA sodium salt is not due to the presence of the sulfo-oxy ester group.

In this research a new series of chemically modified molecules related to ZA scaffold were planned and investigated with the aim to better understand the structural requirements responsible for ZA the anti-biofilm activity. Compounds were characterized by the introduction of substituents at different positions on phenyl ring and several side-chain modifications, such as the removal of the insaturation and the substitution of the carboxylic acid with an alcohol, an aldehyde and ester functionalities. Moreover, both E/Z isomers were prepared in order to explore the role of the double bond.

All these molecules were submitted to a biological screening considering ZA as reference compound and using *E. coli* as model bacterial system. The molecules were tested at different concentrations starting from 1830 µM that is the concentration at which ZA performs its best anti-biofilm activity (Villa et al., 2010). Three % DMSO successfully solubilized the molecules inside the media affecting neither planktonic growth nor cell adhesion. This is in line with the results obtained by Pottz and collaborators (1967) who reported that the bacteriostatic concentration of DMSO for *E. coli* is 10% while the bactericidal concentration is above 30%. Bodini and coauthors (2009) also showed that DMSO did not significantly affect biofilm formation even at close-to-lethal concentrations.

With the aim to identify trends, planktonic growth and cells adhesion data were grouped to obtain a global picture of the biological activity of each ZA related compound at the different concentrations. Molecules showed different biological activity depending on their concentration. At the highest concentrations, most of molecules inhibited biofilm formation and drastically reduced planktonic growth. Therefore, it was assumed that the suppression of biofilm formation was a result from the inhibition of bacterial growth rather than from specific anti-biofilm effects of the substances. Other molecules at the highest concentrations enhanced biofilm formation and also reduced bacteria planktonic growth. In this case the transition to the sessile mode of life was assumed as a protective response to survival in hostile environments (Davey et al., 2000; Donlan et al., 2002; Villa et al., 2012c). At high concentrations the movement of cells toward surfaces could be considered the step immediately before the killing effect as a kind of protecting way against hard stress condition (Plyuta et al., 2013). At the lowest concentrations, an enhancement of biofilm formation was also demonstrated for many of the molecules investigated. Biofilm enhancement by low concentration of small molecules is not new in the biofilm world. Very low concentrations of low-molecular weight compounds released as exudates by plants can act as chemical signals inducing bacteria to colonize specific plant areas developing a complex biofilm that positively interacts with the plant itself (Bais et al., 2006). Plyuta and colleagues (2013) demonstrated that very high concentration of several phenolic acid compounds completely suppressed *Pseudomonas aeruginosa* biofilm as a killing effect. In contrast, *P. aeruginosa* biofilm formation was up to 2- to 3-fold increased and planktonic growth was 20-50% reduced under the action of some phenolic acids compared with the biofilm formed in their absence (Plyuta et al., 2013). Recent evidences also suggested that high concentration of some antibiotics eradicates bacteria while sub-inhibitory concentrations of them induce biofilm formation

(Hoffman et al., 2005; Linares et al., 2006; Migliore et al., 2013; Salta et al., 2013). Zaitseva and coauthors (2009) also observed the same effect for *P. aeruginosa* and *Burkholderia cenocepacia* under the action of some antimicrobial agents as nitrofurans and nitric oxide generators. Plyuta and collaborators (2013) hypothesized that enhancement of biofilm formation at sub-inhibitory concentrations of antibacterial drugs is probably a useful strategy of pathogenic bacteria facilitating their survival after intense antibiotic therapy, when low quantities of drugs remain in the human organism. Biofilm formation by plant pathogenic bacteria might be also an important factor of their protection against antibacterial action of plant-produced phenolics (Walker et al., 2004). However, the mechanisms underlying stimulation of biofilm formation at sub-inhibitory or weakly bacterial growth-suppressing compound concentrations are currently unclear. As biofilm formation is a multi-stage process, these substances can affect several targets (Plyuta et al., 2013).

Each ZA related compound was also associated to a global anti-biofilm performance value, calculated so that to take into account the occurrence that ZA related compounds induced a different bacterial response depending on their concentration and the positive or negative contribution of each single concentration to the global anti-biofilm performance. A reduction of adhered cells were considered a positive contribution to the anti-biofilm performance value, while both the increase of the adhered cells and the decrease of planktonic growth were considered a negative contribution.

The molecules grouped on the basis on both their biological activity and anti-biofilm performance value allowed to recognize some chemical structure require to exert anti-biofilm activity. Structure-activity relationship considerations revealed that the carboxylic acid moiety conjugated to the double bond in *trans* configuration was an essential requirement in ZA chemical structure to guarantee a good anti-biofilm performance, while the deletion of the sulphate ester group seems not to compromise the ZA anti-biofilm activity. Moreover the study revealed that the *para* position on the phenyl ring could be considered a good point for the coupling to a polymer. Indeed *p*-aminocinnamic acid bearing the same ZA active scaffold and an amino group in the para position of the phenyl ring was selected as suitable compounds to form a covalent linkage with appropriate functional groups of the polymeric material.

Among the tested molecules, *p*-coumaric acid and *trans* cinnamaldehyde were previously investigated for their anti-biofilm properties against *E. coli*. Bodini and coauthors (2009) showed that millimolar amounts of *p*-coumaric acid did not affect *E. coli* quorum sensing activity. In our work we found that *p*-coumaric acid is able to reduce bacterial adhesion more than 40%, suggesting that this molecule has an anti-biofilm activity which mechanism is not related to quorum sensing. Niu and collaborators (2004, 2006) reported that at sub-lethal concentration *trans* cinnamaldehyde was effective against *E. coli* biofilm reducing the quorum sensing activity, leading to a morphological damage of cells and decreasing swimming motility. Similarly Brackman and co-authors (2008, 2011) showed that cinnamaldehyde and some cinnamaldehyde derivatives, at concentration that not affect bacterial growth, interfere with autoinducer-2 based quorum sensing in various *Vibrio* spp. by decreasing the DNA-binding activity of the response regulator LuxR. Our data indicated that *trans* cinnamaldehyde did not affect cells adhesion. It is reasonable to suppose that *trans* cinnamaldehyde has an effect during maturation but not in the first step of biofilm formation.

Conclusion

A series of structurally-related compounds was developed and tested and the performed studies highlighted the key role of specific structural features in relation to their anti-biofilm activity. As cinnamic acid showed an inhibitory activity also at 1000-fold minor concentration compared with ZA, it was identified as a promising anti-biofilm agent. In details, the carboxylic acid moiety conjugated to a double bond in *trans* configuration was an essential requirement for the inhibition of the biofilm

growth. Moreover, the anti-biofilm activity was also affected by the nature and the position of substituents on the phenyl ring. In conclusion, the cinnamic acid scaffold could be considered the starting point for the development of a new generation of derivatives characterized by improved activity to study and modulate bacterial adhesion.
A further advance of this work might be the grafting of selected molecules, showing a good anti-biofilm activity and presenting specific functional groups, to a polymeric surface, obtaining a new material able to inhibit the sessile growth.

References

Andersson D., Hughes D. (2010). Antibiotic resistance and its cost: is it possible to reverse resistance? *Nature Reviews Microbiology*, 8:260-271.

Bais H.P., Weir T.L., Perry L.G., Gilroy S., Vivanco J.M. (2006). The role of root exudates in rhizosphere interactions with plants and other organisms. *Annual Review of Plant Biology*, 57:233-266.

Barrios C.A., Xu Q., Cutright T., Newby B.Z. (2005). Incorporating zosteric acid into silicone coatings to achieve its slow release while reducing fresh water bacterial attachment. *Colloids and Surface B: Biointerface*, 41:83-93.

Bodini S.F., Manfredini S., Epp M., Valentini S., Santori F. (2009). Quorum sensing inhibition activity of garlic extract and p-coumaric acid. *Letters in Applied Microbiology*, 49:551-555.

Brackman G., Defoirdt T., Miyamoto C., Bossier P., Van Calenbergh S., Nelis H., Coenye T. (2008). Cinnamaldehyde and cinnamaldehyde derivatives reduce virulence in *Vibrio* spp. by decreasing the DNA-binding activity of the quorum sensing response regulator LuxR. *BMC Microbiology*, 8:149.

Brackman G., Celen S., Hillaert U., Van Calenbergh S., Cos P., Maes L., Nelis H., Coenye T. (2011). Structure-activity relationship of cinnamaldehyde analogs as inhibitors of AI-2 based quorum sensing and their effect on virulence of *Vibrio* spp. *PLoS ONE*, 6: e16084.

Cappitelli F., Polo A., Villa F. (2014). Biofilm formation in food processing environments is still poorly understood and controlled. *Food Engineering Reviews*, 6: 29-42.

Costerton J.W., Cheng K.-J., Geesey G.G., Ladd T.I., Nickel J.C., Dasgupta M., Marrie T.J. (1987). Bacterial biofilms in nature and disease. *Annual Review of Microbiology*, 41: 435-464.

Darouiche R.O. (2007.) Antimicrobial coating of devices for prevention of infection: principles and protection. *The International Journal of Artificial Organs*, 30:820-827.

Davey M.E., O'Toole G.A. (2000). Microbial biofilms: from ecology to molecular genetics. *Microbiology and Molecular Biology Reviews*, 64: 847-867.

De P., Koumba Yoya G., Constant P., Bedos-Belval F., Duran H., Saffon N., Daffé M., Baltas M. (2011). Design, synthesis, and biological evaluation of new cinnamic derivatives as antituberculosis agents. *Journal of Medicinal Chemistry*, 54:1449-1461.

Donlan R.M., Costerton J.W. (2002). Biofilms: survival mechanisms of clinically relevant microorganisms. *Clinical Microbiology Reviews*, 15:167-193.

Donlan R.M. (2011). Biofilm elimination on intravascular catheters: important considerations for the infectious disease practitioner. *Clinical Infectious Diseases*, 52:1038-1045.

Geiger T., Delavy P., Hany R., Schleuniger J., Zinn M. (2004). Encapsulated zosteric acid embedded in poly[3-hydroxyalkanoate] coatings—Protection against biofouling. *Polymer Bulletin*, 52:65-72.

Hall-Stoodley L., Costerton W.J., Stoodley P. (2004). Bacterial biofilms: from the natural environment to infectious diseases. *Nature Review Microbiology*, 2: 95-108.

Hoffman L.R., D'Argenio D.A., MacCoss M.J., Zhang Z., Jones R.A., Miller S.I. (2005). Aminoglycoside antibiotics induce biofilm formation. *Nature*, 436:1171-1175.

Kaplan J.B. (2009). Therapeutic potential of biofilm-dispersing enzymes. *The International Journal of Artificial Organs*, 32:545-554.

Linares J.F., Gustaffson I., Baquero F., Martinez J.L. (2006). Antibiotics as intermicrobial signaling agents instead of weapons. *Proceedings of the National Academy of Sciences USA*, 103:19484-19489.

Migliore L., Rotini A., Thaller M.C. (2013). Low doses of tetracycline trigger the *E. coli* growth: a case of hormetic response. *Dose-Response*, 11:550-557.

Newby B.Z., Cutright T., Barrios C.A., Xu Q. (2006). Zosteric acid-An effective antifoulant for reducing fresh water bacterial attachment on coatings. *The University of Akron*, 3: 69-77.

Niu C., Gilbert E.S. (2004). Colorimetric method for identifying plant essential oil components that affect biofilm formation and structure. *Applied and Environmental Microbiology*, 70:6951-6956.

Niu C., Afre S., Gilbert E.S. (2006). Subinhibitory concentrations of cinnamaldehyde interfere with quorum sensing. *Letters in Applied Microbiology*, 43:489-494.

Plyuta V.A., Lipasovaa V.A., Kuznetsovb A.E., Khmela I.A. (2013). Effect of salicylic, indole-3-acetic, gibberellic, and abscisic acids on biofilm formation by *Agrobacterium tumefaciens* C58 and *Pseudomonas aeruginosa* PAO1. *Applied Biochemistry and Microbiology*, 49: 706-710.

Polo A., Foladori P., Ponti B., Bettinetti R., Gambino M., Villa F., Cappitelli F. (2014). Evaluation of zosteric acid for mitigating biofilm formation of *Pseudomonas putida* isolated from a membrane bioreactor system *International Journal of Molecular Sciences*, 15: 9497-9518.

Pottz G.E., Rampey J.H., Benjamin F. (1967). The effect of dimethyl sulfoxide (DMSO) on antibiotic sensitivity of a group of medically important microorganisms: preliminary report. *Annals of the New York Academy of Sciences*, 141:261-272.

Salta M., Wharton J.A., Dennington S.P., Stoodley P., Stokes K.R. (2013). Anti-biofilm performance of three natural products against initial bacterial attachment. *International Journal of Molecular Sciences*, 14:21757-21780.

Smith A.W. (2005). Biofilms and antibiotic therapy: Is there a role for combating bacterial resistance by the use of novel drug delivery systems? *Advanced Drug Delivery Reviews*, 57: 1539-1550.

Stanley M.S., Callow M.E., Perry R., Alberte R.S., Smith R., Callow J.A. (2002). Inhibition of fungal spore adhesion by zosteric acid as the basis for a novel, non-toxic crop protection technology. *Phytopathology*, 92: 378-383.

Szymanski W., Wu B., Weiner B., de Wildeman S., Feringa B.L., Janssen D.B. (2009). Phenylalanine aminomutase-catalyzed addition of ammonia to substituted cinnamic acids: a route to enantiopure alpha- and beta-amino acids. *The Journal of Organic Chemistry*, 74:9152-9157.

Villa F., Giacomucci L., Polo A., Principi P., Toniolo L., Levi M., Turri S., Cappitelli F. (2009). N-vanillylnonanamide tested as a non-toxic antifoulant, applied to surfaces in a polyurethane coating. *Biotechnology Letters*, 31: 1407-1413.

Villa F., Albanese D., Giussani B., Stewartd P. S., Daffonchio D., Cappitelli F. (2010). Hindering biofilm formation with zosteric acid. *Biofouling*, 26: 739-752.

Villa F., Pitts B., Stewart P.S., Giussani B., Roncoroni S., Albanese D., Giordano C., Tunesi M., Cappitelli F. (2011). Efficacy of zosteric acid sodium salt on the yeast biofilm model *Candida albicans*. *Microbial Ecology*, 62: 584-598.

Villa F., Borgonovo G., Cappitelli F., Giussani B., Bassoli A. (2012a). Sub-lethal concentrations of *Muscari comosum* bulb extract suppress adhesion and induce detachment of sessile yeast cells. *Biofouling*, 28:1107-1117.

Villa F., Remelli W., Forlani F., Vitali A., Cappitelli F. (2012b). Altered expression level of *Escherichia coli* proteins in response to treatment with the antifouling agent zosteric acid sodium salt. *Environmental Microbiology*, 14: 1753-1761.

Villa F., Remelli W., Forlani F., Gambino M., Landini P., Cappitelli F. (2012c). Effects of chronic sub-lethal oxidative stress on biofilm formation by *Azotobacter vinelandii*. *Biofouling*, 28: 823-833.

Villa F., Cappitelli F. (2013). Plant-derived bioactive compounds at sub-lethal concentrations: towards smart biocide-free antibiofilm strategies. *Phytochemistry Reviews*, 12: 245-254.

Von Eiff C., Kohnen W., Becker K., Jansen B. (2005). Modern strategies in the prevention of implant-associated infections. *The International Journal of Artificial Organs*, 28: 1146-1156.

Walker T.S., Bais H.P., Déziel E., Schweizer H.P., Rahme L.G., Fall R., Vivanco J.M. (2004). *Pseudomonas aeruginosa* – plant root interactions. Pathogenicity, biofilm formation, and root exudation. *Plant Physiology*, 134:320-331.

Wong C.C., Cheng K.W., He Q., Chen F. (2008). Unraveling the molecular targets of natural products: insights from genomic and proteomic analyses. *Proteomics Clinical Application*, 2: 338-354.

Zaitseva J., Granik V., Belik A., Koksharova O., Khmel I. (2009). Effect of nitrofurans and generators on biofilm formation by *Pseudomonas aeruginosa* PAO1 and *Burkholderia cenocepacia* 370. *Research in Microbiology*, 160:353-357.

Zwietering M.H., Jongenburger I., Rombouts F.M., van't Riet K. (1990). Modeling of the bacterial growth curve. *Applied and Environmental Microbiology*, 56:1875-1881.

Scansion of *Escherichia coli* proteome for zosteric acid and salicylic acid target identification

Abstract

Recently the natural compounds zosteric acid and salicylic acid have been proposed as alternative biocide-free agents suitable for a preventive or integrative approach against biofilm formation. Beside these important results, the lack of information concerning the mechanism of action and the cellular receptors involved in their anti-biofilm activity limits the efforts to generate more potent derivatives based on the same target and activity structure. In this study, an affinity chromatography proteomic approach was employed to scan the entire *Escherichia coli* proteome with the aim to identify the molecular targets that directly interact with the anti-biofilm compounds zosteric acid and salicylic acid. Mass spectrometry analysis of SDS-PAGE-resolved pull-down proteins reveal that both zosteric acid and salicylic acid in *E. coli* directly interact with the same protein WrbA, suggesting a possible role of this protein in the biofilm formation process. Protein FkpA and Tdh were also identified as possible target for salicylic acid. However, many interpretations about the interaction of zosteric acid and salicylic with these proteins are possible and further experiments are necessary to clarify this question.

Introduction

The worldwide safety is seriously affected by the emergence and spread of microorganisms in form of biofilm, complex differentiated surface-associated microbial community embedded in a self-produced polymeric matrix (Stoodley et al., 2002). All human artefact surfaces like industrial installations, work benches, harbor systems and also medical devices are susceptible to biofilm colonization with important consequences in term of social and economic impact (Hall-Stoodley, 2004). The most detrimental problem is that microorganisms in form of biofilm are up to several orders of magnitude more resistant to antimicrobial agents making their removal from surfaces difficult or even impossible. In addition, increasingly restrictive regulations have banned the use of several biocides hazardous to human health and the environment leading to the inevitable need to develope innovative strategies (Villa et al., 2012).

An innovative approach could be the use of biocide-free anti-biofilm compounds with novel targets, unique modes of action and properties that are different from those of the currently used antimicrobial agents. Nature has been proposed as an important source of new bioactive substances able to exert anti-biofilm properties at sub-lethal concentrations. These behave anticipating biofilm formation by interfering with specific key step of its formation (Villa et al., 2013). Since this approach deprives microorganisms of their virulence properties without affecting their existence, the selection pressure for antibiotics and biocides resistance mutations decrease, posing promising perspective to restore the efficacy of traditional antimicrobial agents (Rasko et al., 2010). Despite the successes, many pharmaceutical companies have scaled down their efforts on natural products in favor of newer and faster combinatorial synthesis technologies. Parallel synthesis allows the rapid construction of compound libraries suitable for high-throughput screening. However, the perceived burst in innovative solutions through combinatorial synthesis has not been materialized. Combinatorial compounds are not so effective as natural compounds often exerting their effects in the micromolar range, in contrast

to high potency exhibited by many natural products (Cong et al., 2012). For these reasons, the interest in natural products has been rekindled. Recently, the emphasis has been placed on approaches that combine the power of natural products and organic chemistry that lead to optimize processes or the synthesis of natural product mimics (Ortholand et al., 2004). The potential bottleneck of this approach is the general lack of information concerning the mechanism of action and cellular receptors of many bioactive natural products. Without an understanding of the nature of products-targets binding, efforts to generate more potent derivatives or mimics through structure-activity relationship studies may prove futile. In addition, identification of targets allows the prediction of potential toxicities in an early stage of drug development and the prioritization of drug candidates (Wong et al., 2008).
Recently, the natural compounds zosteric acid (ZA) and salicylic acid (SA) have been proposed as alternative biocide-free agents suitable for a preventive or integrative approach against biofilm formation. Both ZA and SA were proved to reduce, at sub-lethal concentrations, both bacterial and fungal adhesion and play a role in shaping biofilm architecture, in reducing biofilm biomass and thickness and in extending the performance of antimicrobial agents (Barrios et al., 2005; Villa et al., 2010; Villa et al., 2011; El-Banna et al., 2012; Polo et al., 2014). Proteomic study on *E. coli* suggested that ZA acts as environmental cue leading to global stress on bacterial cells, which favors the expression of various protective proteins, the signal molecule autoinducer-2 production, and the synthesis of flagella, to escape from adverse conditions (Villa et al., 2012). Other researchers hypothesized that SA interferes with bacterial quorum sensing signals involved in biofilm formation and inhibits bacteria motility suggesting the presence of a complex and overlapping effect against biofilm cells (Bandara et al., 2006; Yang et al., 2009; Chow et al., 2011; Lagonenko et al., 2013).
The aim of this research is to elucidate the molecular targets and pathways involved in ZA and SA anti-biofilm activity, as a starting point to develop new improved and more efficient anti-biofilm solutions. In this study, the proteomic approach of the affinity chromatography coupled with mass spectrometry analysis was used for ZA and SA *E. coli* cellular target identification. As this approach identifies the direct binding targets of a compound, the true targets of ZA and SA were isolated among a complex mixture of proteins and no indirect inferences of a target hypothesis were generated. Moreover, in this approach the entire proteome is scanned for targets identification instead of relying on a predefined set of recombinant proteins, as in the case of other approaches offering high selectivity and resolution for the proteins of interest.

Materials and Methods

Escherichia coli strain and growth condition

The best characterized *Escherichia coli* strain K-12 ATCC 25404 wild type was used throughout the study. The strain was stored at –80 °C in suspensions containing 20 % glycerol and 2 % peptone, and was routinely grown in Luria-Bertani broth (LB, Sigma-Aldrich) at 30 °C for 16 h.

Compound synthesis

Cinnamic acid (CA), *p*-aminocinnamic acid (*p*-ACA), salicylic acid (SA), *p*-aminosalicylic acid (*p*-ASA) were purchased by Sigma-Aldrich and were used without any further purification (Figure 1). Zosteric acid (ZA) was synthesized as already described in a previous work by Villa and collaborators (2010).

Biological assay

ZA, CA, *p*-ACA, SA, *p*-ASA were used in planktonic growth, carbon source and biofilm assays at 0 (negative control), 0.183, 1.83, 18.3, 183 and 1830 µM with the addition of 3 % of dimethyl sulphoxyde to make the molecules soluble. All tests were performed as described in Chapter 3 and data were reported as percentage reduction respect to the negative control. Molecules were considered able to

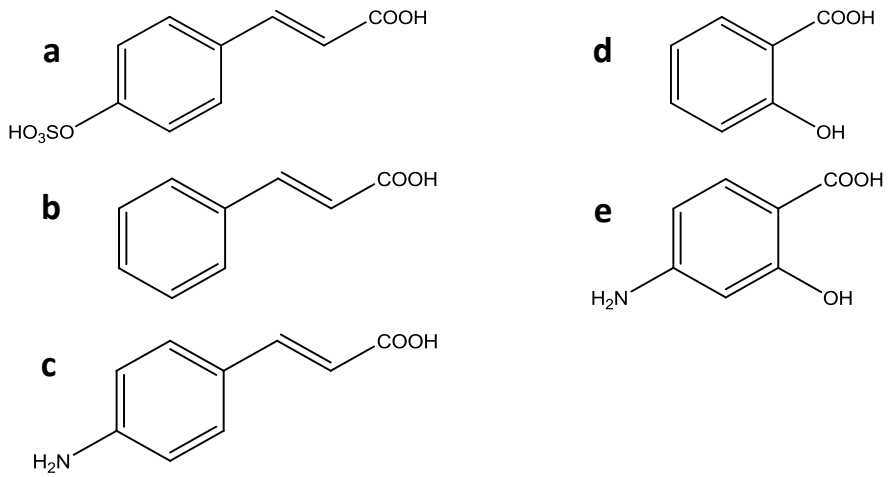

Figure 1. Chemical compounds used in this research: a) zosteric acid (ZA); b) cinnamic acid (CA); c) *p*-aminocinnamic acid (*p*-ACA); d) salicylic acid (SA); e) *p*-aminosalicylic acid (*p*-ASA).

affect planktonic growth when reduced cell growth more than 10 % respect to the negative control and to affect biofilm formation when reduced the number of adhered cells more than 30 % respect to the negative control. Analysis of variance (ANOVA) via a software run in MATLAB (Version 7.0, The MathWorksInc, Natick,USA) was applied to statistically evaluate any significant differences among each concentration of a compound. Tukey's honestly significant different test (HSD) was used for pairwise comparison to determine the significance of the data. Differences were considered significant for $p < 0.05$.

Extraction of total soluble cell proteins

An *E. coli* overnight culture was centrifuged at 5,000 *g* for 15 min at 4 °C three times, washed and resuspended in 200 mM Tris-HCl, 40 mM NaCl buffer (pH 7.5) (protein extraction buffer) to a final concentration of 250 mg of cells for mL. Soluble protein extract was obtained by sonication (seven 1-min sonication cycles followed by 2 min cooling periods, all on ice, in a Sonoplus UW-2070 sonicator) and cell debris was removed by centrifugation at 10,000 *g* for 45 min at 4 °C. The sample protein concentration was determined using the Bradford method with bovine serum albumin as standard (Bradford, 1976).

Matrix functionalization with *p*-aminocinnamic acid/*p*-aminosalicylic acid

Five milliliters of drained NHS-Activated Sepharose 4 Fast Flow (Ge Healthcare Life Sciences, 17090601) were washed 10 times with cold 1 mM HCl and then suspended in 0.2 M $NaHCO_3$, 0.5 M NaCl, 3 % DMSO buffer (pH 8.3) (coupling buffer). *p*-ACA and *p*-ASA dissolved in the coupling buffer at the concentration of 0.4 M were added to the matrix (10 µmol ligand/µmol NHS), mixed in a rotary shaker overnight at 4 °C. After one washing with the coupling buffer, remaining unreacted groups were blocked with 0.5 M ethanolamine, 0.5 M NaCl (pH 8.3). Subsequent 10 washing steps were performed according to the manufacturer's instructions. To generate the control matrix (EA/matrix), matrix was incubated with only coupling buffer and equally treated as described above.

Fluorescent spectra of *p*-aminocinnamic acid and *p*-aminosalicylic acid free in solution and matrix immobilized

Fluorescence spectra of *p*-ACA and *p*-ASA free in solution and matrix-immobilized were independently acquired in a Perkin-Elmer LS 50B spectrofluorometer. Emission spectra were recorded over the 250-600 nm range with emission and excitation slit widths set at 3.0 nm. Spectra of *p*-ACA and *p*-ASA free in solution were recorded by dissolving 2.6 mM *p-ACA* and 5.0 mM *p*-ASA in 0.4 M $NaHCO_3$, 1 M NaCl, 3% DMSO buffer (pH 8.3) (dilution buffer). Spectra of matrix-immobilized *p*-ACA and *p*-ASA were

recorded by suspending respectively 25 µL and 12.5 µL of functionalized matrix in 2 mL of dilution buffer. Control spectra of dilution buffer and ethanolamine-saturated matrix were also acquired at the same experimental conditions.

Matrix hydrolysis

The functionalized matrix was submitted to hydrolysis reaction in order to break the chemical bond between *p*-ACA/*p*-ASA and the matrix. The matrix was hydrolyzed by treatment with a 4 N aqueous solution of NaOH (1 mL). The suspension was stirred at room temperature for 4 hours. Reactions were monitored by thin layer chromatography (TLC) analysis on aluminium-backed Silica Gel 60 plates (0.2 mm, Merck) and were visualized under a UV lamp operating at wavelengths of 254 nm. Visualization was aided by opportune staining reagents. The matrix was filtered off and washed. The aqueous layer was acidified to pH=1 with 2N HCl and then extracted with ethyl acetate (3x1 mL). The combined organic layers were dried over anhydrous sodium sulfate and the solvent was evaporated under reduced pressure. The obtained molecule was submitted to mass spectrometry analysis to be identified.

Mass spectrometry analysis and molecule identification

Products from matrix hydrolysis reaction were analysed by liquid chromatography-electrospray ionization- mass spectrometry (LC-ESI-MS) on an Ultimate 3000 Micro HPLC apparatus (Dionex, Sunnyvale, CA, USA) equipped with a FLM-3000-Flow manager module directly coupled to a LTQ Orbitrap XL hybrid FT mass spectrometer (Thermo Fisher Scientific, Waltham, MA, USA). Reverse-phase chromatography was performed on a Jupiter C18, 5 µm, 150 x 1.0 mm column (Phenomenex, Torrance, CA, USA) and a 31 min run (gradient 0 to 40 % acetonitrile in water with 0.1 % formic acid over 20 min) at a flow rate of 80 µL/min. Mass spectra were collected at 60,000 of resolution in the Orbitrap analyser (mass range 50-1,000 Da). High resolution MS data were elaborated manually using the HPLC-MS apparatus management software (Xcalibur 2.0.7 SP1, Thermo Fisher Scientific).

Protein pull-down

The obtained functionalized matrix was washed with 5 mL of protein extraction buffer, centrifuged at 700 *g* for 2 min at room temperature and incubated with the soluble extracted proteins for 2.5 hours at room temperature in a rotary shaker. Matrix and soluble extracted proteins were packaged into a 15 mL chromatography column (i.d. 10 mm). One hundred mL of washing buffer were loaded into the column and a flow rate of 1.5 mL/min was applied to recover matrix unbound proteins. Proteins specifically bound to the functionalized matrix were recovered by competitive elution by loading into the column 15 mL of 60 mM competitor compound in 200 mM Tris-HCl, 40 mM NaCl buffer (pH 7.5) followed by 50 mL of 200 mM Tris-HCl, 1M NaCl 1 M, buffer (pH 7.5). CA or ZA were used to elute proteins bound to *p*-ACA functionalized matrix (p-ACA/matrix) while SA was used to elute proteins bound to *p*-ASA functionalized matrix (*p*-ASA/matrix). A compact single beam UV-monitor with flow-through cell (GE Healthcare Uvicord SII Code; 280 nm filter) was employed for continuously monitoring protein concentrations during the chromatography. Chromatographic fractions were collected and protein concentration was determined by Bradford assay with bovine serum albumin as standard (Bradford, 1976). To increase the protein concentration, fractions were precipitated using cold 13 % trichloroacetic acid, centrifuged at 13,000 *g* for 30 min at 4 °C and subsequently washed by cold acetone.

Denaturing gel electrophoresis

Precipitated proteins were dissolved in Laemmli sample buffer and were separated by SDS-PAGE according to Laemmli (1970). Coomassie-stained bands and spot were manually excised from gels and subjected to analysis by mass spectrometry.

Mass spectrometry analysis and protein identification

Excised bands were submitted to trypsin digestion as described by Di Pasqua and colleagues (2010). Trypsin digested peptides were analyzed by liquid chromatography-electrospray ionization-tandem mass spectrometry (LC-ESI-MS/MS) on the same HPLC and LTQ Orbitrap mass spectrometer previously reported in 'Mass spectrometry analysis and molecule identification'**.** Reverse-phase chromatography was performed on the same column and at the same flow rate but with different chromatographic conditions: linear gradient 1.6 to 44 % acetonitrile in water with 0.1 % formic acid over 60 min and total LC-run of 95 minutes. Mass spectra were collected in data dependent scan mode (MS scan at 60,000 of resolution in the Orbitrap and MS/MS scan on the three most intense peaks in the linear ion trap, mass range 300-2,000 Da). Selected peptides charge states were isolated with a width of *m/z* 2 and activated for 30 msec using 35% normalized collision energy and an activation q of 0.25. Protein identifications were obtained with the embedded ion accounting algorithm (Sequest HT) of the software Proteome Discoverer (version 1.4, Thermo) after searching a UniProtKB Protein Knowledgebase [release 2013_12 of 11-Dec-13; taxonomical restriction: *Escherichia coli* (strain K12), 4431 sequence entries]. The search parameters were 10 ppm tolerance for precursor ions and 0.6 Da for product ions, 1 missed cleavage, carbamydomethylation of cysteine as fixed modification, oxidation of methionine as variable modification and on a decoy database search calculated false discovery rate under 5 %.

Sequence alignments

Sequences of obtained proteins were aligned with all bacterial and fungal proteome using the National Center for Biotechnology Information (NBCI) protein BLAST tool with a BLOSUM62 matrix and default parameters.

Results

Zosteric acid and salicylic acid chemical structure were modified without affecting their anti-biofilm properties

Since Sepharose 4 Fast Flow matrix prepared with 6-aminohexanoic acid spacer arm and activated by esterification with N-hydroxysuccinimide is prone to form very stable amide linkages with molecules containing a primary amino group in their scaffold, ZA and SA were modified by adding an amino group in the para position of their chemical scaffold so to make them suitable for the chemical linkage with affinity the matrix.

To verify that the deletion of the sulfate ester group in the para position of ZA and the addition of an amino group in the para position of ZA and SA, phenyl ring and did not affect the anti-biofilm performance of the compound, ZA, CA, *p*-ACA, SA and *p*-ASA were submitted to biological assays.

To verify that a possible reduction of the number on adhered cells was given by an inhibition growth effect instead of a real anti-biofilm activity, the ability of each molecule to affect bacterial planktonic growth was performed measuring the maximum specific growth rate of bacteria in the presence of each compound at the different concentrations. ZA did not affect planktonic growth at any concentration while CA, *p*-ACA, SA and *p*-ASA affected planktonic growth only at the maximum concentration tested, showing a significant growth reduction (> 10 %) respect to the negative control (Table 1).

The ability of each compound to be a carbon and energy source for the microorganism was verified. The experiment revealed that *E. coli* did not grow in the presence of each compound as the sole carbon and energy source and showed an OD600 significantly comparable with the negative control.

Finally, the anti-biofilm performance of each compound was proved. As expected, at lethal concentration, molecules showed a reduction of the number of adhered cells, attributable to a killing

effect rather than to their anti-biofilm performance. At sub-lethal concentration, all the molecules showed at least one concentration with excellent anti-biofilm activity with a significant percentage reduction of adhered cells respect to negative control, up to 70 % for ZA, 46 % for CA, 46 % for *p*-ACA, 67 % for SA, 72 % for *p*-ASA (Table 1). Therefore the deletion of the sulfate ester group from ZA scaffold and the addition of the amino group in the para position of the phenyl ring in ZA and SA structure did not affect their anti-biofilm performance. *p*-ACA and *p*-ASA were indeed selected for their covalent coupling with the chromatography affinity matrix.

Cmpd	µM	Planktonic growth	Cell adhesion
ZA	0	0.0±2.0 [a]	0.0±9.5 [a]
	0.183	0.8±3.0 [a]	32.4±12.5 [b]
	1.83	1.8±3.0 [a]	-24.8±11.7 [c]
	18.3	0.1±3.1 [a]	-31.8±12.5 [c]
	183	1.1±3.2 [a]	-27.7±6.9 [c]
	1830	1.2±3.4 [a]	-70.6±6.0 [d]
CA	0	0.0±2.0 [a]	0.0±9.5 [ad]
	0.183	-3.3±3.4 [a]	-46.9±12.2 [bcd]
	1.83	-4.7±0.8 [a]	-38.8±8.7 [bcd]
	18.3	-5.2±2.7 [a]	-7.4±5.4 [acd]
	183	-8.6±2.7 [a]	-30.8±1.3 [abcd]
	1830	-35.1±1.6 [b]	-32.1±8.6 [bcd]
p-ACA	0	0.0±2.0 [a]	0.0±9.5 [abcd]
	0.183	-1.9±3.5 [a]	0.1±0.8 [abce]
	1.83	-3.1±1.6 [a]	-23.5±9.0 [bcd]
	18.3	-3.1±1.8 [a]	-42.1±9.0 [cdf]
	183	-2.4±4.6 [a]	-21.4±4.3 [ce]
	1830	-32.4±1.9 [b]	-46.6±13.1 [df]

Cmpd	µM	Planktonic growth	Cell adhesion
SA	0	0.0±2.0 [a]	0.0±9.5 [a]
	0.183	-1.1±3.6 [a]	-28.8±12.7 [bd]
	1.83	0.3±4.9 [a]	-31.6±13.4 [bd]
	18.3	2.7±0.9 [a]	-47.0±12.2 [bd]
	183	-0.2±3.2 [a]	-67.4±4.8 [cd]
	1830	-44.0±1.0 [b]	-50.0±8.0 [bcd]
p-ASA	0	0.0±2.0 [a]	0.0±9.5 [a]
	0.183	-3.4±2.6 [a]	10.7±18.0 [a]
	1.83	-0.9±4.6 [a]	-70.7±3.4 [b]
	18.3	1.3±2.9 [a]	-72.5±6.4 [b]
	183	2.3±5.8 [a]	-55.6±2.4 [c]
	1830	-22.9±1.0 [b]	-31.0±7.4 [d]

Table 1. Percentage reduction of planktonic growth and adhered cell respect to the negative control. According to post hoc analysis (Tukey's HSD, $p < 0.05$), data sharing the same letter indicates no significant difference.

Matrix functionalization reaction was successfully optimized

Different $\mu mol_{ligand}/\mu mol_{NHS}$ ratio at different pH values were tested to optimize the coupling conditions between *p*-AC and *p*-AS and the matrix. A ratio $\mu mol_{ligand}/\mu mol_{NHS}$ of 10/1 was the maximum tested since above this value molecules was less soluble. Fluorescence measurements using condition followed reported were used to monitor the reaction efficacy. A ratio $\mu mol_{ligand}/\mu mol_{NHS}$ of 10/1 at pH 8.3 was chosen as the best reaction condition (Figure 2).

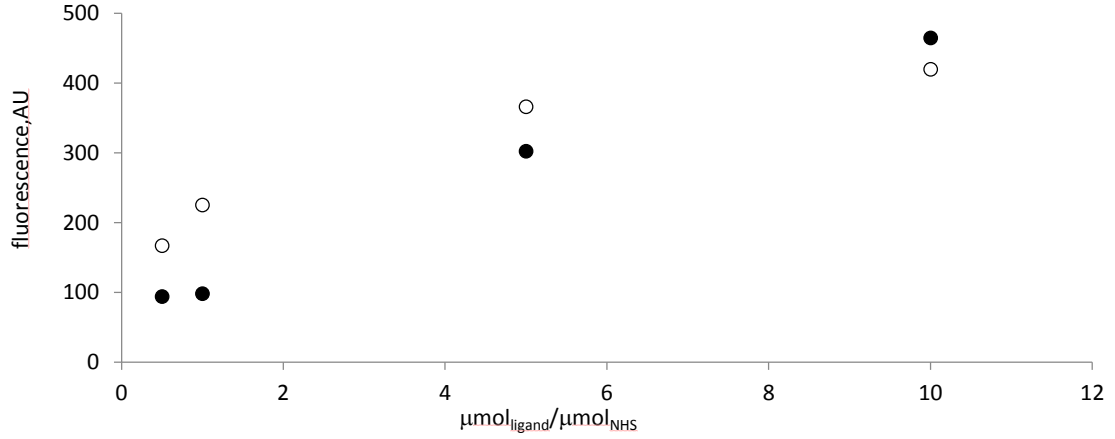

Figure 2. Fluorescence emission spectra of matrix suspension after coupling reaction (pH 8.3) with *p*-ACA (λ_{ex} 350 nm, λ_{em} 426 nm; ●) or *p*-ASA (λ_{ex} 325 nm, λ_{em} 396 nm; ○) at different $\mu mol_{ligand}/\mu mol_{NHS}$ ratios in the optimal pH condition. NHS micromoles were calculated considering NHS density value of 20 μmol_{NHS}/ml drained matrix.

Fluorescence measurements successfully detected the presence of ZA and SA active scaffold on the functionalized matrix

Fluorescence measurements were used to verify *p*-ACA acid and *p*-ASA immobilization process and to highlight any changes in the molecule regions during the coupling reaction by comparing the fluorescence emission spectra of the molecules free in solution and covalently bound to the matrix.

p-ACA excited at 380 nm showed an emission peak at 443 nm while *p*-ASA excited at 325 nm showed an emission peak at 395 nm (Figure 3). Analysis performed on fluorescence data revealed that *p*-ASA was 9-fold lower than *p*-ASA fluorescence at the same concentration. Matrix functionalized with *p*-ACA excited at 350 nm showed an emission peak at 426 nm while matrix functionalized with *p*-ASA excited at 325 nm showed an emission peak at 396 nm (Figure 3). Analysis performed on fluorescence data revealed that *p*-ASA/matrix was 2.4-fold lower than *p*-ASA/matrix fluorescence at the same amount. Since the control matrix did not exhibit fluorescence properties at the same experimental condition, it is possible to ascribe the fluorescence to the immobilized ZA and SA confirming the positive results of the immobilization process. Moreover, the comparison between the free and immobilized molecule spectra revealed that both *p*-ACA and *p*-ASA conserved their fluorescent properties after the immobilization process suggesting that the fluorogenic moieties of *p*-ACA acid and *p*-ASA acid were not altered during the matrix-coupling reaction. Little differences in the spectra between free and immobilized molecules may be ascribed to the different condition during the fluorescence detection (molecule free in solution and molecule immobilized on a suspended matrix).

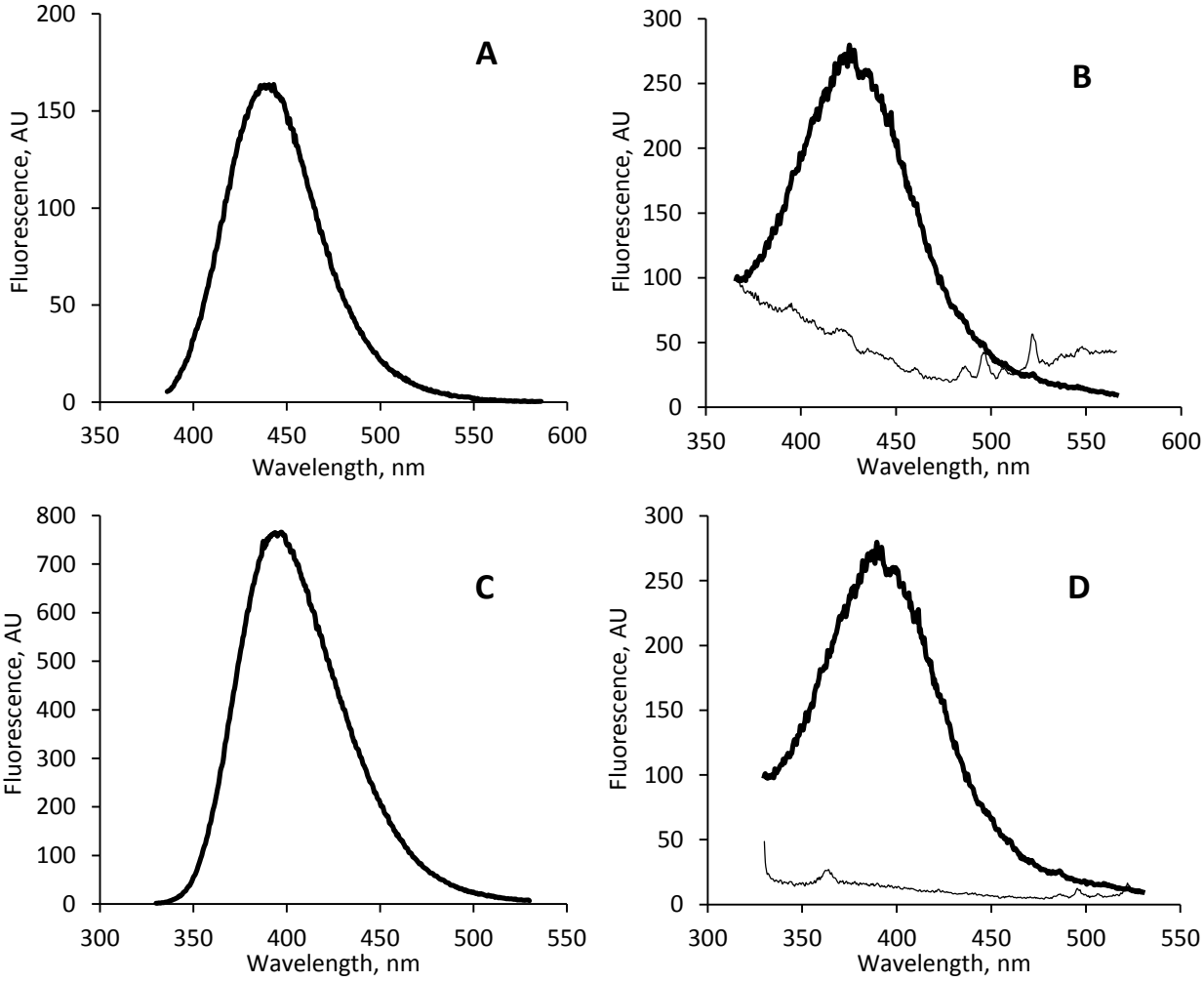

Figure 3. Fluorescent emission spectra of free in solution and matrix immobilized molecules. Panel A: *p*-ACA (λ_{ex} 380 nm); Panel B: ━ *p*-ACA/matrix, — EA/matrix (λ_{ex} 350 nm); Panel C: *p*-ASA (λ_{ex} 325 nm); Panel D: ━ *p*-ASA/matrix, — EA/matrix (λ_{ex} 325 nm).

Mass spectrometric analysis confirmed *p*-ACA and *p*-ASA matrix immobilization

In order to further verify the *p*-ACA and *p*-ASA immobilization process excluding any changes in the chemical scaffold of the molecules as a result of the coupling reaction, functionalized matrix were submitted to hydrolysis in order to break the amide bound between the complex *p*-ACA/matrix and *p*-ASA/matrix and to release *p*-ACA and *p*-ASA in solution. Obtained molecules were analyzed by mass spectrometric techniques and thanks to the high resolution of the MS apparatus, their molecular masses were detected with high precision, confirming their identity. Mass spectrometry analysis registered a monoisotopic single charged mass ($[M+H)^+]$) of 164.069 m/z in the hydrolysates produced by *p*-AC/matrix and a $[M+H]^+$ of 154.049 m/z in the hydrolysates produced by *p*-SA/matrix (Figure 4). The theoretical $[M+H]^+$ for *p*-CA is reported to be 164.071 m/z while the theoretical $[M+H]^+$ for *p*-ASA is reported to be 154.050 m/z. Indeed there is a significant evidence that the product from *p*-ACA/matrix hydrolysis and *p*-ASA/matrix hydrolysis correspond to *p*-ACA and *p*-ASA respectively (experimental mass error of 0.002/0.001 Da) confirming that the matrixes were functionalized with both *p*-ACA and *p*-ASA.

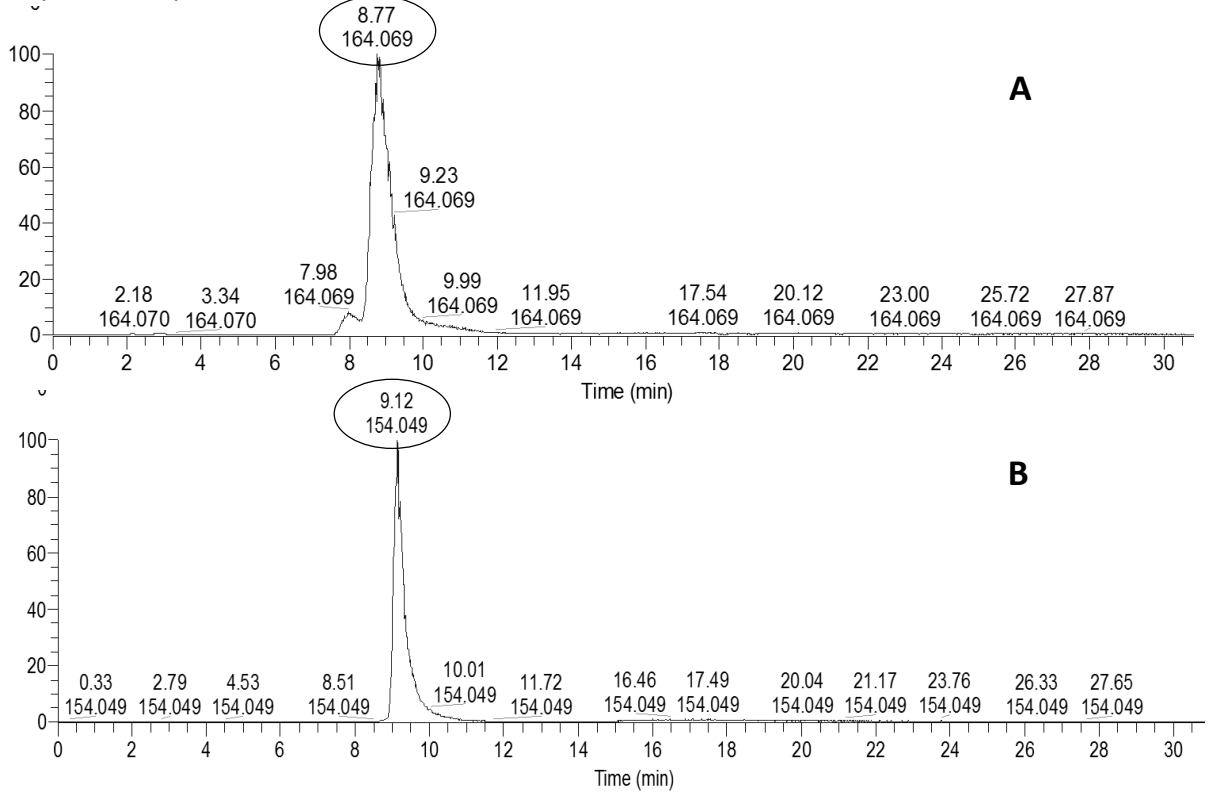

Figure 4. Extracted Ion Current (XIC) profiles of hydrolyzed *p*-ACA/matrix (panel A) and *p*-ASA/matrix (panel B) recorded during the LC-MS run. Retention time and m/z are evidenced.

SDS-PAGE analysis of pull-down revealed bands bound to the matrix

Proteins bound and unbound to the matrix functionalized with *p*-ACA and *p*-ASA were quantified and resolved by SDS-PAGE. Washing fractions were also loaded in the gel to make easier, under comparative conditions, the identification of interesting proteins in the fractions collected during elution by competition.

The SDS-PAGE analysis demonstrated that in three independent experiments one protein of about 20 kDa was eluted from the p-ACA/matrix by competition with both CA (Figure 5) and ZA sodium salt (Figure 5). No proteins were observed to bind the control resin functionalized with ethanolamine and eluted with the same competitors, indicating that the protein isolated on the matrix support specifically bound *p*-ACA (Figure 5).

Three proteins of about 20, 30 and 40 kDa were eluted from the *p*-ASA/matrix by competition with SA (Figure 5) in three independent experiments. No protein was observed to bind the control resin functionalized with ethanolamine and eluted with the same competitor, indicating that the proteins isolated on the affinity support specifically bound *p*-ASA (Figure 5).

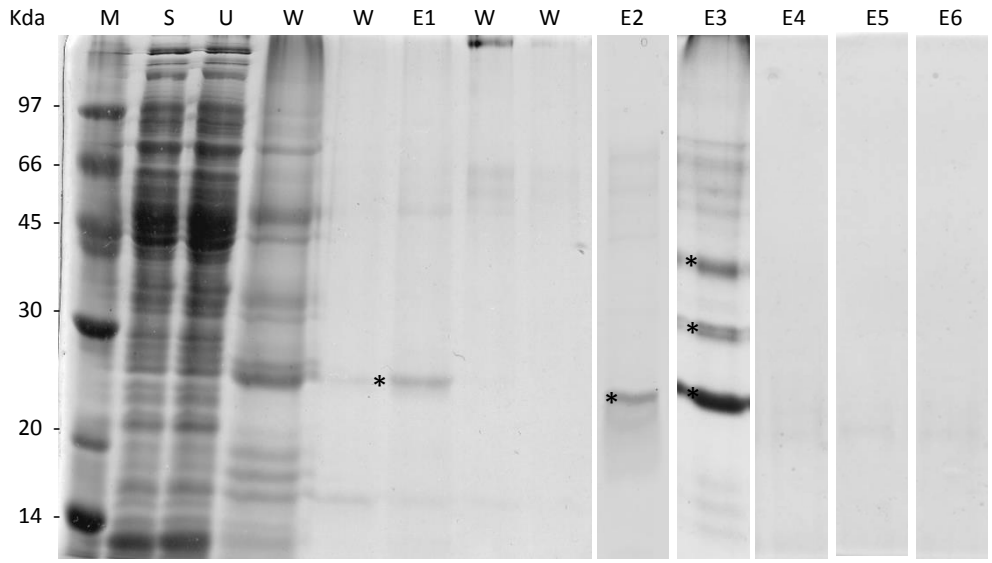

Figure 5. SDS-page analysis of the affinity chromatography of *E. coli* protein extract. Each gel is representative of three independent replicates. M: molecular mass marker, S: total soluble proteins from *E. coli* extract, U: proteins unbound, W: washing fraction E: proteins bound to *p*-ACA/matrix and eluted with CA (E1) and ZA (E2), proteins bound to *p*-ASA and eluted with SA (E3), proteins bound to EA/matrix and eluted with CA (E4), proteins bound to EA/matrix and eluted with ZA (E5), proteins bound to EA/matrix and eluted with SA (E6).

Both ZA and SA interact with the same protein WrbA

Protein specifically bound to functionalized matrix and resolved by SDS-PAGE were cut from the gel and submitted to mass spectrometric analysis in order to be identified. Identified proteins and their characteristics are reported in table 2. In all cases, mass spectrometric analysis gave a result with a high score and coverage percentage, suggesting an unequivocal identification of the proteins.

Mass spectrometric analysis revealed that the same protein WrbA (P0A8G6) was eluted from *p*-ACA/matrix by competition with both sodium cinnamate and ZA confirming that *p*-AC/matrix bound specifically WrbA. WrbA was also eluted from *p*-ASA/matrix by competition with SA. Indeed WrbA was proved to be the possible molecular target for both ZA and SA. Protein FkpA (P45523) and Tdh (P07913) were also eluted from *p*-ASA/matrix by competition with SA.

The blast search assay inside Bacteria and Fungi databases revealed that WrbA sequences exists in a diversity of microorganisms

A BLAST search of all non redundant databases in Bacteria and Fungi was performed with WrbA protein sequence as the query.

The search inside Bacteria databases returned 5792 sequences that had between 40% and 100% identity to WrbA (expect value ≤ 10^{-5}), most of which belonged to different *E. coli* strains, *Shigella* ssp, *Enterobacter* ssp, *Salmonella* ssp, *Klebsiella* ssp, *Cronobacter* ssp, *Yersinia* ssp, *Serratia* ssp, *Burkholderia* ssp and *Pseudomonas* ssp.

The search inside Fungi database returned 490 sequences that had between 36% and 91% of identity to WrbA (expect value ≤ 10^{-5}) including *Candida* spp, *Clavispora* spp, *Aspergillus* spp and *Fusarium* spp.

Matrix[a]	Comp[b]	Accession number[c]	Gene name[d]	Protein[e]	Score[f]	Coverage[g]
p-ACA/matrix	CA	P0A8G6	*wrbA*	NAD(P)H quinone dehydrogenase	189.78	70.2
p-ACA/matrix	ZA	P0A8G6	*wrbA*	NAD(P)H quinone dehydrogenase	684.32	71.72
p-ASA/matrix	SA	P0A8G6	*wrbA*	NAD(P)H quinone dehydrogenase	1079.55	71.72
p-ASA/matrix	SA	P45523	*fkpA*	FKBP-type peptidyl-prolyl *cis-trans* isomerase	156.99	43.33
p-ASA/matrix	SA	P07913	*tdh*	L-threonine 3-dehydrogenase	521.32	59.53

Table 2. Proteins identified by mass spectrometry analysis. a) the matrix from which the protein was eluted; b) the competitor used in the elution step; c) the alphanumeric unique protein sequence identifier; d) the gene name; e) the protein name provided by UniProtKB protein knowledgebase; f) the protein identification's SEQUEST HT Score; g) percentage of protein sequence covered by identified peptides (Coverage).

Discussion

The natural compounds zosteric acid and salicylic acid were previously proved to be suitable molecules for innovative anti-biofilm strategies with novel target and mode of action compare to the traditional less effective antimicrobial agents. Although several studies were performed about their anti-biofilm properties, no information are available concerning their molecular target. The lack of this information represents a potential bottleneck to generate more effective derivatives based on the same target and activity structure. In this study, a pull-down system combined with mass spectrometry-based approach was successfully employed to screen the whole *E. coli* proteome in order to identify the molecular targets implicated in ZA and SA anti-biofilm responses. Biological assays performed on *E. coli* strain confirmed the anti-biofilm performance of ZA and SA and demonstrated that the addition of an amino group in the para position of the phenyl ring in both ZA and SA chemical structure did not affect their anti-biofilm activity. *p*-ACA and *p*-ASA were chosen as suitable molecules to successfully immobilize ZA and SA active scaffold on the solid phase support via an amide bond. Mass spectrometry analysis of SDS-PAGE-resolved pull-down proteins revealed that both ZA and SA in *E. coli* directly interact with the same protein WrbA. Crystallographic studies reported that WrbA is characterized by a tetrameric quaternary structure with a hydrophobic active site pocket that provides an ideal stacking environment for aromatic moieties, indeed well adapted to accommodate phenolic compounds such as ZA and SA and suggesting that interaction of both ZA and SA with WrbA can lead to modulation of the active site function (Andrade et al., 2007).

In the past *E. coli* WrbA was reported to promote complex formation between the tryptophan repressor TrpR and its DNA operator sequences (Grandori et al., 1994). Subsequent experiments demonstrated that WrbA did not specifically bind to DNA and its involvement in transcription regulation was revoked. Anyway, although a direct connection to tryptophan repressor was retracted, a role in the tryptophan metabolism was considered possible especially related to the indole production. Indole is known as a metabolite of tryptophan which has recently been proved to participate in various aspects of bacterial life including virulence induction, cell cycle regulation, stresses resistance, genetic stability, controlling metabolic feedback and it is also proposed to be a quorum sensing signal with an important role in biofilm formation process (Hu et al., 2010; Worthington et al., 2013). Indole is generated by the cytoplasmic enzyme, tryptophanase, which hydrolyses tryptophan to produce indole, pyruvate and ammonia, a reaction that occurs exclusively in bacteria. In *E. coli*, this process is catalysed by the TnaA protein (Li et al., 2013). In normal condition the sigma factor RpoS transcriptional regulator induces the expression of the tryptophanase gene tnaA

promoting tryptophan degradation, producing indole and stimulating WrbA expression to strengthen negative regulation of the trp biosynthetic operon (Lacour et al., 2004; Collect et al., 2007). We hypothesize that ZA and SA interact with WrbA with subsequent consequences on TnaA activity that results in the alteration of the produced indole amount. ZA and SA may negative interact with WrbA reducing its activity and leading to tryptophan accumulation that results in the increased tryptophanase activity and indole synthesis. Alternatively ZA and SA may positive interact with WrbA enhancing its activity so that the availability of tryptophan decreases leading to reduced tryptophanase activity and indole synthesis. In both cases the result is the changing of the amount of indole in the environment that results in a cell to cell communication alteration. Since quorum sensing is essential for biofilm formation, it is clear that the interference with quorum sensing signal leads to the destabilization of biofilm process. It is reported that either too little or too much indole can abolish the ability to increase biofilm formation, in a dose dependent manner and with a strain specific activity. However, although both the hypothesis could be potentially possible to explain ZA and SA mode of action, a WrbA negative modulation by ZA and SA appears more probable. In a previous study, Villa and coauthors (2012) showed that *E. coli* in the presence of ZA exhibited an enhanced tryptophanase activity and an increased synthesis of indole. In addition it is reported that high concentrations (>600 μM) of extracellular indole are produced by *E. coli* when cultured in rich medium and indole has been shown to decrease biofilm formation in *E. coli* in a non-toxic manner (Lee et al., 2007a; Lee et al., 2007b). Domka and colleagues (2007) showed diminished conversion of tryptophan to indole as the biofilm matures, suggesting decreased indole concentrations in developing (15 h) and mature (24 h) biofilms. Indeed these researches validate the idea that increased amount of indole inhibits biofilm formation which is in line with the hypothesis that ZA and SA activity might exert their anti-biofilm performance by negative modulation of WrbA activity.

Recently, WrbA has been reported to be a flavoprotein with the enzymatic activity of a NADH:quinone oxidoreductase (NQO) involved in the maintaining quinones in a fully reduced state (Patridge et al., 2006). Quinones are compounds generally tethered to the plasma membrane or freely traverse the lipid bilayer. Although these compounds are essential for normal electron transport by cycling between the oxidized (hydroquinone) state and the two-electron reduced (hydroquinol) state, it has been demonstrated that such quinonoids also participate in deleterious redox cycling through direct interactions with single electron acceptors such as O_2, leading to the accumulation of reactive oxygen species (ROS) such as superoxide, hydrogen peroxide, and the hydroxyl radical responsible of devastating consequence in the cells (Adams et al., 2005). In order to guard against the production of ROS from one-electron redox cycling, cells have evolved NQO to maintain quinones in a reduced state as a measure of protection against oxidative stress. A previous study by Villa and collaborators (2012) demonstrated that ZA makes *E. coli* cells more prone to accumulate ROS leading a stress condition to which the bacterium responds by activating defensive mechanisms against oxidative damage. Rudrappa and coauthors (2007) suggested that catechol, metabolite of SA by salicylate hydroxylase, plays a direct role in inhibiting *Bacillus subtilis* FB17 biofilm formation on the *Arabidopsis thaliana* root surface, possibly through induction of ROS in the roots, which further mediates the down regulation of gene involved in biofilm formation. Indeed, although further studies will be necessary, we further corroborate the hypothesis that ZA and SA may negatively modulate the oxidoreductase activity of WrbA, maintaining a large amount of quinones in an oxidized state and leading to a ROS accumulation inside the cells with a deleterious impact on biofilm formation. Accumulation of ROS can result in the peroxidation of lipids, the destruction of cofactors, and the hydroxylation of proteins and nucleic acids inside the cells. Recent data also showed the ROS ability to modulate quorum sensing at certain level and their important role in biofilm formation (Čáp et al., 2012). The upset of ROS level caused by ZA and SA interaction with WrbA might interfere with quorum sensing signal destabilizing biofilm formation. Interestingly, some results suggest that ROS play a role in modulating the indole signaling pathway by the induction of tnaA expression (Ren et al., 2004). Kuczyńska-Wisnik (2010a) and co-workers demonstrated that *E. coli* mutant strain that experiences endogenous oxidative stress showed

an enhanced expression of tryptophanase and increased indole production that delayed the biofilm formation. In addition they demonstrated that antibiotics which promote ROS formation inhibit development of *E. coli* biofilm in an indole-dependent way. This means that bacteria also use indole signal to modulate pathways dealing with the oxidative stress and resulting in biofilm repression (Kuczyńska-Wisnik et al., 2010b).
The transcription factor CsgD (curlin subunit gene D) from *E. coli* is considered the master regulator of biofilm formation. The *wrbA* gene was shown to be one of the regulation targets of CsgD and the location distribution of the CgsD-binding regions in the gene suggesting that the expression of *wrbA* is upregulated by CgsD supporting a WrbA role in biofilm formation (Ogasawara et al., 2011).
On the basis of the previous considerations, we propose a possible mechanism by which ZA and SA interact with WrbA negatively modulating its activity and leading to enhanced production of both indole and ROS that cooperate in a complex network of events leading to biofilm growth inhibition. However further studies will be necessary for confirming this hypothesis.
The blast search assay inside Bacteria and Fungi databases revealed that WrbA sequences exist in a diversity of microorganisms with a high percentage of identity, suggesting a possible important role of this protein in the microorganism life, probably associated to the response against environmental stresses. The presence inside other microorganisms of a protein with a similar sequence and activity may suppose that ZA and SA could also interact with these proteins leading to a possible effect on the biofilm development. For example, a number of strains belonged to *Pseudomonas* spp revealed to have in their proteome a NADH quinone oxidoreductase with up to 100 % of similarity to WrbA and in effect it was demonstrated that both SA and ZA are able to significantly reduce *Pseudomonas* spp biofilm (Faber et al., 1993; Polo et al., 2014). Similarly some *Candida* spp presented in their proteome a protein sequence with similarity with WrbA between 60 % and 97 % depending on the species. SA and ZA were described to significantly impact *C. albicans* biofilm reducing biofilm formation up to 90 % (Faber et al., 1993; Villa et al., 2011). Indeed, in this study, the potential of ZA and SA against biofilm formation appears clear, especially because most of microorganisms that had been showed to have homologues sequences to WrbA inside their proteome are involved in human infections or agricultural diseases.
Only related to SA, other two proteins were identified as possible molecular target. FkpA is a peptidyl-prolyl isomerase that in *E. coli* periplasm is found to work in co-operation with other three proteins, PpiA, PpiD, and SurA, known as periplasmic *cis-trans* prolyl isomerases (PPIase) that facilitate the proper protein folding by increasing the rate of transition of proline residues between the *cis* and *trans* states. FkpA also displays chaperone properties that are independent of its PPIase activity implicated in protein aggregation prevention (Saul et al., 2004). Justice and collaborators (2005) proved that genetic inactivation of all four periplasmic isomerases resulted in a viable strain that exhibited a decreased growth rate and increased susceptibility to certain antibiotics but no single or double mutants were shown to have growth defects. The author hypothesized that even if the four periplasmic isomerases are not essential for growth under laboratory conditions, they may have significant roles in survival in environmental and pathogenic niches, demonstrating a possible role in the production of both P and type 1 pili. Pili are composed of multiple subunits that are assembled in a hierarchical manner from the tip to the base with a mechanism in which chaperones actively contribute to the stabilization of the subunit preventing their premature aggregation in the periplasm (Sauer et al., 2004). It is reported that type 1 pili are essential for *E. coli* biofilm formation since are required for both the initial attachment and the movement along the surface. Cells harbouring lesions in genes encoding for the regulation or biogenesis of type I pili are reported not to attach to PVC (Pratt et al., 1998). Indeed it is reasonable to suppose that SA may interact with FkpA altering the PPIase and/or chaperone activity and resulting in incorrect assembling of pili with consequences on biofilm formation. A direct inhibitory effect of SA on swarming, swimming, and twitching motility in different *Pseudomonas aeruginosa* strains were previously illustrated, although any motility system was preferentially indicated as SA target (Chow et al., 2011). It was also shown that FkpA in *E. coli* reduced

the extracellular stress response by alleviating the RpoE-dependant stress response improving cell physiology, and enhancing cell surface display (Narayanan et al., 2008). The SA interaction with FkpA may modulate this protection system in a negative way, leading cells to a stress condition that inhibit bacterial adhesion and subsequent biofilm formation.
The third protein by which SA seems to exert its anti-biofilm activity is Tdh, an L-Threonine 3-dehydrogenase that in both prokaryotes and eukaryotes catalyzes the first step in the L-threonine degradation pathways (Epperly et al., 1990). Threonine has been shown to have an observable effect on the *E. coli* motility, significantly promoting swimming and twitching motility at low concentrations and significantly inhibiting biofilm formation at higher concentration (Goh, 2013). Morehouse and collaborators (2005) has shown that threonine is abundant in the rotor protein FliG, which is important for rotation of flagella in term of directionality. A possible interaction of SA with Tdh could modify the activity of this protein, leading to changes in the threonine amount with effect on bacteria motility and consequently on biofilm formation.
Since SA interacts with different proteins, it probability exerts its anti-biofilm activity by different ways. This is in line with the amount of researches present in the literature that report various effects of SA on bacterial biofilm, suggesting the presence of complex and overlapping regulatory networks controlling quorum sensing, motility and biofilm formation.

Conclusion

In this study, a pull-down proteomic approach has successfully used to identify specific targets involved in ZA and SA anti-biofilm activity, by the screening of all *E. coli* proteome. The same protein WrbA was found to be the molecular target for both ZA and SA, suggesting a possible role of this protein in the biofilm formation process. However, any considerations about the mechanism by which ZA and SA interact with this protein are possible and further experiments are necessary to clarify this question. The confirmation of the relation between the biofilm formation and WrbA will open the way for the development of new and more effective therapies against biofilm formation. In addition, a computational approach could be used to screen and monitor the activity of the molecules, limiting time and cost consumption.

References

Adams M.A., Jia Z. (2005). Structural and biochemical evidence for an enzymatic quinone redox cycle in *Escherichia coli*: identification of a novel quinol monooxygenase. *The Journal of Biological Chemistry*, 280:8358-8363.

Andrade S.L.A., Patridge E.V., Ferry J.G., Einsle O. (2007). Crystal Structure of the NADH: Quinone Oxidoreductase WrbA from *Escherichia coli*. *Journal of Bacteriology*, 189:9101-9107.

Bandara M.B.K., Zhu H., Sankaridurg P.R., Willcox M.D.P. (2006). Salicylic acid reduces the production of several potential virulence factors of *Pseudomonas aeruginosa* associated with microbial keratitis. *Investigative Ophthalmology and Visual Science*, 47: 4453-4460.

Barrios C.A., Xu Q., Cutright T., Newby B.Z. (2005). Incorporating zosteric acid into silicone coatings to achieve its slow release while reducing fresh water bacterial attachment. *Colloids and Surface B: Biointerface*, 41:83-93.

Bradford M.M. (1976). Rapid and sensitive method for the quantitation of microgram quantities of protein utilizing the principle of protein-dye binding. *Analytical Biochemistry*, 72:248-254.

Čáp M., se Váchová L., Palková Z. (2012). Reactive oxygen species in the signaling and adaptation of multicellular microbial communities. *Oxidative Medicine and Cellular Longevity*, ID 976753.

Chow S., Gu K., Jiang L., Nassour A. (2011). Salicylic acid affects swimming, twitching and swarming motility in *Pseudomonas aeruginosa*, resulting in decreased biofilm formation. *Journal of Experimental Microbiology and Immunology*, 15:22-29.

Collet A., Vilain S., Cosette P., Junter G.A., Jouenne T., Phillips R.S., Di Martino P. (2007). Protein expression in Escherichia coli S17-1 biofilms: impact of indole. *Antonie van Leeuwenhoek*, 91:71-85.

Cong F., Cheung A.K., Huang S-M.A. (2012). Chemical genetics–based target identification in drug discovery. *Annual Review of Pharmacology and Toxicology*, 52:57-78.

Di Pasqua R., Mamone G., Ferranti P., Ercolini D., Mauriello G. (2010). Changes in the proteome of *Salmonella enterica* serovar Thompson as stress adaptation to sublethal concentrations of thymol. *Proteomics*, 10: 1040-1049.

Domka J., Lee J., Bansal T., Wood T.K. (2007). Temporal gene-expression in *Escherichia coli* K-12 biofilms. *Environmental Microbiology*, 9:332-346.

El-Banna T., Sonbol F.I., Abd El-Aziz A.A., Abo-Kamar A., Seif-Eldin D.W. (2012). Effect of the combination of salicylate with aminoglycosides on bacterial adhesion to urinary catheters. *International Research Journal of Pharmaceuticals*, 2:39-45.

Epperly B.R., Dek E.E. (1990). L-threonine dehydrogenase from *Escherichia coli*. Identification of an active site cysteine residue and metal ion studies. *The Journal of Biological Chemistry*, 266:6086-6092.

Faber B.F., Wolff A.G. (1993). Salicylic acid prevents the adherence of bacteria and yeast to silastic catheters. *Journal of Biomedical Materials Research*, 27:599-602.

Goh S.N. (2013). Effects of different amino acids on biofilm growth, swimming motility and twitching motility in escherichia coli BL21. *Journal of Biology and Life Science*, 4:103-115.

Grandori R., Carey J. (1994). Six new candidate members of the α/β twisted open-sheet family detected by sequence similarity to flavodoxin. *Protein Science*, 3:2185-2193.

Hall-Stoodley L., Costerton W.J., Stoodley P. (2004). Bacterial biofilms: from the natural environment to infectious diseases. *Nature Review Microbiology*, 2: 95-108.

Hu M., Zhang C., Mu Y., Shen Q., Feng Y. (2010). Indole Affects Biofilm Formation in Bacteria. *Indian journal of Microbiololy*, 50:362-368.

Justice S.S., Hunstad D.A., Harpe J.R., Duguay A.R., Pinkner J.S., Bann J., Frieden C., Silhavy T.J., Hultgren S.J. (2005). periplasmic peptidyl prolyl *cis-trans* isomerases are not essential for viability, but SurA is required for pilus biogenesis in *Escherichia coli*. *Journal of Bacteriology*, 187:7680-7686.

Kuczynska-Wisnik D., Matuszewska E., Laskowska E. (2010a). *Escherichia coli* heat-shock proteins IbpA and IbpB affect biofilm formation by influencing the level of extracellular indole. *Microbiology*, 156:148-157.

Kuczyńska-Wisnik D., Matuszewska E., Furmanek-Blaszk B., Leszczyńska D., Grudowska A., Szczepaniak P., Ewa Laskowska E. (2010b). Antibiotics promoting oxidative stress inhibit formation of Escherichia coli biofilm via indole signalling. *Research in Microbiology*, 161:847-853.

Lacour S., Landini P. (2004). σ^S-Dependent gene expression at the onset of stationary phase in *Escherichia coli*: function of σ^s-dependent genes and identification of their promoter sequences. *Journal of Bacteriology*, 186:7186-7195

Laemmli U.K. (1970). Cleavage of structural proteins during the assembly of the head of bacteriophage T4. *Nature*, 227: 680-685.

Lagonenko L., Lagonenko A., Evtushenkov A. (2013). Impact of salicylic acid on biofilm formation by plant pathogenic bacteria. *Journal of Biology and Earth Science*, 3: B176-B181.

Lee J., Jayaraman A., Wood T.W. (2007a). Indole is an inter-species biofilm signal mediated by SdiA. *BMC Microbiology*, 7:42.

Lee J., Bansal T., Jayaraman A., Bentley W.E., Wood T.K. (2007b). Enterohemorrhagic *Escherichia coli* biofilms are inhibited by 7-hydroxyindole and stimulated by isatin. *Applied and Environmental Microbiology*, 73:4100-4109.

Li G., Young K.D. (2013). Indole production by the tryptophanase TnaA in *Escherichia coli* is determined by the amount of exogenous tryptophan. *Microbiology*, 159:402-410.

Morehouse K. A., Goodfellow I.G., Sockett R.E. (2005). A chimeric N-terminal Escherichia coli-C-terminal *Rhodobacter sphaeroiders* FliG rotor protein supports bidirectional *E. coli* flagellar rotation and chemotaxis. *Journal of Bacteriology*, 187:1695-1701.

Narayanan N., Chou C.P. (2008). Periplasmic chaperone FkpA reduces extracytoplasmic stress response and improves cell-surface display on *Escherichia coli*. *Enzyme and Microbial Technology*, 42:506-513.

Ogasawara H., Yamamoto K., Ishihama A. (2011). Role of the biofilm master regulator CsgD in cross-regulation between biofilm formation and flagellar synthesis. *Journal of Bacteriology*, 193:2587-2597.

Ortholand J-Y., Ganesan A. (2004). Natural products and combinatorial chemistry: back to the future. *Current Opinion in Chemical Biology*, 8:271-280.

Patridge E.V., Ferry J.G. (2006). WrbA from *Escherichia coli* and *Archaeoglobus fulgidus* is an NAD(P)H: quinone oxidoreductase. *Journal of Bacteriology*, 188: 3498-3506.

Pratt L.A., Kolter R. (1998). Genetic analysis of *Escherichia coli* biofilm formation: roles of flagella, motility, chemotaxis and type I pili. *Molecular Microbiology*, 30:285-293.

Polo A., Foladori P., Ponti B., Bettinetti R., Gambino M., Villa F., Cappitelli F. (2014). Evaluation of zosteric acid for mitigating biofilm formation of *Pseudomonas putida* isolated from a membrane bioreactor system *International Journal of Molecular Sciences*, 15: 9497-9518.

Rasko D.A., Sperandio V. (2010). Anti-virulence strategies to combat bacteria-mediated disease. *Nature Reviews Drug Discovery*, 9:117-128.

Ren D., Bedzyk L.A., Thomas S.M., Ye R.W., Wood T.K. (2004). Gene expression in Escherichia coli biofilms. *Applied Microbiology and Biotechnology*, 64:515-524.

Rudrappa T., Quinn W.J., Stanley-Wall N.R., Bais H. P. (2007). A degradation product of the salicylic acid pathway triggers oxidative stress resulting in down-regulation of *Bacillus subtilis* biofilm formation on *Arabidopsis thaliana* roots. *Planta*, 226:283-297.

Sauer F. G., Remaut H., Hultgren S.J., Waksman G. (2004). Fiber assembly by the chaperone-usher pathway. *Biochimica et Biophysica Acta*, 1694:259-267.

Saul F.A., J.-P. Arié J-P., Vulliez-le Normand B., Kahn R., Betton J-M., Bentley G.A. (2004). Structural and functional studies of Fkpa from *Escherichia coli*, a *cis/trans* peptidyl-prolyl isomerase with chaperone activity. *Journal of Molecular Biology*, 335:595-608.

Stoodley P., Sauer K., Davies D.G., Costerton J.W. (2002). Biofilms as complex differentiated communities. *Annual Review of Microbiology*, 56: 187-209.

Villa F., Albanese D., Giussani B., Stewartd P. S., Daffonchio D., Cappitelli F. (2010). Hindering biofilm formation with zosteric acid. *Biofouling*, 26: 739-752.

Villa F., Pitts B., Stewart P.S., Giussani B., Roncoroni S., Albanese D., Giordano C., Tunesi M., Cappitelli F. (2011). Efficacy of zosteric acid sodium salt on the yeast biofilm model *Candida albicans*. *Microbial Ecology*, 62: 584-598.

Villa F., Remelli W., Forlani F., Vitali A., Cappitelli F. (2012). Altered expression level of *Escherichia coli* proteins in response to treatment with the antifouling agent zosteric acid sodium salt. *Environmental Microbiology*, 14: 1753-1761.

Villa F., Cappitelli F. (2013). Plant-derived bioactive compounds at sub-lethal concentrations: towards smart biocide-free antibiofilm strategies. *Phytochemistry Reviews*, 12: 245-254.

Wong C.C., Cheng K.W., He Q., Chen F. (2008). Unraveling the molecular targets of natural products: insights from genomic and proteomic analyses. *Proteomics Clinical Application*, 2: 338-354.

Worthington R.J., Richards J.J., Melander C. (2012). Small molecule control of bacterial biofilms. *Organic and Biomolecular Chemistry*, 10: 7457-7474.

Yang L., Rybtke M.T., Jakobsen T.H., Hentzer M., Bjarnsholt T., Givskov M., Tim Tolker-Nielsen (2009). Computer-aided identification of recognized drugs as *Pseudomonas aeruginosa* quorum-sensing inhibitors. *Antimicrobial Agents and Chemotherapy*, 53:2432-2443.

New bio-hybrid anti-biofilm surfaces functionalized with zosteric acid and salicylic acid compounds

Abstract

Recently the natural molecules zosteric acid and salicylic acid have been proposed as alternative biocide-free agents suitable for a preventive or integrative approach against biofilm formation. Beside this promising results, the lack of a system to efficiently spread and use these compounds leave this technology far from a real application. In this research zosteric acid and salicylic acid were successfully covalently immobilized on low density polyethylene surface, providing new no-leaching bio-hybrid materials available for a wide range of applications. O_2 plasma treatment was firstly employed to activate the low density polyethylene surface. Subsequently, the graft-polymerization with 2-hydroxyethyl methacrylate and the immobilization of the selected bioactive molecules on the polymeric surface successfully provided the new materials. The functionalized materials were proved to significantly reduce *E. coli* biofilm biomass up to 60 % respect to the non-functionalized control surface, with a mechanism that not affected bacterial viability. CLSM analysis also revealed a dramatic impact of immobilized zosteric acid and salicylic acid on biofilm morphology, showing a biofilm with a significantly reduced thickness and polysaccharide matrix amount. Moreover, biofilm grown on functionalized surfaces showed enhanced susceptibility to ampicillin and ethanol, further reducing biofilm biomass on functionalized surfaces up to 95 %.

Introduction

The spread and development of microorganisms in form of biofilm is recognized to be one of the most social and economic problem in all medical and industrial setting, causing devastating consequences in term of economic and social impact, also because biofilms present some features that make them extremely more resistant to the effects of antimicrobial agents (Hall-Stoodley, 2004). This consistent problem has motivated a lot of researchers and industrial companies to develop new materials as new solutions against biofilm formation, especially in the medical area where the biofilm formation is become an important cause of systemic infections. Altering the surface properties of polymeric material is one of the main issues to prevent or decrease biofilm infections. A number of disinfectants, antiseptics and antibiotics has been incorporated into different polymeric surfaces developing leachable anti-infective systems with a broad-spectrum of antimicrobial activity available to counteract infections (Coenye et al., 2011). This approach, however, suffers from problems. The release of the active compound is temporary, typically no longer than 24 h, and indeed unuseful for applications that required a longer protection. In addition, the prerequisite for a good performance is the continuous and constant elution of the anti-biofilm molecules from the surface, with a sufficient release rates to deter bacterial attachment and slow enough to ensure the long service life of the coating (Barrios et al., 2005). Unluckily, in most of cases these materials exhibit discontinuous release rate according to first-order kinetics with an initially high release and afterwards an exponential decrease of the released, providing the perfect condition for development of the anti-microbial resistance (von Eiff et al., 2005).

Heavy metal silver was also used as an anti-biofilm agent in the medical area by depositing silver on the surfaces of bio-materials using coating technology (Jiang et al., 2004). However coating medical devices with silver ions or metallic silver has disappointing results. Moreover silver nanoparticles could have genotoxic and cytotoxic effects on human cells (Rai et al., 2009; Jena et al., 2012).
An alternative approach is to inhibit the tendency of surface-adhered bacteria to form biofilms, rather than to kill them. Recently, the natural compounds zosteric acid (ZA) and salicylic acid (SA) have been proposed as new solutions able to affect biofilm development interfering with key steps of its formation (i.e. microbial adhesion and cell-to-cell communication signal) without affecting microbial existence and with a low risk for development of resistant mutations. Related studies proved the ability of ZA and SA to significantly reduce bacterial and fungal adhesion and play a role in shaping biofilm architecture, in reducing biofilm biomass and thickness and in extending the performance of antimicrobial agents, at a concentration that does not affect microbial life (Barrios et al., 2005; Villa et al., 2010; Villa et al., 2011; El-Banna et al., 2012; Polo et al., 2014). The aim of this work is to develop new anti-biofilm materials by covalently anchoring zosteric acid and salicylic acid to a polyethylene polymeric surface with in mind to create new anti-biofilm materials available for a wide range of applications and with a mode of action distinct to the traditional antimicrobial-based anti-biofilm technologies. In this approach, molecules are permanently attached to the surface. Thanks to the knowledge of their active side (see Chapter 4), the molecules are all oriented to externally exhibit their active scaffold, allowing the material to exert its anti-biofilm performance directly interacting with bacterial cells even at the early stages of biofilm formation. In addition, since no molecules are leached from the surface, their concentration remains constantly below the lethal levels, reducing the risk of developing resistant strains. The proved low toxicity of both zosteric acid and salicylic acid poses the basis to spread this technology to different sectors resulting in new, safe and eco-friendly types of products available for a wide range of applications.

Materials and Methods

Materials and sample preparation
Low density polyethylene (LDPE) was purchased from Alfa Aesar as sheets and was prepared in the form of 1.6 mm thick round shape coupons (d=1.27cm). LDPE coupons were washed with a 3% aqueous solution of a neutral detergent efficient in removing greasy residues (AUSILAB 101, Carlo Erba Reagents) and an aqueous 1 M HCl solution. Then they were treated by extraction with acetone overnight and dried prior each plasma treatment.

LDPE low pressure oxygen plasma treatment
LDPE coupons were exposed to a low pressure oxygen plasma treatment in order to introduce new carbon-oxygen functionalities to LDPE surface. The apparatus used in this study consists in a parallel-electrodes, capacitive-coupled plasma enhanced chemical vapor deposition (PECVD) system, made up of a cylindrical stainless steel vacuum chamber of 25 cm inner diameter with an asymmetric electrode configuration. The powered electrode is connected to a 13.56 MHz power supply, associated to an automatic impedance matching unit, while the other electrode is grounded and works as sample holder. The treatment was performed for 60 s at a total plasma process pressure of about 15 Pa, kept constant by balancing the incoming oxygen flux with the system pumping speed. Commercially (99.998% purity) available oxygen was supplied into the discharge vessel through a mass flow controller. The total gas pressure was measured by a capacitive vacuum gauge. Plasma treatment was performed as a function of RF power of 100 W. At first low pressure is created in the process reactor by means of a turbo-molecular pump combined with a rotary pump. At a pressure of 0.026 mbar,

oxygen was fed into the chamber (O_2 flow= 15sccm). When the working pressure was achieved, the generator was switched on and the process gas become ionized.

Grafting procedure
For the polymerization processes, monomers are introduced into the chamber and react chemically among each other to form polymers and then settle down as a layer onto the treated part. LDPE samples were immersed for 10 s in a solution of 2-hydroxyethyl methacrylate (HEMA, 97 %, contains ≤ 250 ppm monomethyl ether hydroquinone as inhibitor, used as-received without further purification; Sigma Aldrich) in ethanol (>99.8 %, Sigma Aldrich). Concentration of HEMA solutions was varied from 0.05 M to 1 M. Immersed LDPE samples were dried in air and then oxygen plasma treated in order to promote the graft-polymerization of the monomer. Oxygen pressure and treatment time were varied in order to optimize the process. Input power was kept constant at 100W to prevent any damages to the substrates. Finally, the samples were ultrasonically washed in ethanol for 5 minutes in order to remove the ungrafted macromolecules and dried in air at room temperature. The result of the treatment is a LDPE-HEMA-OH surface (LDPE-OH).

Preparation of carboxylic acid derivatized LDPE-HEMA-OH surface
The LDPE-HEMA-OH surface was treated with succinic anhydride to obtain LDPE-HEMA-COOH surface (LDPE-COOH). The LDPE-HEMA-OH coupons were immersed in 10 mL dichloromethane (DCM, Sigma Aldrich) with the addition of dry pyridine (2.5 eq, Sigma Aldrich). Succinic anhydride (2.5 eq; Sigma Aldrich) dissolved in 10 mL of tetrahydrofuran (Sigma Aldrich) was added to the reaction mixture. The reaction was allowed to proceed at room temperature for 24 h. The surface was washed with copious amounts of dichloromethane (10 x 10 mL) prior to dry in air.

Immobilization of ZA and SA active scaffold via an amide bond formation
LDPE-COOH was bound to *p*-aminocinnamic acid and *p*-aminosalicylic acid amino group via a condensation reaction to allow their binding to the surfaces. LDPE-COOH coupons (1 eq of carboxylic acid groups) were suspended in DCM (10 mL) and were activated with N-hydroxysuccinimide (1.2 eq, Sigma Aldrich) and N,N-dicyclohexylcarbodiimide (1.2 eq; 685178, Sigma Aldrich) for 20 min at room temperature under a nitrogen atmosphere. *p*-aminocinnamic acid and *p*-aminosalicylic acid (1.2 eq) were independently poured in the suspension with the activated carboxylic acid on coupons and the resulting mixture was stirred at room temperature for 16 h. The coupons were filtered off and washed with dichloromethane for many times (10 x 5 mL). Additional washes with dimethylformamide (3 x 3 mL, Sigma Aldrich) were necessary to remove the remaining dicyclohexylurea (Sigma Aldrich). The resulted ZA and SA functionalized coupons (LDPE-ZA, LDPE-SA) were dried in vacuum to allow analytical analysis.

Surface characterization by Attenuated Total Reflectance Fourier Transform Infrared spectroscopy
Attenuated Total Reflectance Fourier Transform Infrared spectroscopy analysis (ATR-FTIR) measurements were performed using a SpectrumOne spectrophotometer (Perkin-Elmer, USA), by placing non-functionalized (LDPE, LDPE-OH, LDPE-COOH) and functionalized (LDPE-ZA, LDPE-SA) coupons on a diamond crystal mounted in ATR cell (Perkin-Elmer, USA). The spectra were collected over the wavenumber region 4000−650 cm^{-1} at 4 cm^{-1} resolution and 128 scans. The ATR-FTIR measurements provide mostly semi-quantitative information on the chemical changes of the near-surface region, because the measured thickness of the layer is limited to 4 µm. Experiments were carried out under ambient conditions.

Surface characterization by Confocal Laser Scanner Microscope
Functionalized (LDPE-ZA, LDPE-SA) and non-functionalized coupons (LDPE, LDPE-OH, LDPE-COOH) were visualized using a Leica SP5 Confocal Laser Scanning Microscope (CLSM) (405 nm laser excitation

line, blu channel) before and after 10-fold used. Images were captured with a 40x, 0.8 NA water immersion objective and analyzed with the software Imaris (Bitplane Scientific Software, Zurich, Switzerland). The experiments were repeated two times.

***Escherichia coli* strain and growth condition**

The well characterized *E. coli* MG1655 was used as a model system for bacterial biofilms. The strain was stored at –80 °C in suspensions containing 20 % glycerol and 2 % peptone, and was routinely grown in Luria-Bertani broth (LB, Sigma-Aldrich) at 37 °C.

Biofilm growth in the CDC Reactor

E. coli biofilm was grown on functionalized and non-functionalized coupons in the Center for Disease Control Bioreactor (CDC reactor, Biosurface Technologies, Bozeman, MT, USA). Inoculum of the bioreactor was prepared by inoculating 400 mL of sterile LB medium with an overnight culture of *E. coli* MG1655 strain and growing this culture at 37°C with continous strirring for 24 hours. After the 24-h adhesion phase, the peristaltic pump was started and sterile 10 % LB medium was continuously pumped into the reactor at a rate of 8.3 mL/min. After 48 hours of dynamic phase, functionalized and non-functionalized coupons were removed, gently washed with PBS and processed to be analyzed.

Plate count viability assay

Collected coupons were transferred to 5 mL PBS. Sessile cells were removed from the coupon surface by 30 s vortex mixing, 2 min sonication (Branson 3510, Branson Ultrasonic Corporation, Dunburry, CT) followed by other 30 s vortex mixing. Using this procedure, all the cells were dislodged from the coupons. Serial dilutions of the resulting cell suspensions were plated on Tryptic Soy Agar (TSA, Fisher Scientific) and incubated overnight at 37 °C. CFUs were determined by standard colony counting method. The $\log_{10}$ number of viable bacterial cells was calculated. Data were normalized to the $\log_{10}$ number for the control sample and percentage reduction respect to the negative control was also calculated. The experiments were repeated three times.

Biofilm Imaging by Epifluorescence microscopic analysis

Biofilm grown on both functionalized and non-functionalized coupons was stained using the Live/Dead BacLight viability kit (Molecular Probes-Life Technologies) enabling differentiation between cells with intact versus permeable membranes. Biofilms were directly incubated on the coupon with using 2 µL of each component per mL of sterile filtered PBS at room temperature in the dark for 25 min and then rinsed with sterile PBS, according to the manufacture instruction.

Direct staining of total biofilm mass on both functionalized and non-functionalized coupons was also achieved using 1x commercial solution of CellMask plasma membrane orange stain (Molecular Probes-Life Technologies) in sterile PBS. CellMask orange staining does not distinguish between live and dead cells, but rather allows for the visualization of total cell mass. Biofilms were allowed to incubate for 30 min in the dark at room temperature and then rinsed with sterile PBS.

Coupons without biofilm were also stained with the dyes in order to exclude any false positive signals. Biofilm samples were visualized using a Nikon Eclipse E800 epifluorescent microsope with excitation at 480 nm and emission at 516 nm for the green channel and excitation at 581 nm and emission at 644 nm for the red channel. Images were captured with a 60x, 1.0 NA water immersion objective and analyzed via MetaMorph 7.5 software (Molecular Devices, Sunnyvale, CA, USA). Percent area threshold of stained cells was performed by calculating at least ten random images for each sample for at least three coupons per experiment. The efficacy of the anti-biofilm material was calculated as percentage reduction in stained cells threshold area respect to the control images. Live/dead ratio was also determined by dividing percent area threshold of the alive stained cells by the percent area threshold of the dead stained cells in each sample.

Biofilm Imaging by Confocal Laser Scanning Microscopy

Biofilm grown on both functionalized and non-functionalized coupons was stained using the lectin Concanavalin A-Texas Red conjugate (Molecular Probes-Life Technologies) to visualize the polysaccharide component of the EPS and Sybr green I fluorescent nucleic acid stain (Molecular Probes-Life Technologies) to display biofilm cells. Biofilm were incubated with 200 µg/mL of ConA and 1:1000 of commercial Sybr green dye solution in PBS at room temperature in the dark for 30 min and then rinsed with PBS. Coupons without biofilm were also stained in order to exclude any false positive signals. Biofilm samples were visualized using a Leica SP5 CLSM with excitation at 488 nm, and emission <530 nm (green and red channel). Images were captured with a 63x, 0.9 NA water immersion objective and analyzed with the software Imaris (Bitplane Scientific Software, Zurich, Switzerland). Bio-volume of both cells and matrix was calculated by summing the stained cells/matrix threshold area of each single plane. Cells and matrix bio-volumes were calculated considering at least five random images for each sample for at least three coupons per experiment. The efficacy of the anti-biofilm material was calculated as percentage reduction in bio-volume respect to the control images. Cells/matrix bio-volume ratio was also determined by dividing bio-volume of cells with the bio-volume of matrix in each sample.

Antibiotic and biocide susceptibility test

Biofilm on functionalized and non-functionalized coupons were independently soaked in 15 mL of 100 µg/mL Ampicillin (Amp, Fisher Scientific) and 20 % ethanol for respectively 24 h and 20 min. Functionalized and non-functionalized coupons were also soaked in 15 mL of water for 24 h and 20 min as a negative control. The incubation time was chosen to mimic antibiotic therapies and daily disinfection procedures in hospital and industrial settings. After the treatment, coupons were soaked in distilled water for 10 min in order to neutralize the antimicrobial agent. Cells in the biofilm were collected in PBS for colony counting, as previously reported in the plate count viability assay section. Dispersed cells in the bulk liquid were washed by centrifugation at 8,000 g for 30 min and suspended in PBS for colony counting. Obtained data were expressed as $\log_{10}/cm^2$ survived bacteria. The antimicrobial efficacy percentage was also calculated as (no. of viable cells from bulk liquid x 100)/(no. of viable cells from bulk liquid + no. of viable cells from the remaining biofilm). All antimicrobial experiments were conducted in triplicate.

The susceptibility of biofilm on functionalized and non-functionalized 20 % ethanol was also carried out using the FC 270 flow cell apparatus (BioSurface Technologies, Bozeman, MT), performing the setup according to the manufacturer's recommendations. The method consisted in determining the decrease in fluorescence intensity of cells previously stained with the syto-9 green fluorescent nucleic acid stain solution within the biofilm during exposure to ethanol using direct time-lapse confocal microscopy inside intact biofilm. Biofilms on functionalized and non-functionalized coupons were stained with 5 mM of SYTO-9 (Molecular Probes-Life Technologies) in PBS at room temperature in the dark for 30 min and then rinsed with PBS. A solution of 20 % ethanol was pumped through the flow cells at a rate of 1 mL/min rate for 20 min. The decrease in fluorescence intensity of the cells in the biofilm was imaged using a Leica SP5 CLSM with excitation at 488 nm, and emission <530 nm (green channel). Images were captured with a 63x, 0.9 NA water immersion objective and analyzed with the software Imaris (Bitplane Scientific Software, Zurich, Switzerland). The cells bio-volume of each single frame was calculated as previously reported in biofilm imaging by confocal laser scanning microscopy section and plotted against time. The bio-volume of each single frame was also used to calculate a mathematical model for ethanol susceptibility.

Statistical Analysis

ANOVA, via a software run in MATLAB environment (Version 7.0, The MathWorks Inc, Natick, USA), was applied to statistically evaluate any significant differences among the samples. Tukey's honestly

significant different test (HSD) was used for pairwise comparison to determine the significance of the data. Statistically significant results were depicted by *p*-values < 0.05.

Results

ATR-FTIR successfully detect the presence of ZA and SA active scaffold on the functionalized surfaces

Attenuated Total Reflectance Fourier Transform infrared spectroscopy (ATR-FTIR) analyses were carried out, in order to detect the presence of the ZA and SA active scaffold grafted on the surfaces.

The LDPE surface analysis showed a typical polyethylene spectrum with a small number of characteristic peaks (Figure 1). After plasma exposure, the surface spectra did not change and no evidences for -OH or -COOH peaks were shown. No changes were also observed in both LDPE-OH and LDPE-COOH surfaces.

After the covalent linkage with *p*-aminocinnamic acid and *p*-aminosalicylic acid the shape of the spectra changed (Figure 1), with significant differences respect to LDPE surface especially in the infrared-region between 1.600-1.800 cm^{-1} (C-O stretching, N-H bending). The spectra showed typical peaks of the amide bond confirming the presence of a covalent bond between ZA and SA active scaffold and LDPE surfaces.

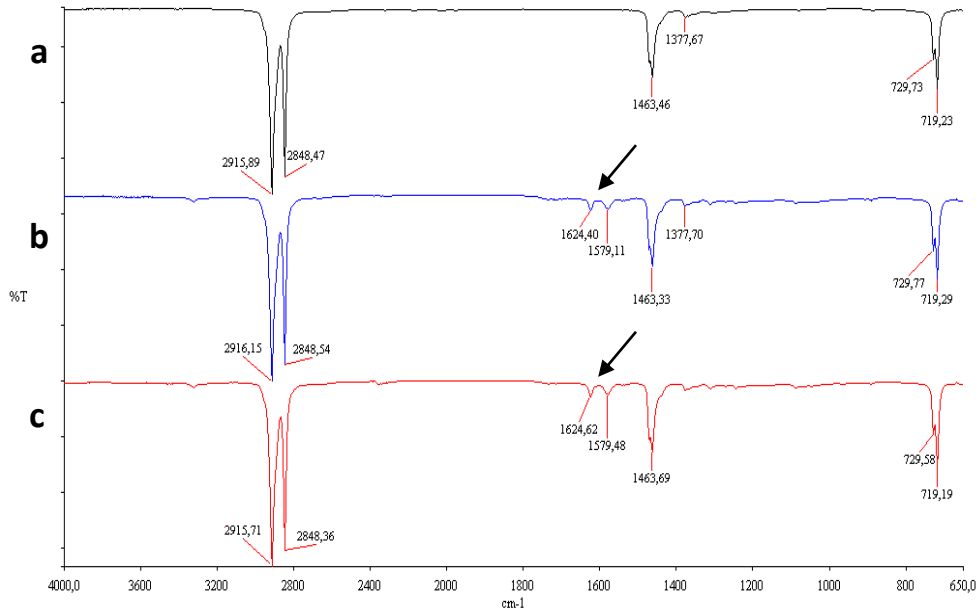

Figure 1. Representative ATR-FTIR spectra of functionalized and non-functionalized surfaces. a) LDPE, b) LDPE-ZA, c) LDPE-SA. Black lines show the typical peaks of an amide bond confirming the successful of ZA and SA immobilization process.

CLSM analysis successfully demonstrated the polyethylene surface functionalization

The auto-fluorescence of ZA and SA immobilized scaffold (data shown in chapter 4) was used to verify the surface functionalization by Confocal Scanning Laser Microscopy (CLSM). Acquired pictures of LDPE, LDPE-OH and LDPE-COOH control samples revealed a completely black background with the absence of fluorescence. On the contrary acquired picture of LDPE-ZA and LDPE-SA samples revealed the presence of an intense fluorescence signal that, since no fluorescence was detected in the control samples, could be attributable to the ZA and SA fluorescence moieties immobilized on the surface, demonstrating the successful of the functionalization process (Figure 2). To prove the retention and stability of the functionalized material, the CSLM analysis was repeated on 10-fold used coupons.

Pictures of LDPE, LDPE-OH and LDPE-COOH 10-fold used control coupons revealed a completely black background with the absence of fluorescence. Picture of LDPE-ZA and LDPE-SA 10-fold used coupons revealed the presence of an intense fluorescence signal comparable to that unused corresponding coupons, demonstrating that the coupons are not altered by their usage and that ZA and SA are successfully retained by the surface (Figure 2).

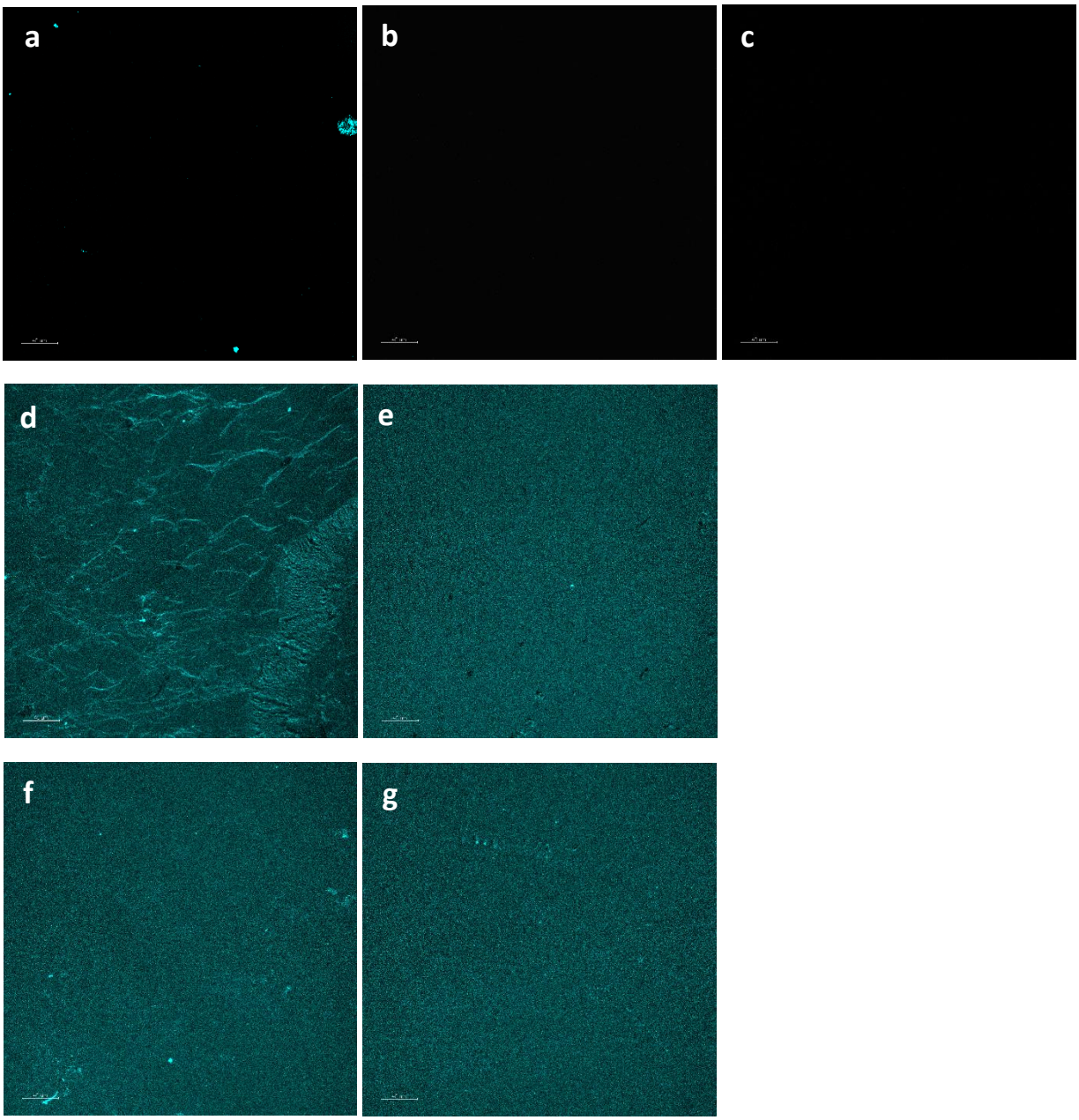

Figure 2. Representative CLSM images of unused and 10-fold used functionalized and non-functionalized polyethylene surfaces (405 nm laser excitation line; 40×, 0.8 NA water immersion objective). Blue fluorescence corresponds to the molecule presence on the surface. No-used coupon: a) LDPE, b) LDPE-OH, c) LDPE-COOH, d) LDPE-ZA, e) LDPE-SA. Ten-fold used coupon: f) LDPE-ZA, g) LDPE-SA. Scale bar=40µm.

Plate count viability assay demonstrated the efficacy of the functionalized polyethylene surface to reduce *E. coli* adhered cells

Biofilm formation on both functionalized and non-functionalized coupons was monitored, measuring biofilm biomass by colony counting. CDC reactor was used to grow the biofilm to create flow condition normally encountered in vivo. After 24 h of static conditions followed by 48 h of dynamic conditions, the biofilm growth revealed significant differences in viable cell adhesion between the control sample (LDPE) and the functionalized material (LDPE-ZA and LDPE-SA) (viable adhered cells: LDPE 7.01±0.06 $\log_{10}$ CFU/cm^2; LDPE-ZA 6.55±0.17 $\log_{10}$ CFU/cm^2; LDPE-SA 6.62±0.10 $\log_{10}$ CFU/cm^2). No significant differences were detected in viable cells adhesion between the control sample LDPE and the linker control sample LDPE-OH and LDPE-COOH (viable adhered cells: LDPE-OH 7.00±0.08 $\log_{10}$ CFU/cm^2; LDPE-COOH 6.99±0.08 $\log_{10}$ CFU/cm^2), suggesting that the used linker does not affect biofilm biomass and consequently that the anti-biofilm performance of the functionalized materials is totally attributable to ZA and SA immobilized on the surface. The experiment revealed that LDPE-ZA and LDPE-SA exploited an optimal anti-biofilm performance reducing viable adhered cells by 61.6 % and 60.0 % respectively in comparison to the LDPE control surface (Figure 3).

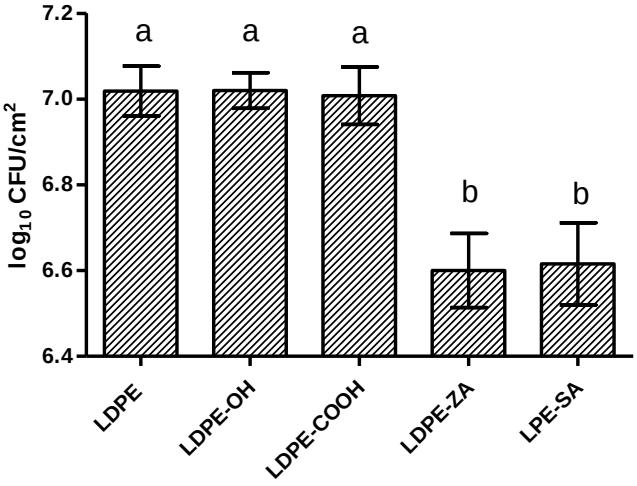

Figure 3. *E. coli* biofilm growth on functionalized and non-functionalized polyethylene surfaces. Error bars display the honestly significant difference (HSD) intervals using Tukey multiple comparison with a 95 % confidence level (Tukey's HSD, $p < 0.05$). According to post-hoc analysis, means sharing the same letter are not significantly different from each other. Values are based on results from at least three separate experiments.

Functionalized polyethylene surfaces reduce *E. coli* biofilm biomass without affecting cell viability

Plate count analysis revealed a reduced viability of bacteria recovered from the functionalized polyethylene surfaces. Epifluorescence microscopic techniques were additionally used to provide image analysis and quantification of bacterial cells in situ.

Direct microscopic visualization of the total biofilm biomass on functionalized and non-functionalized coupon is shown in Figure 4, where in situ biofilms have been stained with the CellMask plasma membrane orange stain. Pictures analysis showed significant differences in the percentage area threshold of stained cells between the control LDPE and the functionalized LDPE-ZA and LDPE-SA materials (percentage threshold area of total cells: LDPE 91.04±3.88 %; LDPE-ZA 29.96±6.06 %; LDPE-SA 35.45±4.54 %) (Figure 5). No significant differences were detected in the threshold area of stained cells between the LDPE control sample and the LDPE-OH and LDPE-COOH linker control samples (percentage threshold area of total cells: LDPE-OH 87.40±3.73 %; LDPE-COOH 92.76±1.00 %), confirming that the used linker does not affect biofilm biomass (Figure 5). The analysis of the picture

revealed that ZA and SA functionalized material reduced biofilm biomass by 73.7 % and 61.06 % respect to the control LDPE. Coupons without biofilm and stained with the same dye did not produce detectable fluorescence suggesting that false positive signals were not produced (data not shown).

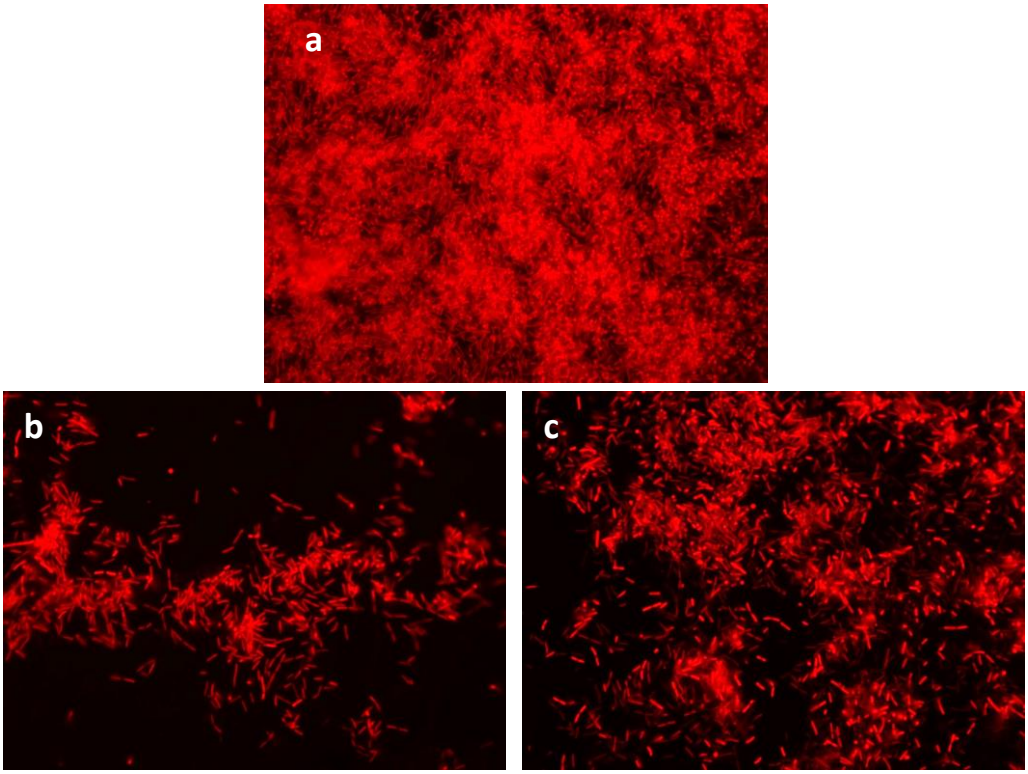

Figure 4. Representative epifluorescence microscope images of *E. coli* biofilm stained with CellMask plasma membrane orange and grown on functionalized and non-functionalized polyethylene surfaces (60x, 1.0 NA water immersion objective): a) LDPE, b) LDPE-ZA, c) LDPE-SA. Red fluorescence corresponds to *E. coli* cells. λ_{ex}: 554 nm and λ_{em}: 567. Scale bar = 20 µm.

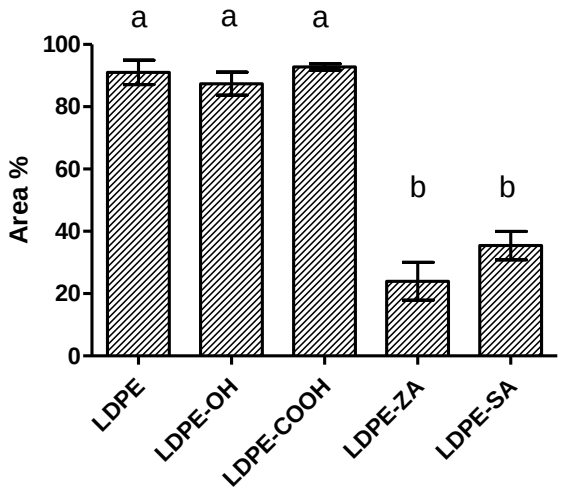

Figure 5. Percentage area threshold of CellMask plasma membrane orange stained cells on functionalized and non-functionalized polyethylene surfaces. Error bars display the honestly significant difference (HSD) intervals using Tukey multiple comparison with a 95 % confidence level (Tukey's HSD, $p < 0.05$). According to post-hoc analysis, means sharing the same letter are not significantly different from each other. Values are based on results from at least three separate experiments.

Staining for live and dead cells was also used to visualize biofilm biomass on functionalized and non-functionalized surface. Direct imaging of biofilms indicated that both functionalized and non-functionalized surface resulted in few dead cells (red) within the biofilm structures with any significant difference in the threshold area between the different surface. On the contrary, pictures analysis showed significant differences in the percentage threshold area of live cells between the control LDPE and the functionalized LDPE-ZA and LDPE-SA material (percentage threshold area of live cells: LDPE 59.89±4.86 %; LDPE-ZA 26.89±5.11 %; LDPE-SA 17.61±3.34 %) (Figure 6-7). The analysis of the pictures revealed that LDPE-ZA and LDPE-SA functionalized material reduced the number of live cells by 55.0 % and 70.6 % respect to the control LDPE. No significant differences were detected in the threshold area of live cells between the control sample LDPE and the linker control samples LDPE-OH and LDPE-COOH (percentage threshold area of live cells: LDPE-OH 55.79±4.24 %; LDPE-COOH 51.10±7.48 %) (Figure 6). The relative percentage of live versus dead cells was also calculated in order to directly compare the number of live bacterial cells versus dead bacterial cells in each surface samples. Statistical analysis of live/dead ratio revealed no significant difference between LDPE, LDPE-OH and LDPE-COOH ratio while live/dead ratio significantly decreased on LDPE-ZA and LDPE-SA functionalized surfaces respect to LDPE (live/dead ratio: LDPE 8.70±0.55; LDPE-OH 7.83±0.75; LDPE-COOH 7.69±1.28; LDPE-ZA 4.77±1.21; LDPE-SA 2.67±0.62) (Figure 6). Coupons without biofilm and stained with the same dye did not produce detectable fluorescence suggesting that false positive signals were not produced (data not shown).
These data suggested that i) the LDPE-OH and LDPE-COOH linker neither affect biofilm biomass nor cells viability; ii) LDPE-ZA and LDPE-SA functionalized surface reduced biofilm biomass with a mechanism that does not affect bacterial viability.

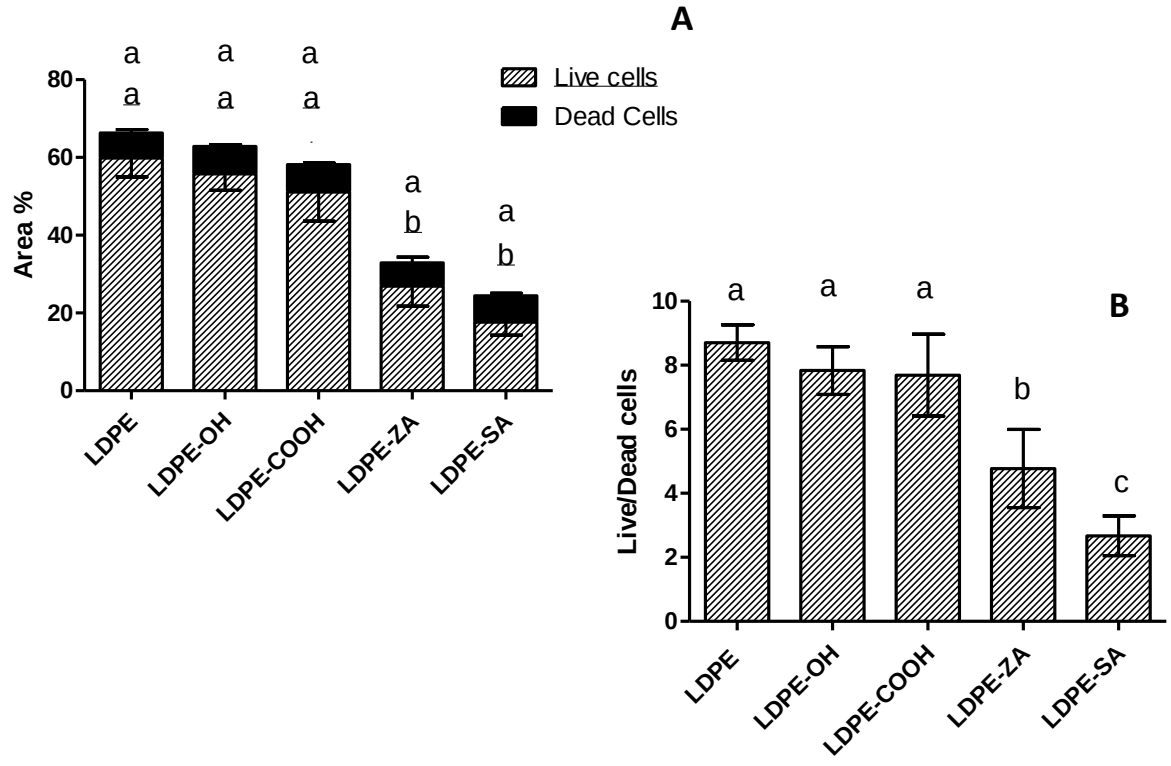

Figure 6. Percentage area threshold of Live/Dead BacLight viability stained cells on functionalized and non-functionalized polyethylene surfaces. Panel A: percentage area threshold of live and dead cells within the biofilm; Panel B: live/dead cells ratio within the biofilm. Error bars display the honestly significant difference (HSD) intervals using Tukey multiple comparison with a 95 % confidence level (Tukey's HSD, $p < 0.05$). According to post-hoc analysis, means sharing the same letter are not significantly different from each other. Values are based on results from at least three separate experiments.

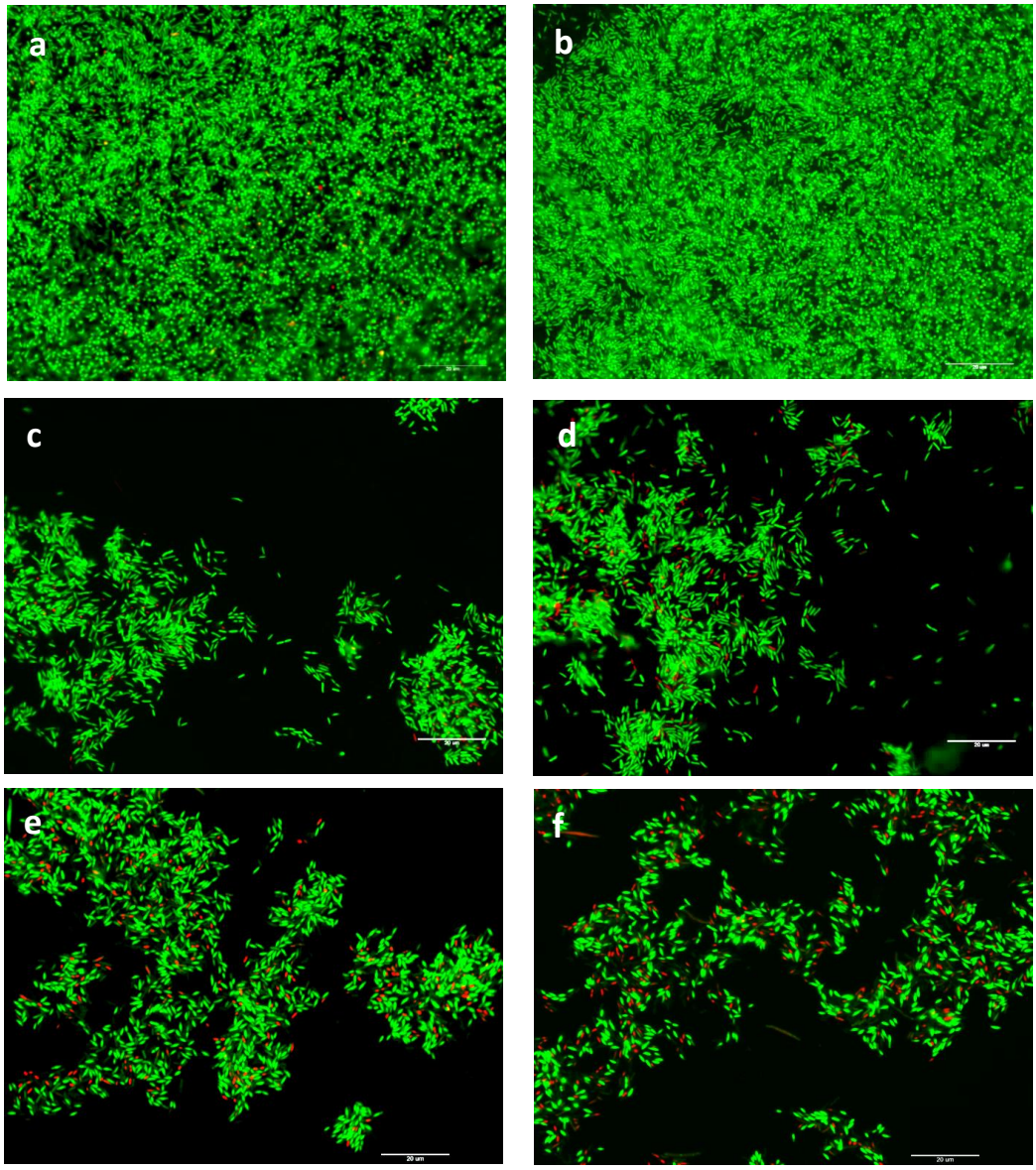

Figure 7. Representative epifluorescence microscope images of *E. coli* biofilm stained with Live/Dead BacLight viability kit and grown on functionalized and non-functionalized polyethylene surfaces (60x, 1.0 NA water immersion objective): a) and b) LDPE, c) and d) LDPE-ZA, e) and f) LDPE-SA. Red fluorescence corresponds to *E . coli* dead cells (λexcitation: 581 nm and λemission: 644 nm while green fluorescence corresponds to *E. coli* live cells (λ_{exc}: 480 nm and λ_{em}: 516 nm). Scale bar = 20 μm.

Functionalized polyethylene surfaces affect the morphology of *E. coli* biofilm

Three-D morphology of biofilm growth on control (LDPE) and LDPE-ZA and LDPE-SA functionalized polyethylene surface was detected by CLSM, with cells within the biofilm stained with Sybr green I nucleic acid dye and EPS polysaccharide matrix stained with Concanavalin A-Texas Red conjugate dye. As presented in figure 9, projection analysis as well as 3D-reconstructed images revealed a complex biofilm on LDPE, LDPE-OH, LDPE-COOH control polyethylene surface, with an intense red and green signal corresponding to multi-layers of cells organized in macro-colonies inside a well-structured polysaccharide matrix. On the contrary biofilm growth on LDPE-ZA and LDPE-SA functionalized surfaces showed a significant decrease in thickness with a mono-layer of dispersed cells and very low presence of polysaccharide matrix. In particular, on LDPE-ZA the matrix is completely disappeared.

Bio-volume percentages of both cells and polysaccharide matrix component were calculated. The analysis of the pictures revealed that LDPE-ZA and LDPE-SA functionalized material significantly reduced cells bio-volume by 91.4 % and 89.2 % respectively in comparison to the LDPE control sample (cells bio-volume percentage: LDPE 30.67±10.64 %; LDPE-ZA 2.61±0.06 %; LDPE-SA 3.31±0.58 %) (Figure 8). Picture analysis also revealed that LDPE-ZA and LDPE-SA functionalized material significantly reduced polysaccharide matrix bio-volume by 99.9 % and 94.0 % respectively in comparison to the LDPE control surface (matrix bio-volume percentage: LDPE 45.22±4.59 %; LDPE-ZA 0.03±0.05 %; LDPE-SA 2.70±0.71 %) (Figure 8).
No significant differences were detected in both cells and polysaccharide matrix bio-volumes between the biofilm grown on the LDPE, LDPE-OH and LDPE-COOH control sample surfaces (cells bio-volume percentage: LDPE-OH 37.40±12.38 %; LDPE-COOH 30.63±9.18; 2.61±0.06 %; matrix bio-volume percentage LDPE-OH 34.31±9.10 %; LDPE-COOH 38.56±5.43) (Figure 8). The relative percentage of each biofilm component (matrix versus cells) was also calculated in order to directly compare the amount of matrix versus the amount of cells on each surface. Statistical analysis of matrix/cells ratio revealed no significant difference between LDPE, LDPE-OH and LDPE-COOH surfaces, with a ratio value over 1 meaning a predominance of matrix respect to the cellular component (matrix/cells ratio: LDPE: 1.60±0.34; LDPE-OH 1.30±0.25; LDPE-COOH 1.28±0.39). A significant reduction of matrix/cells ratio were found in the biofilm grown on LDPE-ZA and LDPE-SA functionalized surfaces, with value under 1, confirming the relevant decrease in the matrix amount respect to the biofilm grown on the control surfaces (matrix/cells ratio: LDPE-ZA 0.00±0.00; LDPE-SA 0.56±0.15) (Figure 8).
Coupons without biofilm and stained with the same dye did not produce detectable fluorescence suggesting that false positive signals were not produced (data not shown).

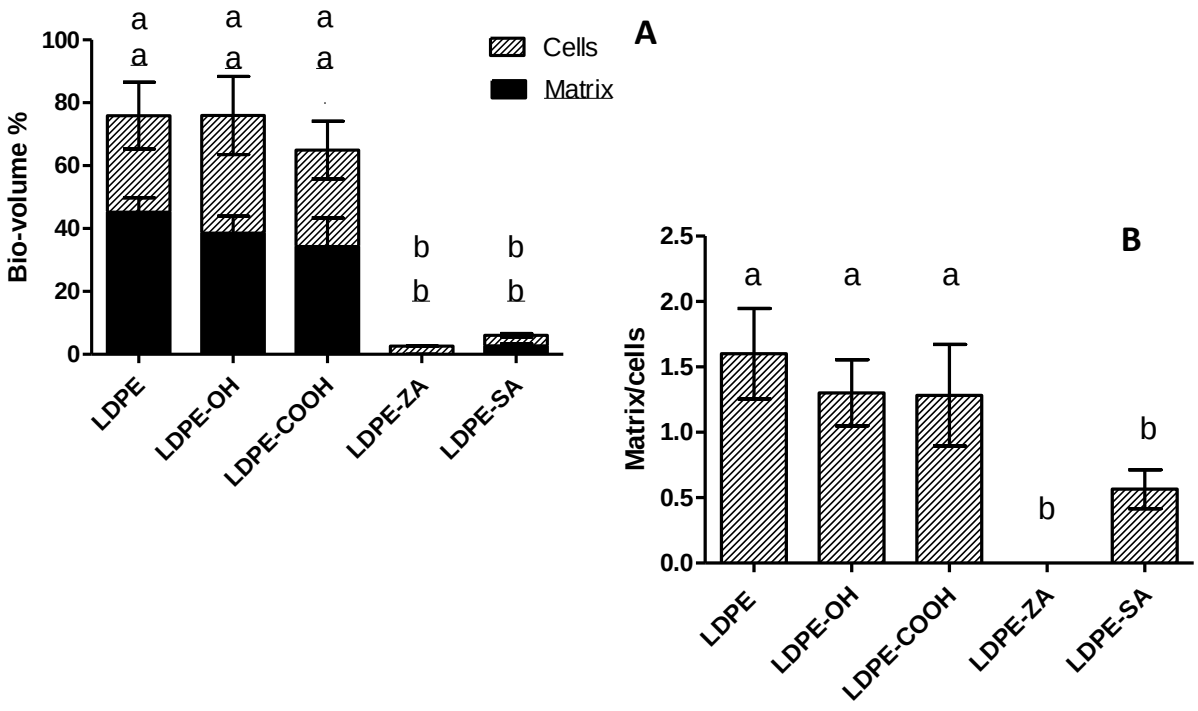

Figure 8. Bio-volume of the cells and polysaccharide matrix biofilm component grown on control and functionalized polyethylene surfaces. Panel A: bio-volume of cells and matrix within the biofilm; Panel B: cells/matrix bio-volume ratio within the biofilm. Error bars display the honestly significant difference (HSD) intervals using Tukey multiple comparison with a 95% confidence level (Tukey's HSD, $p < 0.05$). According to post-hoc analysis, means sharing the same letter are not significantly different from each other.

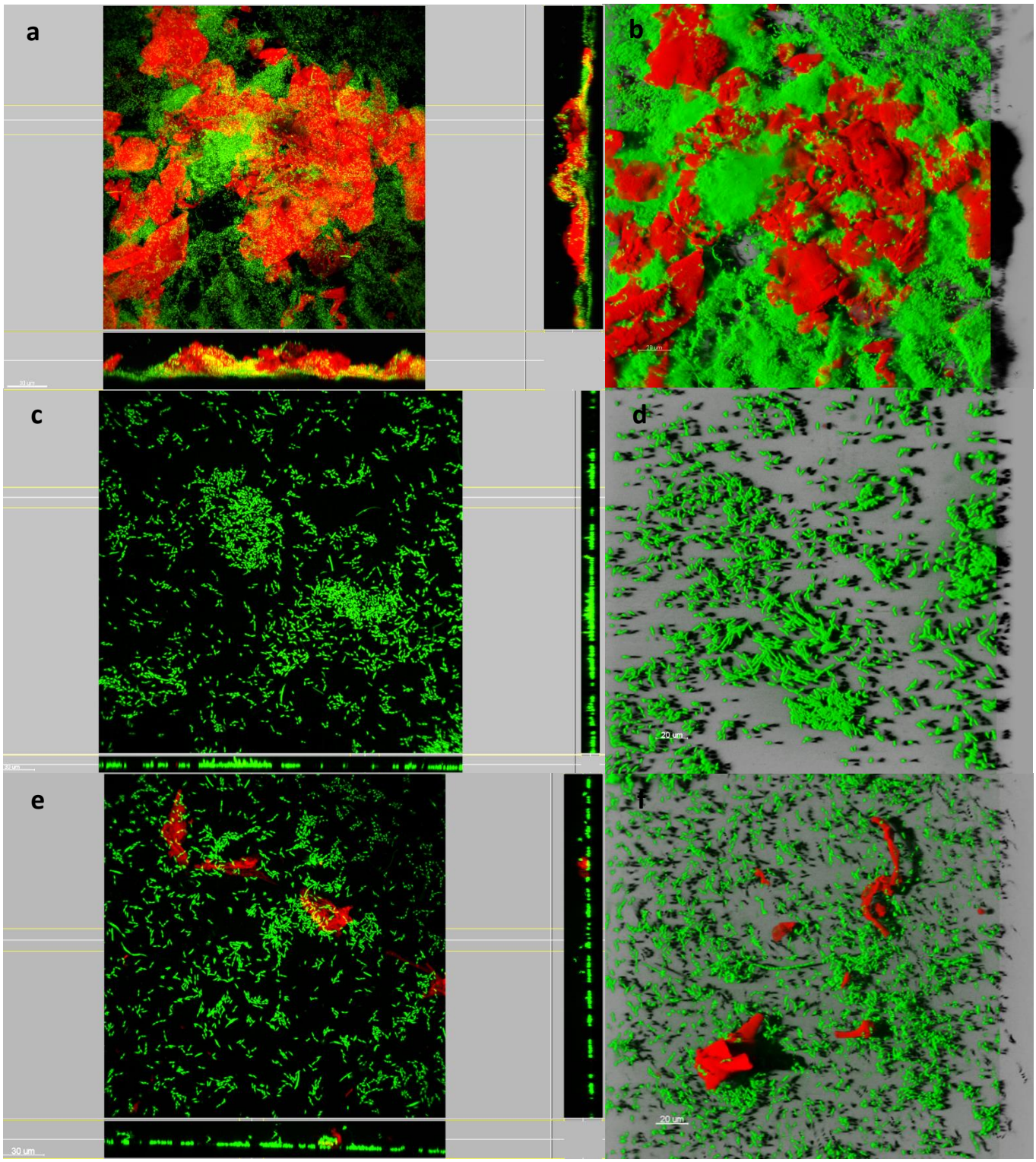

Figure 9. Representative CLSM images of *E. coli* biofilm on functionalized and non-functionalized polyethylene surfaces (λ_{ex} at 488 nm, and λ_{em} < 530 nm , 60x, 1.0 NA water immersion objective): a) and b) LDPE, c) and d) LDPE-ZA, e) and f) LDPE-SA. Live cells were stained green with Syber green I, whereas the polysaccharide component of the EPS matrix was stained red with Texas Red-labelled ConA. Scale bar = 20 or 30 µm.

Enhanced antimicrobial agent susceptibility of *E. coli* biofilm formed on functionalized polyethylene surfaces

To evaluate the susceptibility of *E. coli* biofilm to 100 µg/mL ampicillin and 20 % ethanol on control LDPE and LDPE-ZA and LDPE-SA functionalized surfaces, viable cells in both the biofilm and the bulk liquid were quantified by plate count analysis.

The treatment with ampicillin did not significantly affect the number of viable cells in biofilm grown of LDPE surface, since the number of viable cells in biofilm treated with ampicillin did not show significant differences respect to the biofilm grown on the same surface but treated with PBS (viable adhered cells: LDPE/PBS 7.05±0.07 $\log_{10}$ CFU/cm^2; LDPE/Amp 6.87±0.18 $\log_{10}$ CFU/cm^2) (Figure 10). On the contrary, the treatment with ampicillin drastically decreased the number of viable cells within the biofilm grown on both LDPE-ZA and LDPE-SA functionalized surfaces, in comparison to the corresponding negative control treated with PBS (viable adhered cells: LDPE-ZA/PBS 6.75±0.11 $\log_{10}$ CFU/cm^2; LDPE-ZA/Amp 5.64±0.01 $\log_{10}$ CFU/cm^2; LDPE-SA/PBS 6.70±0.05 $\log_{10}$ CFU/cm^2; LDPE-SA/Amp 5.71±0.08 $\log_{10}$ CFU/cm^2) (Figure 10). The enhanced susceptibility of the biofilm grown on functionalized surfaces to ampicillin was also confirmed by the antimicrobial efficacy percentage that appeared significantly higher on LDPE-ZA and LDPE-SA surfaces respect to LDPE surface (ampicillin efficacy percentage: LDPE/Amp 47.56±7.13 %; LDPE-ZA/Amp 85.59±0.84 %; LDPE-SA/Amp 85.47±1.92 %)(Figure 10). The combination of both LDPE-ZA and LDPE-SA with ampicillin resulted in 96.2 % and 95.5 % biofilm biomass reduction respectively.

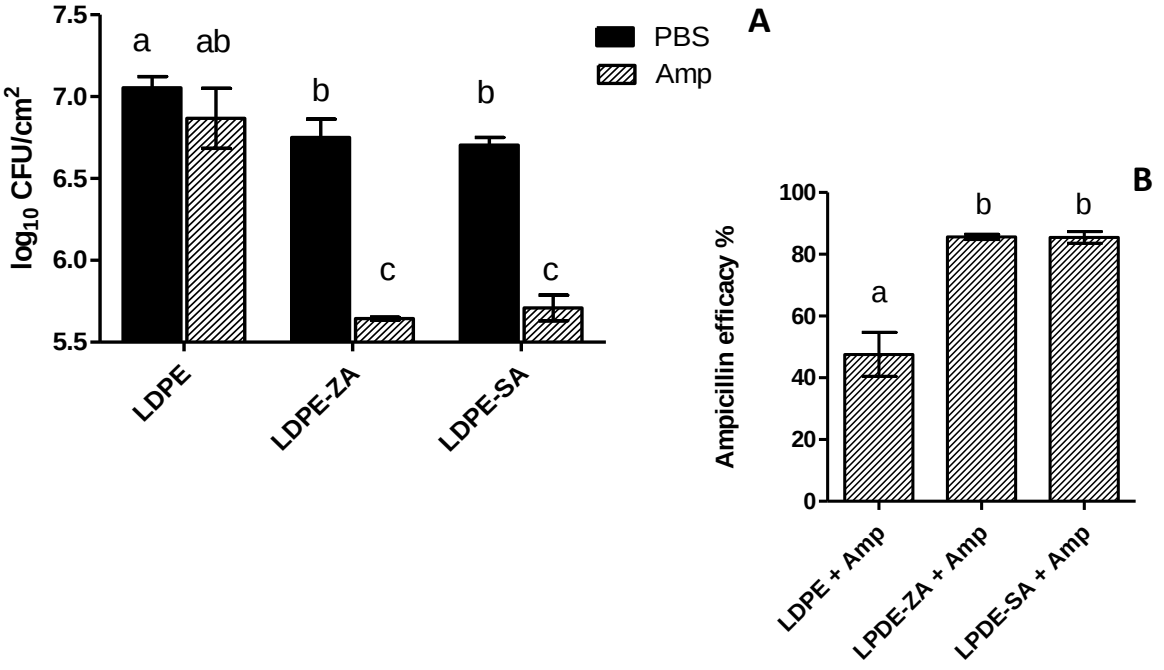

Figure 10. Ampicillin susceptibility test against *E. coli* biofilm pre-grown on functionalized and non-functionalized polyethylene surfaces. Panel A: Biofilm growth after 24 h treatment with 100 µg/mL ampicillin and PBS (negative control). Panel B: 100 µg/mL ampicillin efficacy percentage. Error bars display the honestly significant difference (HSD) intervals using Tukey multiple comparison with a 95 % confidence level (Tukey's HSD, $p < 0.05$). According to post-hoc analysis, means sharing the same letter are not significantly different from each other. Values are based on results from at least three separate experiments.

The treatment with 20 % ethanol significantly affected biofilm biomass on both the control and functionalized surface. The experiment showed a significant reduction in viable cells within the biofilm grown on both LDPE and LDPE-ZA and LDPE-SA functionalized surfaces respect to the corresponding negative control treated with PBS (viable adhered cells: LDPE/PBS 7.63±0.05 $\log_{10}$ CFU/cm^2; LDPE/EtOH

6.56±0.02 log_{10} CFU/cm^2; LDPE-ZA/PBS 6.72±0.04 log_{10} CFU/cm^2; LDPE-ZA/EtOH 6.26±0.06 log_{10} CFU/cm^2; LDPE-SA/PBS 6.64±0.08 log_{10} CFU/cm^2; LDPE-SA/EtOH 6.26±0.08 log_{10} CFU/cm^2) (Figure 11). However, the biofilm grown on the functionalized polyethylene surfaces appeared significantly more vulnerable to the ethanol treatment respect to the biofilm grown on non-functionalized surface. Statistical analysis performed on antimicrobial efficacy data revealed that the ethanol efficiency against biofilm grown on LDPE-ZA and LDPE-SA functionalized surfaces was significantly higher than ethanol efficiency against biofilm on LDPE surface (ethanol efficacy percentage: LDPE/EtOH 17.45±2.10 %; LDPE-ZA/EtOH 70.52±2.12 %; LDPE-SA/EtOH 57.37±3.68 %) (Figure 11). Anyway the combination of both LDPE-ZA and LDPE-SA with ethanol allowed a further decrease in the number of viable adhered cells, with a reduction of 82.8 % and 83.1% in biofilm biomass on respectively LDPE-ZA and LDPE-SA in comparison to LDPE surface.

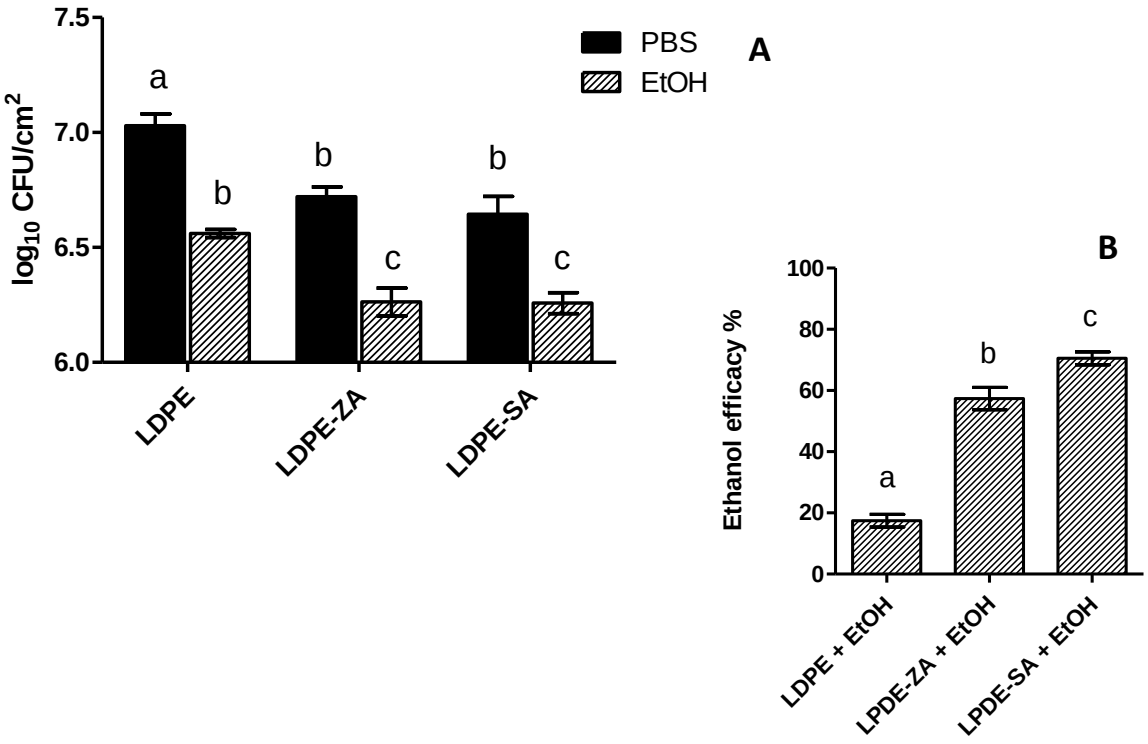

Figure 11. Ethanol susceptibility test against *E. coli* biofilm pre-grown on functionalized and non-functionalized polyethylene surfaces. Panel A: Biofilm growth after 20 min treatment with 20 % ethanol and PBS (negative control). Panel B: 20 % ethanol efficacy percentage. Error bars display the honestly significant difference (HSD) intervals using Tukey multiple comparison with a 95 % confidence level (Tukey's HSD, $p < 0.05$). According to post-hoc analysis, means sharing the same letter are not significantly different from each other. Values are based on results from at least three separate experiments.

To corroborate these results, a direct time-lapse confocal microscope analysis of the 20% ethanol effect on a pre-formed biofilm grown on both control LDPE and LDPE-ZA and LDPE-SA functionalized surfaces was performed by flowing for 20 min the antimicrobial agent directly on the surface. The ethanol effect was measured as decrease in the fluorescence intensity of cells previously stained with the syto-9 green fluorescent nucleic acid stain solution able to bind intact live cells. The time-lapse image analysis revealed that ethanol treatment did not affect the cells green fluorescent of biofilm grown on LDPE control surface within the 20 min of the experiment, except for an initial non-significant decrease probably achievable to the detachment of a portion of biofilm from the surface for the presence of the flow. On the contrary, the ethanol treatment on biofilm grown on both LDPE-ZA and LDPE-SA functionalized surface significantly affected the biofilm biomass integrity, leading to a rapid completely loss in cells fluorescent intensity. Biofilm grown on LDPE-ZA completely lost its green

fluorescent within 15 min while biofilm grown on LDPE-SA completely lost its green fluorescent within 4 min (Figure 12).

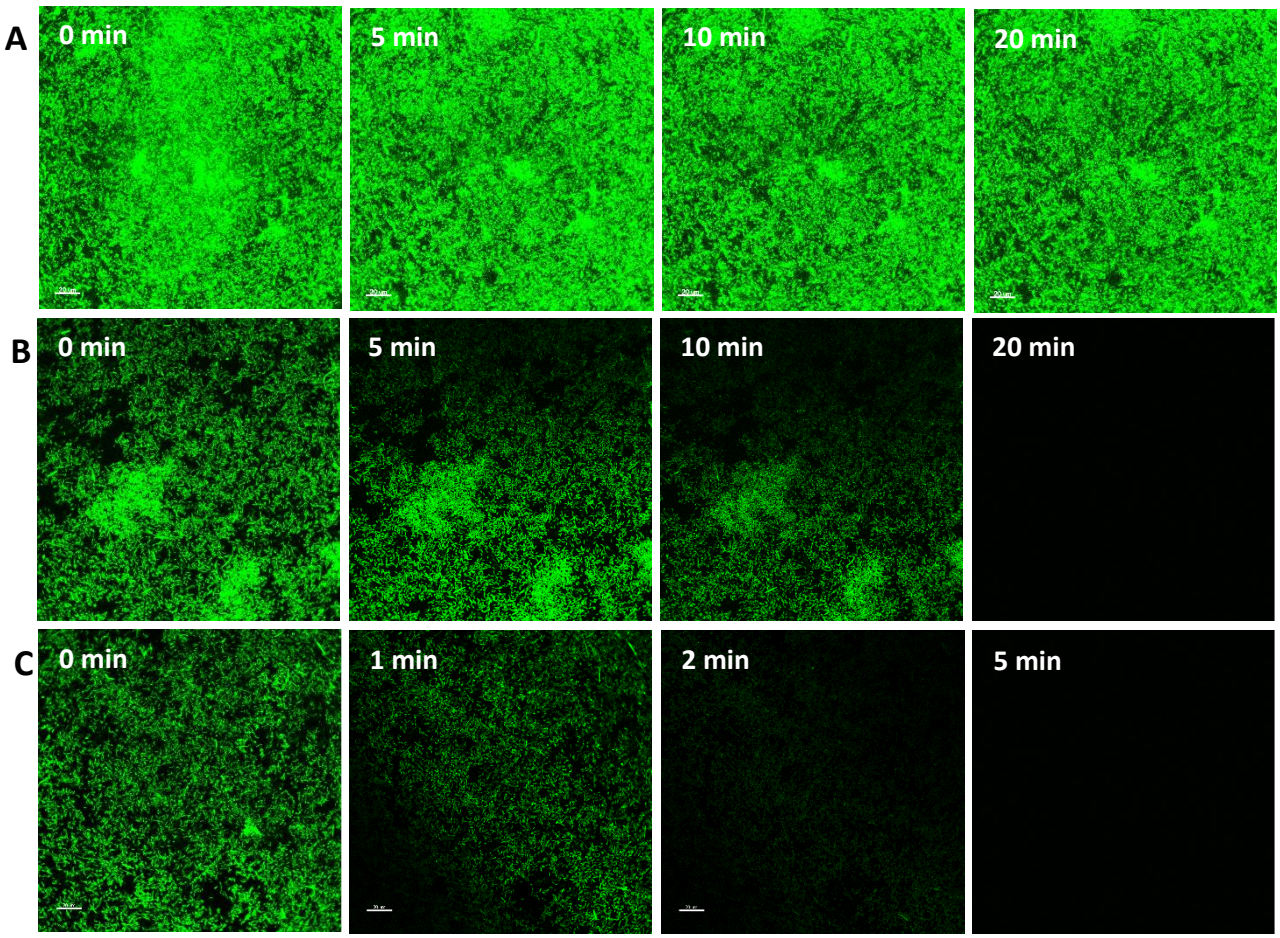

Figure 12. Time-lapse CLSM representative images of the 20 % ethanol action against *E. coli* biofilm pre-grown on functionalized and non-functionalized polyethylene surfaces within 20 min. Live cells were stained green with Syto 9 (λ_{ex} 488 nm, and λ_{em} <530 nm , 60x, 1.0 NA water immersion objective). Line A: Biofilm pre-growth on LDPE control surface; Line B: Biofilm pre-growth on LDPE-ZA functionalized surface; Line C: Biofilm pre-growth on LDPE-SA functionalized surface. Scale bar = 20 µm.

The cells bio-volume of each single frame was calculated and used to re-elaborate a mathematical model explaining the biofilm cells response against the ethanol treatment in term of bio-volume reduction in function of the time x (equation 1). The model considered a first step in which the bio-volume fluorescence gradually decreased with an exponential trend (equation 2) and a second step following a logistic trend (equation 3) in which the bio-volume fluorescence rapidly decreased until reaching 0 value.

(1) $y(x)g(x)$

(2) $$y(x) = \frac{y_0 \cdot (a \cdot s_0 + y_0) \cdot \exp\left[r \cdot (x - p)\right]}{a \cdot s_0 + y_0 \cdot \exp[r \cdot (x - p)]}$$

(3) $$g(x) = \exp\left[k \cdot (x - p)\right]$$

$$y_0 = 150000 \quad s_0 = 100000 \quad a = 0.5 \quad p = 9 \quad r = -8 \quad k = -15$$

Discussion

The natural compounds zosteric acid (ZA) and salicylic acid (SA) were previously proved to be powerful anti-biofilm compounds able to counteract biofilm formation at sub-lethal concentration. Despite these promising results, a real application of these compounds is not feasible due to the lack of a suitable technology able to efficiently retain the anti-biofilm molecules over a working timescale. In the past, some researches were performed with the aim to incorporate ZA and SA in different polymeric materials able to gradually release the anti-biofilm molecules in the surrounding area (Geiger et al., 2004; Barrios et al., 2005; Bryers et al., 2006; Rosenberg et al., 2008; Guinta et al., 2011; Nowatsky et al., 2012; Lo et al., 2014). However, in most of cases these systems showed several problems such as the non-uniform distribution of the anti-biofilm compounds inside the material and the formation of aggregates due to the incomplete miscibility of the molecules in the polymers. In addition, a constant release rate of the active compound has neither been achieved nor monitored, limiting the effectiveness of the technology to only a short period of time and making this system often unfeasible for a wide range of practical applications (Barrios et al., 2005; Nowatsky et al., 2012).
In this research a new improved anti-biofilm solution based on ZA and SA surface immobilization process was presented, providing a new class of bio-hybrid active materials with a novel target and mode of action. Here ZA and SA were successfully covalently bound to a low density polyethylene (LDPE) surface, in a procedure that allowed the anti-biofilm compound to preserve the biological function upon the conjugation process. In the previous chapters, ZA and SA chemical determinants responsible of their anti-biofilm activity were investigated. Moreover, the addition of an amino group in the para position of the phenyl ring in both ZA and SA chemical structure was proved not affecting the anti-biofilm activity of both molecules. Indeed, in this study a specific protocol to expose AZ and SA active scaffold on the external surface of the polymeric material via an amide bond was set up, allowing the anti-biofilm compound active moieties to directly interact with bacterial cells and successfully exerting their function.
Low pressure glow discharge O_2 plasma has been firstly used to increase wettability in a LDPE film in order to improve its adhesion properties by the formation of some polar species on the exposed surface. LDPE plasma treatment causes the breakdown of some C–H bonds and the generation of activated species. The subsequent exposure of the activated surface to air causes oxygen incorporation on the LDPE surfaces, leading to surface oxidation and the formation of peroxide and hydroperoxide species. The use of plasma treatments has grown in interest in the last decades since it is an environmentally efficient process that provides activated surfaces characterized by high uniformity. Moreover, the use of low pressure conditions allows to perform plasma treatments at low or moderate temperatures, reducing the material degradation that could occur with a different type of treatment and maintaining the bulk properties of the materials unchanged (Sanchis et al., 2006). Subsequently, the graft-polymerization with 2-hydroxyethyl methacrylate (HEMA) and the conversion of the terminal hydroxyl groups of HEMA side chains into the carboxylic acid derivatives by treatment with succinic anhydride provided the chemical condition to allow the amide bond formation between the modified LDPE surface and ZA and SA molecules bearing an amino group in the *para* position on their phenyl ring.
The characteristics of the functionalized material were evaluated in each step by means of both contact angle measurements and Fourier Transform Infrared Spectroscopy (AFT-FTIR) analysis. The experiments revealed that O_2 plasma treatment and HEMA graft-polymerization considerably reduced surface contact angle confirming that the procedure successfully improved surface wettability with a marked hydrophilic nature (data not shown). Theoretically, after plasma exposure significant changes in the measured ATR-FTIR spectra respect to untreated surface should have also been observed for the presence of some -OH or -OOH groups incorporated into the surface, with the appearance of two

broad peaks between 3.600-3.050 cm^{-1} and 1.800-1.520 cm^{-1}. In this study, recorded spectra did not show evidence for -OH or -OOH peaks after plasma treatment. Moreover, no changes were observed after the graft-polymerization procedure (LDPE-OH) and the subsequent oxidation to carboxylic acid derivatives (LDPE-COOH), probably for the low concentration of the polar species undetectable by the instrument. However, after the covalent linkage with ZA and SA the shape of the spectra changed, showing significant differences respect to LDPE surface and displaying typical peaks of the amide bond, indeed confirming the presence of a covalent bond between ZA and SA active scaffold and LDPE surface. The auto-fluorescence of ZA and SA immobilized scaffold was also used to verify the surface functionalization by Confocal Scanning Laser Microscopy (CLSM). LDPE pictures acquired in each step of the functionalization procedure revealed the presence of an intense fluorescent signal after the last functionalization process, only attributable to the presence of ZA and SA active scaffold on the LDPE surface. The analysis repeated on 10-fold used coupons showed a maintained intense fluorescent signal, suggesting that ZA and SA were successfully retained by the surface and that the surface coupons were not affected by their usage. Further accurate analysis, such as X-ray Photoelectron Spectroscopy (XPS) measurements to determine the elemental composition of the surface and Scanning Electron Microscopy (SEM) analysis to provide an image of the physical modifications of the material were also performed confirming the success of the functionalization procedure (data not shown).

The anti-biofilm performance of the modified materials were tested by using a standardized in vitro system aimed at replicating hydrodynamic flow conditions normally encountered in vivo. The Center for Disease Control (CDC) biofilm reactor was used to produce *E. coli* biofilm under continuous liquid shear to simulate conditions to which surfaces of a wide range of applications are subjected during their use.

Biofilm biomass grown on functionalized and non-functionalized materials were collected and quantified by viable plate count assay. Epifluorescence microscopic techniques were additionally used to provide image analysis and quantification of bacterial cells in situ. Accordingly, all the experiments revealed a significant decrease in biofilm biomass and viable cells between the control sample (LDPE) and the functionalized material (LDPE-ZA and LDPE-SA). On the contrary, no significant differences were detected in biofilm biomass and cells viability between the LDPE control sample and the LDPE-OH and LDPE-COOH control linker sample. This result suggested that no functionalization step introduce modification in LDPE structure that affect biofilm biomass and cell viability. Consequently, the anti-biofilm performance of the functionalized materials is totally attributable to the ZA and SA active moieties covalently immobilized on the surface. Direct images of biofilms stained for live and dead cells revealed that both functionalized and non-functionalized surface resulted in a few dead cells within the biofilm with no significant differences between the different surfaces. This result confirmed that ZA and SA functionalized surface reduced biofilm biomass with a mechanism that not affect bacterial viability, creating the prerequisite to reduce the risk of developing resistant microbial strains. In the past, Villa and collaborators (2010) reported that 500 mg/mL ZA was able to reduce cells adhesion up to 70 % while El-Banna and colleagues (2012) reported that SA at a concentration between 10 and 100 µg/mL inhibited *E. coli* biofilm production up to 68 %. In this research it was proved that ZA and SA functionalized surfaces reduced biofilm formation of 62 % and 60 % respectively, proving the ability of ZA and SA to exert the anti-biofilm activity even immobilized on the surface, with a performance comparable to that they exert free in solution.

Confocal Laser Scanner Microscope Analysis revealed a dramatic impact of immobilized ZA and SA on biofilm morphology. ThreeD-reconstructed images analysis showed a complex biofilm on LDPE, LDPE-OH, LDPE-COOH control surfaces, with an intense fluorescence signal corresponding to multi-layers of cells organized in macro-colonies inside a well-structured polysaccharide matrix. On the contrary, biofilm grown on ZA and SA functionalized surfaces showed a significant decrease in thickness with a mono-layer of dispersed cells and significant lower bio-volume of polysaccharide matrix. Indeed the new materials provided new anti-biofilm solutions, not only able to affect biofilm biomass and cells

adhesion, but also able to deeply affect biofilm structure with massive changes especially in the biofilm thickness and matrix amount.
It is well known that the susceptibility of *E. coli* biofilm to many conventional antimicrobial agents is reduced, compared to the susceptibility of planktonic cells (Hall-Stoodley, 2004). Indeed, the sensitivity of a biofilm grown on functionalized surfaces to conventional antimicrobial agents was examined, to prove the ability of these new materials to improve the antimicrobial efficacy. In this study ampicillin, an antibiotic with a wide range spectrum of activity, and ethanol, widely used to disinfect surfaces, were selected to be tested for their performance against an *E. coli* biofilm pre-formed on both control and ZA and SA functionalized surfaces. In particular, ethanol was chosen since it might be a promising solution because of its antimicrobial activity against a broad range of planktonic bacteria and fungi, its low cost and its universal availability. In addition, there are no evidences of acquired resistance to concentrated ethanol despite its extensive and long standing use as an antiseptic (Balestrino et al., 2009). Both ampicillin and ethanol significantly reduced the number of viable adhered cells on functionalized materials respect to the corresponding sample treated with PBS and the antimicrobial efficacy value of both ampicillin and ethanol resulted significantly improved on LDPE-ZA and LDPE-SA functionalized biofilm, confirming the enhanced susceptibility of biofilm grown on ZA and SA functionalized material to the antimicrobial agents. The combination of the functionalized surface with both ethanol and ampicillin reduced viable biomass up to 92% with the antibiotic treatment and up to the 83 % with the biocide treatment. The direct time-lapse confocal microscope analysis of the 20% ethanol effect on a pre-formed biofilm grown on both control LDPE and LDPE-ZA and LDPE-SA functionalized surfaces also corroborated this result. The decrease in the green syto 9 dye fluorescence related to live cells was more rapid in the biofilm grown on ZA and SA functionalized material respect to biofilm grown on the control surface suggesting a faster penetration of ethanol in the biofilm grown on the functionalized surfaces.
Ethanol penetration was described with a mathematical model that predicted an initial exponential trend followed by a logistic trend. Ethanol is known to eliminate bacterial cells by denaturing proteins and causing membrane leakage in a procedure that starts with the loss of respiratory activity (Balestrino et al., 2009). We suggest that in the exponential first step of fluorescent decreased bacterial cell respiratory activity start to decrease and cells respond to the adverse condition by the activation of protecting systems. However, the further treatment with ethanol led the cell to an extreme stress condition that resulted in its death with the quickly loss of fluorescence (logistic trend).
It is reported that the restricted susceptibility of biofilms to antimicrobials depends on some characteristic that allow them to counteract environmental stress. The presence of a diffusion barrier provided by the EPS is recognized to be an important factor with the potential to reduce the antimicrobial penetration within the biofilm, either by physically slowing their diffusion or chemically reacting with them (Pace et al., 2006). CLSM analysis revealed that biofilm grown of ZA and SA functionalized surfaces is deeply damaged with a very low or no amount of polysaccharide matrix. Indeed it is reasonable that biofilm grown on ZA and SA functionalized material appears to be more susceptible to both antibiotic and biocide treatment that more easily penetrate within the biofilm exerting their effect even at a concentration below those normally used in the traditional applications. The experiments did not give evidence if the treatment caused the killing or the removal of the biomass from the biofilm. The plate count assay of cells in the bulk liquid after both antibiotic and ethanol treatment performed in the previous experiments, suggested the presence of some still alive cells. However, more experiments are required to clarify this hypothesis.

Conclusion

In this research ZA and SA were successfully immobilized on a LDPE surface in a procedure that allowed their active moiety to exert the anti-biofilm activity even immobilized on a surface providing a new, improved solution able to reduce the incidence of biofilm formation. In this approach, no molecules are leached from the surface, sidestepping the problem of the compound release kinetics, providing long term protection against bacterial colonization, and reducing the risk of developing resistant microbial strains, as the concentration of the anti-biofilm agent is constantly below the lethal concentration. The biological assays demonstrated a dramatic impact of immobilized ZA and SA on biofilm formation, proving the efficacy of these materials. Moreover, biofilm grown on ZA and SA functionalized surfaces showed enhanced susceptibility to the traditional antimicrobial agents, even at concentrations below those normally used in the currently application. This study also posed the basis for the exciting possibility to extend the functionalization procedure to other types of polymeric materials creating new anti-biofilm bio-hybrid materials available for a wide range of application.

References

Balestrino D., Souweine B., Charbonnel N., Lautrette A., Aumeran C., Traor´e O., Forestier C. (2009). Eradication of microorganisms embedded in biofilm by an ethanol-based catheter lock solution. *Nephrology Dialysis Transplantation*, 10:3204-3209.

Barrios C.A., Xu Q., Cutright T., Newby B.Z. (2005). Incorporating zosteric acid into silicone coatings to achieve its slow release while reducing fresh water bacterial attachment. *Colloids and Surface B: Biointerface*, 41:83-93.

Bryers J.D., Jarvis R.A., Lebo J., Prudencio A., Kyriakides T.R., Uhrich K. (2006). Biodegradation of poly(anhydride-esters) into non-steroidal anti-inflammatory drugs and their effect on *Pseudomonas aeruginosa* biofilms in vitro and on the foreign-body response in vivo. *Biomaterials*, 27:5039-48.

Coenye T., De Prijck K., Nailis K., Nelis H.J. (2011). Prevention of *Candida albicans* biofilm formation. *The Open Mycology Journal*, 5:9-20.

El-Banna T., Sonbol F.I., Abd El-Aziz A.A., Abo-Kamar A., Seif-Eldin D.W. (2012). Effect of the combination of salicylate with aminoglycosides on bacterial adhesion to urinary catheters. *International Research Journal of Pharmaceuticals*, 2:39-45.

Geiger T., Delavy P., Hany R., Schleuniger J., Zinn M. (2004). Encapsulated zosteric acid embedded in poly[3-hydroxyalkanoate] coatings—Protection against biofouling. *Polymer Bulletin*, 52:65-72.

Guinta R.A., Carbone L.A., Rosenberg E.L., Uhrich E.K., Tabak M., Chikindas L.M. (2011). Slow release of salicylic acid from degrading poly(anhydride ester) polymer disrupts bimodal pH and prevents biofilm formation in *Salmonella typhimurium* MAE52. In Bailey W.C. (ed), Biofilms: Formation, Development and Properties, Nova Science Publishers, New York, pp. 649-658

Hall-Stoodley L., Costerton W.J., Stoodley P. (2004). Bacterial biofilms: from the natural environment to infectious diseases. *Nature Review Microbiology*, 2:95-108

Jena P., Mohanty S., Mallick R., Jacob B., Sonawane A. (2012). Toxicity and antibacterial assessment of chitosan-coated silver nanoparticles on human pathogens and macrophage cells. *International Journal of Nanomedicine*, 7:1805-1818.

Jiang H., Manolache S., Wong A.C.L., Denes F.S. (2004). Plasma-enhanced deposition of silver nanoparticles onto polymer and metal surfaces for the generation of antimicrobial characteristics. *Journal of Applied Polymer Science*, 93:1411-1422.

Lo J., Lange D., Chew B.H. (2014). Ureteral stents and Foley catheters-associated urinary tract infections: the role of coatings and materials in infection prevention. *Antibiotics*, 3: 87-97.

Nowatzki P.J., Koepsel R.R., Stoodley P., Min K., Harper A., Murata H., Donfack J., Hortelano E.R., Ehrlich G.D., Russell A.J. (2012). Salicylic acid-releasing polyurethane acrylate polymers as anti-biofilm urological catheter coatings. *Acta Biomaterialia*, 8: 1869-1880.

Pace J.L., Rupp M.E., Finch R.G. (2006). Biofilms, Infection, and Antimicrobial Therapy. Taylor & Francis Group, Boca Raton.

Polo A., Foladori P., Ponti B., Bettinetti R., Gambino M., Villa F., Cappitelli F. (2014). Evaluation of zosteric acid for mitigating biofilm formation of *Pseudomonas putida* isolated from a membrane bioreactor system *International Journal of Molecular Sciences*, 15: 9497-9518.

Rai M., Yadav A., Gade A. (2009). Silver nanoparticles as a new generation of antimicrobials. *Biotechnology Advances*, 27:76-83.

Rosenberg L.E., Carbone A.L., Römling U., Uhrich K.E., Chikindas M.L. (2008). Salicylic acid-based poly(anhydride esters) for control of biofilm formation in *Salmonella enterica* serovar Typhimurium. *Letters in Applied Microbiology*, 46: 593-599.

Sanchis M.R., Blanes V., Blanes M., Garcia D., Balart R. (2006). Surface modification of low density polyethylene (LDPE) film by low pressure O_2 plasma treatment. *European Polymer Journal*, 42:1558-1568.

Villa F., Albanese D., Giussani B., Stewartd P. S., Daffonchio D., Cappitelli F. (2010). Hindering biofilm formation with zosteric acid. *Biofouling*, 26: 739-752.

Villa F., Pitts B., Stewart P.S., Giussani B., Roncoroni S., Albanese D., Giordano C., Tunesi M., Cappitelli F. (2011). Efficacy of zosteric acid sodium salt on the yeast biofilm model *Candida albicans*. *Microbial Ecology*, 62: 584-598.

Von Eiff C., Kohnen W., Becker K., Jansen B. (2005). Modern strategies in the prevention of implant-associated infections. *The International Journal of Artificial Organs*, 28:1146-1156.

Conclusion

The increase impact of biofilms on human society and their recalcitrant resistance to the antimicrobial agent has put a tremendous pressure on the scientific community to find alternative approaches for the treatment of surface associate biofilms. In this study, the idea to combine commonly used materials with small natural molecules that do not act as antibiotics but elicit biofilm formation was developed. Zosteric acid (ZA) and salicylic acid (SA) were previously reported as alternative biocide-free agents able to significantly reduce, at sub-lethal concentrations, both bacterial and fungal adhesion and to play a role in shaping biofilm architecture, in reducing biofilm biomass and thickness and in extending the antimicrobial agents performance.

In this research a new improved anti-biofilm solution based on ZA and SA surface immobilization process was presented. This strategy provided a new class of bio-hybrid active materials with a novel target and mode of action.

The functionalization process was carried with a procedure that did not compromise the molecule active site conformation and function. A detailed study to identify the ZA and SA chemical structure and molecular target involved in their anti-biofilm activity was performed. The study highlighted that the carboxylic acid moiety conjugated to the double bond in *trans* configuration is an essential requirement in ZA chemical structure to guarantee a good anti-biofilm performance, while the deletion of the sulphate ester group seems not to compromise the ZA anti-biofilm activity. Moreover, the *para* position on ZA and SA phenyl ring could be considered a good point for the coupling to a polymer. Proteomic study also revealed that ZA and SA directly interact with the same protein WrbA, suggesting its possible role in the biofilm formation process. However, any consideration about the mechanism triggered by the interaction of ZA and SA with this protein is possible and further experiments are necessary to clarify this question.

Based on this information, **ZA and SA were successfully covalently bound to a low density polyethylene (LDPE) surface, overcoming the challenge to preserve the ZA and SA biological function upon the conjugation process and over a working timescale**. A specific protocol to expose ZA and SA active scaffold on the external surface of the polymeric material via an amide bond was set up. This allowed the anti-biofilm compound active moieties to directly interact with bacterial cells and successfully exerting their function. The developed protocol resulted in new materials in which the problem of the molecule release was sidestepped. In addition an effective local concentration of anti-biofilm agent was maintained over an extended period of time. Moreover, this preventive biocide-free strategy offers a solution to mitigate bacterial selection pressure with the potential to restore the efficacy of antimicrobial agents that are ineffective against sessile microorganisms. Biological assays revealed a dramatic impact of these materials on biofilm formation. Biofilm grown on functionalized material appeared deeply altered in both the number of adhered cells and morphology. In addition, biofilm grown on functionalized material presented enhanced susceptibility to the traditional antimicrobial agents.

As ZA and SA low toxicity was widely proved, the delivery methods set up in this research could become a robust technological platform which could be adaptable to many applications such as engineering system surfaces and work benches but also to other materials such as for medicine and food packaging. The major industries and/or public organizations might pick up these successful developments and integrate them with their existing strategies. Indeed it appeared clear that this new technology could be the breakthrough in the fight against biofilm development.

The understanding of ZA and SA mode of action represents a relevant achievement toward future researches aims to develope improved and more efficacy anti-biofilm technology. In the last years, combinatorial chemistry has evolved important and sophisticated design strategies able to manipulate

molecules proving new compounds with enhanced activity. In this research a platform of biologically active chemical structures with anti-biofilm activity and their cellular targets were identified. In the future the combination of this knowledge with the potentiality of the combinatorial chemistry could provide new effective anti-biofilm strategies in terms of efficacy and selectivity for the target. ZA and SA active structures could be used as structural scaffolds or simply as building block to provide analogues or designed hybrid molecules with an increased chance to exert a potent biological activity. On the other hand the ZA and SA cellular targets could be used to predict the anti-biofilm potentiality of new molecules avoiding the in vivo screening of the compounds that appears ineffective since the early stage of the research.

In conclusion this research allowed to create a new antibiotic free, eco-friendly, cost effective, anti-biofilm technology based on natural molecule immobilization process that is available for a wide range of application, also posing the basis for the development of further improved anti-biofilm solutions.

Collaborations

Dr. Stefania Villa and Dr. Arianna Gelain
Department of Pharmaceutical Sciences
Università degli Studi di Milano

Prof. Domenico Albanese
Department of Chemistry
Università degli Studi di Milano

Dr. Alberto Vitali and Dr. Francesco Secundo
Institute of chemistry of molecular recognition – Roma/Milano
National Research Council

Prof. Garth James
Center for Biofilm Engineering
Montana State University, MT, USA

Acknowledgements

I would like to express my gratitude to Dr. Fabio Forlani and Dr. Francesca Cappitelli. They offered me many helpful suggestions, important advice and constant attention during the course of this work.

There are many people that have contributed to the completion of this work. They gave me interesting feedback, suggestions and technical support. I would like to thank: Dr. Federica Villa, Dr. Andrea Polo, Dr. Stefania Villa, Dr. Arianna Gelain, Silvia Carolina Dell'Orto, Dr. Alberto Vitali, Dr. Valeria Marzano, Dr. Francesco Secundo, Eugenio Spadoni Andreani, Prof. Domenico Albanese. Thanks to Prof. Garth James, Dr. Kelly Kirker, Dr. Elinor de Lancey Pulcini, Laura Broegli, Steve Fisher of the Medical Biofilm Laboratory at the CBE, Montana State University. It was a great pleasure to work with them.

Furthermore, I would like to thank my colleagues Anna, Annalisa, Aristodemo, Aurora, Besma, Bessem, Davide, Elena, Eleonora, Elisa, Emanuela, Erica, Federica, Francesca, Maurizio, Giuseppe, Jessica, Lucia, Luigi, Michela, Matteo, Marco, Marta, Mauro, Ramona, Sara, Stefania, Violetta.

Finally, thanks to all people who helped me during this period of my life.

fondazione cariplo

anfomat

Anfomat Project – 2012-2014

Novel materials for medical devices based on biofunctionalized surfaces with antifouling properties.

grant no. 2011-0277

ATENEO ITALO-TEDESCO
DEUTSCH-ITALIENISCHES HOCHSCHULZENTRUM

German-Italian bilateral Vigoni Project – 2012-2014

Seagrass compounds inhibit biofilm formation -from the identification to the application.

grant no. 54644032